

SEDIMENTOLOGICAL CHARACTERISTICS OF STORM DEPOSITS INDUCED BY THE
TROPICAL STORM PABUK ALONG THE WESTERN COAST OF THE GULF OF THAILAND



A Dissertation Submitted in Partial Fulfillment of the Requirements
for the Degree of Doctor of Philosophy in Geology
Department of Geology
Faculty Of Science
Chulalongkorn University
Academic Year 2023

ลักษณะเฉพาะทางตะกอนวิทยาของชั้นตะกอนพายุที่เกิดจากพายุโซนร้อนปาบึกบริเวณชายฝั่งอ่าว
ไทยด้านตะวันตก



วิทยานิพนธ์นี้เป็นส่วนหนึ่งของการศึกษาตามหลักสูตรปริญญาวิทยาศาสตรดุษฎีบัณฑิต
สาขาวิชาธรณีวิทยา ภาควิชาธรณีวิทยา
คณะวิทยาศาสตร์ จุฬาลงกรณ์มหาวิทยาลัย
ปีการศึกษา 2566

Thesis Title	SEDIMENTOLOGICAL CHARACTERISTICS OF STORM DEPOSITS INDUCED BY THE TROPICAL STORM PABUK ALONG THE WESTERN COAST OF THE GULF OF THAILAND
By	Miss Chanakan Ketthong
Field of Study	Geology
Thesis Advisor	Professor MONTRI CHOOWONG, Ph.D.
Thesis Co Advisor	Assistant Professor SUMET PHANTUWONGRAJ, Ph.D.

Accepted by the FACULTY OF SCIENCE, Chulalongkorn University in Partial
Fulfillment of the Requirement for the Doctor of Philosophy

..... Dean of the FACULTY OF SCIENCE
(Professor PRANUT POTIYARAJ, Ph.D.)

DISSERTATION COMMITTEE

..... Chairman
(Professor Panya Charusiri, Ph.D.)

..... Thesis Advisor
(Professor MONTRI CHOOWONG, Ph.D.)

..... Thesis Co-Advisor
(Assistant Professor SUMET PHANTUWONGRAJ, Ph.D.)

..... Examiner
(Assistant Professor VICHAI CHUTAKOSITKANON, Ph.D.)

..... Examiner
(Associate Professor THANOP THITIMAKORN, Ph.D.)

ชนกานต์ เกตุทอง : ลักษณะเฉพาะทางตะกอนวิทยาของชั้นตะกอนพายุที่เกิดจากพายุโซนร้อนปาบึกบริเวณชายฝั่งอ่าวไทยด้านตะวันตก. (SEDIMENTOLOGICAL CHARACTERISTICS OF STORM DEPOSITS INDUCED BY THE TROPICAL STORM PABUK ALONG THE WESTERN COAST OF THE GULF OF THAILAND) อ.ที่ปรึกษาหลัก : ศ. ดร.มนตรี ชูวงศ์, อ.ที่ปรึกษา
ร่วม : ผศ. ดร.สุเมธ พันธุ์จักราช

พายุโซนร้อนปาบึกขึ้นฝั่งที่ชายฝั่งด้านตะวันตกของอ่าวไทยในวันที่ 4 มกราคม พ.ศ. 2562 ก่อให้เกิดคลื่นซัดฝั่งในระดับสูงและยังทั้งตะกอนคลื่นซัดฝั่งไว้ตามพื้นที่ชายฝั่ง หลังเหตุการณ์พายุผู้วิจัยดำเนินการสำรวจชายฝั่งเบื้องต้นจำนวน 44 จุด เพื่อตรวจสอบลักษณะทางตะกอนวิทยา วัตถุประสงค์ขยหาด รวบรวมข้อมูลความรุนแรงทางอุทกพลศาสตร์ รวมถึงสภาพธรณีสัณฐานวิทยาของพื้นที่ จากนั้นคัดเลือกพื้นที่ศึกษาหลัก 4 พื้นที่ ได้แก่ หาดเจ้าสำราญ (เพชรบุรี) บ้านทุ่งน้อย (ประจวบคีรีขันธ์) ทุ่งตะโก (ชุมพร) และแหลมตะลุมพุก (นครศรีธรรมราช) เพื่อศึกษารายละเอียดทางตะกอนวิทยา การสำรวจยังลึกลงด้วยสัญญาณเรดาร์ 3 ความถี่ และการวิเคราะห์ที่ต่อเนื่องในตะกอนพายุ ทั้ง 4 พื้นที่ศึกษานี้มีความแตกต่างในสภาพแวดล้อมการสะสมตัวรวมถึงระยะทางจากจุดที่พายุขึ้นฝั่ง การศึกษานี้เป็นการนำเสนอบันทึกของตะกอนพายุโซนร้อนซึ่งขึ้นฝั่งที่อ่าวไทยด้านตะวันตกในรอบ 57 ปี ผลการศึกษาสรุปได้ว่า ระยะห่างจากจุดที่พายุขึ้นฝั่งมีผลต่อความหนาและระยะสะสมตัวของตะกอนพายน้อยกว่าปัจจัยเชิงพื้นที่อื่นได้แก่ ระดับน้ำขึ้นสูงสุดของพื้นที่ ความสูงของคลื่นพายุคลื่นฝั่ง ความสูงคลื่นระดับความสูงของสันทราย โครงสร้างจากมนุษย์ และปริมาณตะกอนที่เข้ามาเติม (sediment supply) ตะกอนพายุโซนร้อนปาบึกมีขนาดตั้งแต่ทรายละเอียดมากถึงทรายหยาบมาก โดยมีองค์ประกอบหลักเป็นทรายขนาดปานกลาง การคัดขนาดแยกกว่าตะกอนพื้นเดิมที่อยู่ด้านล่าง มีลักษณะความหนาลดลงไปทางแผ่นดิน ความหนาสูงสุด 40 ซม. และความหนาเฉลี่ย 25-30 ซม. ตะกอนเหล่านี้สามารถแบ่งได้ 3 หน่วยซึ่งสะท้อนถึงการไหลของกระแส 3 รูปแบบ หน่วยตะกอน A เป็นชั้นของตะกอนขนาดละเอียดกว่าชั้นอื่นซึ่งวางตัวเป็นชั้นบางในแนวระดับแบบขนาน มีการวางชั้นแบบเรียงขนาดไม่ปกติ (reverse grading) ซึ่งสะสมตัวจากการเคลื่อนที่ของตะกอนแบบพัดพาบนพื้นที่ท้องน้ำในกระแสที่มีปริมาณตะกอนมากในระยะเริ่มต้นของพายุซึ่งมีพลังงานต่ำ หน่วยตะกอน B ซึ่งอยู่ตรงกลางมีขนาดตะกอนใหญ่กว่าชั้นอื่น ทั้งยังประกอบไปด้วยเปลือกหอยและเศษหอยขนาดใหญ่ โครงสร้างแบบชั้นเฉียงระดับจะพบอยู่ในชั้นนี้เท่านั้น เช่น ชั้นเฉียงแบบมุมต่ำ (3° - 9°) ไปจนถึงมุมสูง (20°) และเป็นทรายด้านน้ำ การเปลี่ยนแปลงโครงสร้างการวางตัวแบบแนวระดับไปสู่ชั้นเฉียงก็ปรากฏในชั้นนี้ด้วยเช่นกัน หน่วยตะกอนนี้สะสมตัวจากการเคลื่อนที่ของตะกอนแบบพัดพาบนพื้นที่ท้องน้ำในช่วงความรุนแรงสูงสุดหรือช่วงที่ระดับน้ำสูงที่สุด หน่วยตะกอน C ซึ่งอยู่ด้านบนสุดเป็นตะกอนละเอียดถึงเนื้อเดียว (semi massive) จนถึงชั้นบางซึ่งวางตัวในแนวระดับ มีการวางชั้นแบบเรียงขนาดปกติ (normal grading) เป็นส่วนใหญ่ โครงสร้างเหล่านี้สะท้อนถึงช่วงสุดท้ายของการเกิดน้ำท่วมของเหตุการณ์พายุซึ่งจะเอื้อให้ตะกอนค่อยๆ ตกสะสมตัว ชั้นโคลนบางซึ่งปิดทับด้านบนสุดก็สามารถพบได้เช่นกัน โครงสร้างทางตะกอนขนาดใหญ่บางชนิดไม่สามารถสังเกตได้จากหลุมตะกอน อย่างไรก็ตาม การสำรวจยังลึกลงด้วยสัญญาณเรดาร์สามารถช่วยตรวจสอบโครงสร้างเหล่านี้ได้เป็นอย่างดี เรดาร์ความถี่ 200 และ 400 เมกะเฮิรตซ์สามารถแสดงภาพที่ความลึก 5-6 ม. และ 2.5 ม. ตามลำดับ ในขณะที่เรดาร์ความถี่ 900 เมกะเฮิรตซ์ให้ภาพความละเอียดสูงที่สุดด้วยความลึก 75 ซม. จึงเหมาะกับตะกอนพายุซึ่งมีลักษณะดิน สามารถแบ่งสัญญาณภาพออกได้เป็นพื้นผิวสัญญาณ 3 รูปแบบ และชุดลักษณะสัญญาณ 7 ชุด สัญญาณดังกล่าวแสดงภาพโครงสร้างชั้นเฉียงเข้าไปทางแผ่นดินในตะกอนพายุของพื้นที่ทุ่งตะโกซึ่งไม่สามารถมองเห็นได้ในหลุมตะกอนขนาดแคบ นอกจากนี้ชั้นลาดแนวดินดอน (foreset bedding) ของพายุโบราณจากเหตุการณ์คลื่นซัดฝั่งในอดีตของพื้นที่แหลมตะลุมพุกก็สามารถตรวจเจอได้เช่นกัน ความหลากหลายของไดอะตอมในตะกอนพายุพบตั้งแต่ชนิดที่อาศัยอยู่ในทะเลและชนิดที่อาศัยอยู่ในน้ำจืดซึ่งปรากฏอย่างน้อย 22 ชนิด ไดอะตอมชนิดที่อาศัยอยู่ในน้ำจืดบ่งชี้ถึงเหตุการณ์ฝนตกหนักจนทำให้เกิดน้ำท่วมซึ่งเอ่อล้นมาจากแม่น้ำในพื้นที่

สาขาวิชา ธรณีวิทยา

ปีการศึกษา 2566

ลายมือชื่อนิสิต

ลายมือชื่อ อ.ที่ปรึกษาหลัก

ลายมือชื่อ อ.ที่ปรึกษาร่วม

6171932323 : MAJOR GEOLOGY

KEYWORD: Storm deposits, Tropical storm Pabuk, Gulf of Thailand (GOT), Ground Penetrating Radar, Diatom, Washover deposits, Storm surge

Chanakan Ketthong : SEDIMENTOLOGICAL CHARACTERISTICS OF STORM DEPOSITS INDUCED BY THE TROPICAL STORM PABUK ALONG THE WESTERN COAST OF THE GULF OF THAILAND. Advisor: Prof. MONTRI CHOOWONG, Ph.D. Co-advisor: Asst. Prof. SUMET PHANTUWONGRAJ, Ph.D.

Tropical storm Pabuk (TS-Pabuk) attacked the western coast of the Gulf of Thailand (W-GOT) on January 4th, 2019, generating high storm surge levels, high wave height and leaving washover sediments along the coastal areas. Soon after the storm, an initial survey was set up for 44 localions to described sedimentary characteristics, measured beach topography, hydrodynamic intensities and geomorphological conditions. Then, the 4 main locations including Chao Samran beach (CSR), Ban Thung Noi (BTN), Thung Tako (TTK), and Talumphuk (TLP) were selected to study sedimentary detail, ground penetrating radar (GPR) with 3 frequencies and diatom analysis on their storm deposits. These 4 locations vary in depositional environments and distances in ascending order to the landfall site. Here the first modern record of tropical storm deposits in Thailand landfalling on the W-GOT in the past 57 years is presented. The conclusion is that distance from landfall site has less influence than local factors; local high tide level, storm surge height, wave runup height, elevations of dune crest, artificial structure and sediments supply. The TS-Pabuk sediments range from very fine to very coarse sand with mainly medium sand, poorer sorted than the underlying original sediment, thinning landward, maximum thickness is 40 cm and average is 25-30 cm. They show at least 3 units reflecting 3 sets of flow. The lower unit A is planar horizontal laminations of finer grains with reverse grading that deposited in bedload transportation of grain flow during an initial stage of low energy. The middle unit B is coarser than others and contains much and large shell fragments and valves. Inclined structures can be found only in this unit such as low-angle (3°- 9°) to high-angle (20°) cross laminations and antidune. Lateral changing of horizontal structure to inclined structure was also observed. This unit was formed in bedload transportation during the peak intensity or maximum inundation level. The uppermost unit C is semi-massive to horizontal laminations of finer grain with normal grading in most locations. This reflects the late stage of the storm inundation regime allowing the sediments to settle down. Thin mud contents at the top are also presented. Some large sedimentary structures cannot be noticed. However, Ground penetrating radar (GPR) can solve this problem helpfully. The 200 and 400 MHz frequency provided 5-6 m and 2.5 m depth, respectively. Whereas, the 900 MHz GPR gave the best resolution with 75 cm depth which is suitable for shallow deposits of storm. GPR were classified into 3 radar surfaces and 7 radar facies. The signals provide landward inclined structure within storm deposits at TTK that was invisible in the narrow sediment pits. Moreover, foreset bedding of paleostorm from previous storm surge events at TLP was also captured. Diatom diversity ranging from marine to freshwater were identified at least 22 species. The freshwater diatoms indicate heavy precipitation that causes overbank river flooding.

Field of Study: Geology

Academic Year: 2023

Student's Signature

Advisor's Signature

Co-advisor's Signature

ACKNOWLEDGEMENTS

My sincere gratitude devoted to Professor Dr. Montri Choowong, thesis advisor and Assistant Professor Dr. Sumet Phantuwongraj, co-advisor for supporting all processes of my study life since undergraduate to Ph.D. Thank you for supporting my fieldworks, collecting samples, reshaping my ideas, commenting, giving feedback and managing the exchange laboratory works in Japan until the Ph.D. thesis was finished very well.

My appreciation also extended to Associate Professor Dr. Fujino Shigehiro and Professor Dr. Ken-Ishiro Hisada from Faculty of Life and Environmental Sciences, University of Tsukuba, for my laboratory work (grain size analysis) and all experiences as a one-year exchanged students in Japan and Dr. Yuki Swai from National Institute of Advanced Industrial Science and Technology (AIST), Japan for diatom knowledges. Professor Dr. Punya Charusiri, Associate Professor Dr. Thanop Thitimakorn for GPR work, Assistant Professor Dr. Vichai Chutakositkanont, Professor Dr. Santi Pailoplee for mental health supportive during my severe time, Associate Professor Dr. Thasinee Charoentitirat for microfossils, all teachers and staffs in Department of Geology, Chulalongkorn University, as well as the 100th Anniversary of Chulalongkorn University and the 90th Anniversary of Chulalongkorn University Fund for financial support.

Fieldworks cannot be accomplished without Dr. Peerasit Surakiatchai, Dr. Stapan Kongsan, Dr. Sirawat Udomsak, Ms. Chanista Chansom and Mr. Pitipat Punsap.

Thanks to all friends in department of Geology for research advice and all fruitful vibe in my study life.

Lastly, my heartfelt appreciation goes to my aunt and my love who standing by me when I was overcoming the hard times. Your sympathy and best wish encouraged me to complete my duties “steadily as the beating drum”.

Chanakan Ketthong

TABLE OF CONTENTS

	Page
ABSTRACT (THAI)	iii
ABSTRACT (ENGLISH)	iv
ACKNOWLEDGEMENTS	v
TABLE OF CONTENTS	vi
LIST OF TABLES.....	x
LIST OF FIGURES.....	xii
CHAPTER 1 INTRODUCTION	24
1.1 Rationale (Pabuk importance).....	24
1.2 Study Area.....	25
1.3 Objectives	27
1.4 Output.....	27
1.5 Methodology	27
1.5.1 Collecting samples and sedimentary analysis.....	28
1.5.2 Ground Penetrating Radar (GPR).....	31
1.5.3 Topographic survey and Hydrodynamic parameters	34
CHAPTER 2 LITERATURE REVIEW.....	35
2.1 Paleotempestology.....	35
2.2 Regional of washover deposits.....	36
2.2.1 Overwash regimes.....	36
2.2.2 Beach morphology changes.....	38

1) Erosional features.....	38
2) Depositional features	38
2.2.3 Sedimentary characteristics of washover sediments	40
2.3 Analytical techniques for washover sediments.....	45
2.3.1 Grain size analysis	45
1) Sieving	45
2) Sedimentation or Settling	46
3) Laser Diffraction Analysis (Mastersizer)	46
4) Digital image analysis (Camsizer)	47
2.3.2 Microfossil analysis	47
2.3.3 Ground Penetrating Radar (GPR).....	52
2.4 Washover deposits in Thailand.....	55
CHAPTER 3 HYDRODYNAMIC CONDITIONS AND WASHOVER MORPHOLOGY.....	59
3.1 Hydrodynamic conditions	59
3.1.1 Wind speeds.....	60
3.1.2 Wave height.....	60
3.1.3 Tidal range and inundation in the GOT	60
3.2 Damages and erosional features	63
3.3 Washover Morphology	67
3.3.1 Surface morphology	67
3.3.2 Sedimentary structures.....	69
CHAPTER 4 STORM DEPOSITS AND MICROFOSSILS.....	73
4.1 Storm Deposits	73
4.1.1 Chao Samran Beach (CSR)	73

1) Proximal zone (A).....	75
2) Middle zone (B).....	75
3) Near distal zone (C)	76
4) Distal zone (D).....	80
5) Ripple zone (E).....	81
4.1.2 Ban Thung Noi (BTN).....	83
4.1.3 Thung Tako (TTK).....	89
4.1.4 Talumphuk (TLP).....	95
4.2 Microfossils in storm deposits.....	100
CHAPTER 5 GROUND PENETRATING RADAR.....	105
5.1 Radar Surfaces and Radar Facies.....	106
5.2 Ban Thung Noi (BTN).....	109
5.3 Thung Tako (TTK).....	110
5.4 Talumphuk (TLP).....	115
CHAPTER 6 DISCUSSIONS.....	120
6.1 Hydrodynamic conditions in ascending order to distances from landfall site	120
6.1.1 Storm intensity and inland extent of washover deposits.....	120
6.1.2 Thickness of storm deposits.....	122
6.2 Characteristics of Tropical storm deposits and flow conditions.....	123
6.2.1 Three dominant stratigraphies of event deposits in trench scale.....	124
6.2.2 Horizontal variation of storm deposits in transect scale	127
6.3 Local geomorphological controlling factors, storminess regime and storm deposits.....	128
6.4 Comparison of Pabuk and other modern storm deposits.....	132

6.5 GPR for shallow deposits induced by storm and possible paleostorms captured by 900 MHz frequency GPR.....	137
CHAPTER 7 CONCLUSIONS.....	139
REFERENCES.....	143
VITA.....	152



LIST OF TABLES

	Page
Table 1.1 Summary table of analysis technique using for each transect line in 4 areas; CSR, BTN, TTK and TLP.....	31
Table 2.1 Comparison of geomorphic setting, washover type, flow condition, and sedimentary characteristic in washover deposits induced by monsoons and low pressure systems from many locations in the western coast of the Gulf of Thailand (Phantuwoongraj et al., 2013).....	41
Table 2.2 Comparison of local geomorphic setting, hydrodynamic conditions and sedimentary textures and structures of Typhoon Haiyan deposits in many locations of Philippines coasts (Soria et al., 2017).	43
Table 2.3 Comparison of local setting, meteorology, hydrodynamic conditions and sedimentary signatures in transect and trench scale of the Typhoon Haiyan and other recent storms of comparable intensity (Soria et al., 2017).	43
Table 2.4 Particle size ranges with optimal analytical techniques. (López, 2016)	47
Table 3.3.1 Summary of morphology setting, depositional and erosional features, sedimentary structures and inundation detail from each surveying sites. (PF: Perched Fan, WT: Washover Terrace, * Wind blowing from land to sea, Site 1 = Songkhla, Site 2-13 = Nakhon Si Thammarat, Site 14-17 = Suratthani, Site 18-31 = Chumphon, Site 32-41 = Prachuap Khiri Khan and Site 42-44 = Phetchaburi).....	65
Table 4.1 Summary of diatom species found in BTN, TTK and TLP areas.	102
Table 5.1 Summary table of GPR frequencies used in this research, depth (m), horizontal resolution (cm) and internal structures found in each frequency.	119
Table 6.1 Meteorology, hydrology and sedimentary characteristics of TS-Pabuk deposits and Typhoon Haiyan, Cyclone Yasi and Hurricane Ike.	135
Table 6.2 Meteorology, hydrology and sedimentary characteristics of TS-Pabuk deposits and Cyclone Sidr, Typhoon Durian, Hurricane Rita and Isabel.	136

Table 7.1 Summary of storm deposits from the tropical storm Pabuk at CSR, BTN,
TTK and TLP..... 142



LIST OF FIGURES

	Page
Figure 1.1 Map showing tracts of recent tropical cyclones made landfall at the western coast of the Gulf of Thailand (TS: Tropical Storm, T: Typhoon) (modified from Williams et al., 2016 and Kongsen et al., 2021).....	25
Figure 1.2 Study area (a) Location of the western coast of the Gulf of Thailand (W-GOT) (b) Satellite image showing the W-GOT and surveying point (yellow circles) and the 4 main study sites (red square) including CSR, BTN, TTK and TLP (c) Photos of washover deposits induced by the TS-Pabuk found in the 4 main study sites.....	26
Figure 1.3 Flow chart of methodology using for this research.....	28
Figure 1.4 Images illustrate the process of collecting sediment samples. (a) Several shallow pits were excavated in a transect line perpendicular to the shore. The pits are about 50 cm width. (b) Collecting layer-by-layer sediment samples for grain size analysis. (c) Weighting sediment samples for 1 g before wet sieve (d) 63 μm sieve mesh for wet sieve technique and (e) Camsizer for grain size analysis.....	29
Figure 1.5 Diatom analysis using detergent solution for step 1.....	30
Figure 1.6 Process of collecting GPR data. (a) Dragging GPR antenna on the surface of washover lobes to collect GPR signals. (b) GPR profile signal recorded from the field that was processed by RADAN 6.0 software.....	32
Figure 1.7 Example of processing GPR raw data from TTK-1 900 MHz signals. (a) raw data (b) after position correction (c) after elevation adjustment (d) after stacking and (e) after gaining.....	33
Figure 2.1 Model showing variables used in scaling the impact of storms on beach barrier. R_{high} and R_{low} represent elevations of swash. D_{high} and D_{low} represent elevations of dune. (Sallenger, 2000).....	37

Figure 2.2 Schematic illustration of the Four storminess regimes developed under the conceptual model of Sallenger (2000) consisting of swash, collision, overwash and inundation (Goslin & Clemmensen, 2017).....	37
Figure 2.3 Erosional and depositional features induced by storms including a. Dune Erosion, b. Channel Incision, c. Washout, d. Perched Fans, e. Washover Terrace and f. Sheetwash Lineations. (Morton & Sallenger, 2003).....	39
Figure 2.4 Cross-shore topography and beach ridge configurations parallel to shoreline of three areas; BT, LT and MR that control washover types. (a) A uniform beach configuration with large back-ridge swale inducing washover terrace at BT area. (b) A non-uniform beach configuration with flat and high coastal plain inducing perched fan at LT area. (c) A non-uniform beach configuration with low-lying tidal floodplain inducing sheetwash lineation superimposed by perched fan at MR area. (Phantuwongraj et al., 2013).....	40
Figure 2.5 (a) Washover deposits induced by 2010 NE monsoon at Laem Talumphuk, Thailand. (b) Illustrated image of the deposits showing two sediment units and thin organic layer at distal part between the two units. (c) Thin organic layer. (d) Shell base of unit 2 and (e) Normal grading in both units (Phantuwongraj et al., 2013).....	41
Figure 2.6 (a) Sediment units of Typhoon Haiyan deposits in Philippines overlie pre-Haiyan unit with sharp contact. unit 1 is magnetite-rich medium sand with coarsening upward trends and unit 2 is light grey coarse sand with fining upwards trend (Soria et al., 2017). (b) Haiyan deposits showing massive sand of unit 1 and laminated sand of unit 2 (Brill et al., 2016).....	42
Figure 2.7 Sedimentary characteristics of tsunami and storm deposits. (Morton et al., 2007).....	45
Figure 2.8 Mollusca and foraminifera found in washover deposits induced by NE monsoon and low-pressure system during the years 2007 to 2011 in the Gulf of Thailand coast. a) <i>Cerithidea cingulate</i> . b) <i>Siliquaria</i> . c) <i>Natica</i> . d) <i>Pseudoneptunea varicose</i> . e) <i>Nuculana (Thestyleda) soyoae</i> . f) <i>Vepricardium</i> . g)	

Anadara. h) <i>Antalis dentalis</i> . i) <i>Antalis vulgaris</i> . j) <i>Elphidium crispum</i> . (Phantuwongraj, 2012)	49
Figure 2.9 An example of microfossil assemblage changes in Typhoon Haiyan deposits in Philippines (Basey). (a) Elevation profile, sampling locations (black circle) and washover thickness. (b) Presence of testate amoebae (freshwater organisms), calcareous and agglutinated foraminifera (intertidal and marine organisms). (c) Foraminifera's concentration per 5 cm ³ . (d,e) Abundances of dominant foraminifera species. (f) Taphonomic condition of calcareous foraminifera. (g) Abundances of small and large tests. (Pilarczyk et al., 2016)	50
Figure 2.10 Fossil diatom assemblages of core B-1 induced by the Cyclone Sidr from Kuakata coast, Bangladesh (Haque et al., 2021).	51
Figure 2.11 An example of 500 MHz GPR reflection showing contacts between tsunami, paleotsunami and non-tsunami layers. (Gouramanis et al., 2015)	53
Figure 2.12 The 250 MHz GPR signals and interpretation of BP area located at the northern part of Florida and confronting Ivan (2004) and Dennis (2005) Hurricane. The GPR profile shows truncated dune, subhorizontal stratification, inclined tabular foresets formed when washover prograded into the bay on the land, water table (wt) and radar surface interpreted as the base of Hurricane Ivan deposits (lv). (Wang & Horwitz, 2007)	54
Figure 2.13 An example of 100 MHz antennas frequency GPR profile on the Bay-Bay Spit, Bicol, Central Philippines. Red lines show erosional surfaces induced by Typhoon Durian and Pre-Durian events. Yellow lines are interpreted as beach progradation. Green lines represent overwash deposits and the continuous blue line is water table. (Pile et al., 2016)	55
Figure 2.14 Tracks of recent tropical cyclones landfalling in the Gulf of Thailand. (Williams et al., 2016)	57
Figure 2.15 Map showing track and intensity of the tropical storm Pabuk on the 4 th of January 2019 (Wikipedia, 2019)	58

Figure 3.1 (a) Wind speeds and (b) wave height during an arrival of the tropical storm Pabuk from January 2nd to 6th, 2019 obtained from WRF-ROMS (Thaigeo) model (Hydro-Informatics Institute Thailand, 2019). (c) Predicted and recorded tidal level above mean tide level (MTL) recorded by the Royal Thai Navy.....59

Figure 3.2 Example of predicted tide (broken red line) and recorded tide (solid blue line) from Chumphon tide gauge station (CP) showing high tide level in normal condition and recorded high tide level that is significantly higher than usual at the midday of January 5th, 2019 which is an effect of the TS-Pabuk. The difference between normal high tide and recorded tide is storm surge height, while the combination of them is storm tide level.....61

Figure 3.3 The tropical storm Pabuk track (red line), the 44 initial surveying sites (black dot) and the 7 tide gauge stations (red triangle) along the Gulf of Thailand (GOT) supported by the Marine Department (2019) and Hydrographic Department (2019) of the Royal Thai Navy including 5 stations from the western GOT; Nakhon Si Thammarat (NST), Chumphon (CP), South-Prachuap Khiri Khan (S-PKK), North-Prachuap Khiri Khan (N-PKK), Samut Songkhram (SS) and from the eastern GOT; Chonburi (CB) and Rayong (RY).....62

Figure 3.4 (a), (c) and (d) Knocked down trees at Nakhon Si Thammarat and Chumphon. (b) Washover sediments covering local road were partly cleared out at Laem Talumphuk, Nakhon Si Thammarat. (e) and (f) Knocked down electric pole at Laem Talumphuk.63

Figure 3.5 a), (b) and (c) Beach scarp Chumphon, Prachuap Khiri Khan and Nakhon Si Thammarat with the maximum height of about 80 cm. (d) Heavy mineral at Nakhon Si Thammarat. (e) and (g) mud rip-up clasts on sand beaches at Chumphon. (f) Mud rip-up clast at muddy beaches in Prachuap Khiri Khan.64

Figure 3.6 a), (b) and (c) Washover terrace at sites 12, 23 and 19, respectively. (d), (e), (f), (g) and (h) perched fans at sites 20, 39, 22, 17 and 16, respectively.68

Figure 3.7 (a) Linguoid current ripple at Nakhon Si Thammarat (site 5). (b) Sinuous current ripple at Phetchaburi (site 44). (c) Straight to sinuous current ripple on

pre-Pabuk mud and Pabuk sand (site 44). (d) Straight current ripple at Nakhon Si Thammarat (site 6). (e), (f) and (g) Truncation sediment lobes at Phetchaburi (site 44). (h) A unique current ripple on the surface of younger truncating lobes.....70

Figure 3.8 (a) Stratification at Nakhon Si Thammarat, erosional base was overlaid by shelly thick bed and horizontal sediment laminations overtopped by inclined laminations dipping landward of much shell sediments and less shell sediments. (b) Stratification at Prachuap Khiri Khan, sharp contact located at the base overlaid by sub-horizontal bed of sands. Inclined laminations dipping landward located as a middle layer and overtopped by horizontal laminations. (c) Foreset bedding at a pond near river mouth in Chumphon. The inclined bed deposited on a sloping surface and dip landward into the pond. (d) Stratification at Nakhon Si Thammarat, this picture was looked into the land. The contact between Pabuk469 and Pre-Pabuk does not notable but the sequence start with thick planar laminations and overlaid by the inclined laminations dipping to the south. (e) Stratification at Prachuap Khiri Khan showing only sharp contact and planar laminations. (f) Three distinct layers at Phetchaburi, sub-horizontal bed over a sharp contact, cross laminations and overtopped again by horizontal laminations.....71

Figure 4.1 Chao Samran Beach (CSR) at Phetchaburi province, western coast of the Gulf of Thailand (a) Satellite images showing washover terrace along the coast with 2 offshore breakwater and studied transect line (A-A') (b) Washover terrace with ripple zone at the distal landward part (c) Current ripple found at distal part of storm deposits (d) Topography of transect line with mean tide level (MTL), high tide level (HT), storm surge level and storm tide above mean tide level in meters (e) positions of pit number 1 to 5 (from landward to seaward) and 12 stratigraphic logs of storm deposits from proximal part (CSR-5), middle part (CSR-4), near distal part (CSR-3.1 to 3.5), distal part (CSR-2.1 to 2.2) and ripple zone (CSR-1.1 to 1.3) though the length of 16 m inland extent. The vertical scale is depth in cm, while horizontal scale is grain size in phi (ϕ) scale.74

Figure 4.2 Sedimentological characteristics of TS-Pabuk deposits (yellow part) and pre-Pabuk (brown part) at CSR in proximal part (CSR-5) and middle part (CSR-4) showing mud content (%), mean grain size, sorting, skewness and kurtosis. CSR-5 shows fining upward trend with a thin layer of coarse sand capping at the surface. CSR-4 was organized as 3 distinct layers of unit 1 (coarsening upward), unit 2 (largest grain size and poorest sorted) and unit 3 (fining upward). The vertical scale is depth in cm, while horizontal scale is grain size in phi (ϕ) scale.76

Figure 4.3 Sedimentological characteristics of TS-Pabuk deposits (yellow part) and pre-Pabuk (brown part) at CSR in near distal part (CSR-3.1 to 3.5) located far from the landward avalanched face for about 4 m. (a) photo of near distal part of 100 cm lengths with the sampling position (red triangle on the horizontal scale). The cross laminated angles (broken red line) are steeper landward from 9° to 20°. (b) sedimentological characteristics of 5 sampling points including mud content (%), mean grain size, sorting, skewness and kurtosis. This part presented the 3 units pattern of storm deposits including the lower unit 1, the middle unit 2 with cross-lamination and the upper unit 3. Coarsening upward at base and fining upward at top are clearly presented. The vertical scale is depth in cm, while horizontal scale is grain size in phi (ϕ) scale.79

Figure 4.4 Sedimentological characteristics of TS-Pabuk deposits (yellow part) and pre-Pabuk (brown part) at CSR in distal part (CSR-2.1 to 2.2) and ripple zone (CSR-1.1 to 1.3) showing mud content (%), mean grain size, sorting, skewness and kurtosis. The vertical scale is depth in cm, while horizontal scale is grain size in phi (ϕ) scale.82

Figure 4.5 Ban Thung Noi (BTN). (a) Location of BTN in Prachuap Khiri Khan province, Western coast of the Gulf of Thailand. (b) BTN located at between the 2 Permian limestone headlands. (c) Satellite images of BTN on 2017 January, 24th before an arrival of TS-Pabuk. (d) Satellite images of BTN on 2019 February, 24th after TS-Pabuk made landfall at Nakhon Si Thammarat on 2019 January, 4th.83

Figure 4.6 Pit BTN-1.2. (a) a photo of open pit with 80 cm width. The Pabuk sediments was classified into 2 subunits; U1A, U1B and Unit 2 lying above pre-Pabuk sediments with sharp erosional surface. (b) sedimentary characteristics of BTN-1.2 including mud contents (%), mean grain size, sorting, skewness and kurtosis. The vertical scale is depth in cm, while horizontal scale is grain size in phi (ϕ) scale.85

Figure 4.7 Sedimentological characteristics of TS-Pabuk deposits (yellow part) and pre-Pabuk (brown part) at BTN line 1 with 4 pits (BTN-1.1 to 1.4) showing mud content (%), mean grain size, sorting, skewness and kurtosis. The vertical scale is depth in cm, while horizontal scale is grain size in phi (ϕ) scale.86

Figure 4.8 Sedimentological characteristics of TS-Pabuk deposits (yellow part) and pre-Pabuk (brown part) at BTN line 2 with 6 pits (BTN-2.1 to 2.6) showing mud content (%), mean grain size, sorting, skewness and kurtosis. The vertical scale is depth in cm, while horizontal scale is grain size in phi (ϕ) scale.87

Figure 4.9 Sedimentological characteristics of TS-Pabuk deposits (yellow part) and pre-Pabuk (brown part) at BTN line 3 with 7 pits (BTN-3.1 to 3.7) showing mud content (%), mean grain size, sorting, skewness and kurtosis. The vertical scale is depth in cm, while horizontal scale is grain size in phi (ϕ) scale.88

Figure 4.10 Thung Tako (TTK). (a) Location of TTK in Chumphon province, Western coast of the Gulf of Thailand. (b) BTN located semi-bay beach open to the sea. (c) Satellite images of TTK on 2017 September, 9th before an arrival of TS-Pabuk showing mudflat, narrow beach and swale between the beach and main road. (d) Satellite images of TTK on 2019 February after TS-Pabuk made landfall at Nakhon Si Thammarat on 2019 January, 4th showing an intrusion of storm deposits into the back-beach environments (large swale).89

Figure 4.11 Sedimentological characteristics of TS-Pabuk deposits (yellow part) and pre-Pabuk (brown part) at TTK line 1 with 6 pits (TTK-1.1 to 1.6) showing mud content (%), mean grain size, sorting, skewness and kurtosis. The vertical scale is depth in cm, while horizontal scale is grain size in phi (ϕ) scale.92

- Figure 4.12 Sedimentological characteristics of TS-Pabuk deposits (yellow part) and pre-Pabuk (brown part) at TTK line 2 with 5 pits (TTK-2.1 to 2.5) showing mud content (%), mean grain size, sorting, skewness and kurtosis. The vertical scale is depth in cm, while horizontal scale is grain size in phi (ϕ) scale.....93
- Figure 4.13 Sedimentological characteristics of TS-Pabuk deposits (yellow part) and pre-Pabuk (brown part) at TTK line 3 with 6 pits (TTK-3.1 to 3.5) showing mud content (%), mean grain size, sorting, skewness and kurtosis. The vertical scale is depth in cm, while horizontal scale is grain size in phi (ϕ) scale.....94
- Figure 4.14 Talumphuk (TLP). (a) Location of TLP in Nakhon Si Thammarat province, Western coast of the Gulf of Thailand where is a bit north of the TS-Pabuk landfall location. (b) TLP located near the tip part of Laem Talumphuk cape sand spit. (c) Satellite image of TLP on 2018 September, 18th before an arrival of TS-Pabuk showing narrow sand beach and previous washover deposits invading into shrimp ponds between beach and main road. (d) Satellite image of TLP on 2020 April, 11st after TS-Pabuk made landfall on 2019 January, 4th. The presence of Pabuk sediments in this image is unclear because the land surface was disturbed more than in fieldwork which were finished within 2019.....95
- Figure 4.15 Satellite images of TLP from 2000 to 2020 showing at least 2 overwash events during 2000 to 2009 and 2009 to 2012 before the 2019 TS-Pabuk event. The 1st event during 2000 to 2009 caused small amount of sediment invaded the shrimp ponds along the coast. The 2nd event during 2009 to 2012 caused a huge amount of sand overflowing into the ponds. The last event was the 2019 TS-Pabuk that allowed sediments to deposit on top of the previous washover deposits.....97
- Figure 4.16 Sedimentological characteristics of TS-Pabuk deposits (yellow part) and pre-Pabuk (brown part) at TLP line 1 with 6 pits (TLP-1.1 to 1.6) showing mud content (%), mean grain size, sorting, skewness and kurtosis. The vertical scale is depth in cm, while horizontal scale is grain size in phi (ϕ) scale.....98

Figure 4.17 Sedimentological characteristics of TS-Pabuk deposits at TLP line 2 with 6 pits (TTK-2.1 to 2.6) showing mud content (%), mean grain size, sorting, skewness and kurtosis. However, the deposits in this line cannot be differentiated from the original sediments both in naked eye from pit walls and in sedimentological parameters. The vertical scale is depth in cm, while horizontal scale is grain size in phi (ϕ) scale.99

Figure 4.18 Pit TLP-1.2. (a) a photo of open pit with 110 cm width. The Pabuk sediments was classified into 4 subunits; U1A, U1B, U1C and U2 lying above pre-Pabuk sediments with sharp erosional surface. U1A, U1B and U1C are horizontally organized with different grain size and sorting, whereas the U2 is 6° to 7° landward inclined laminations. (b) sedimentary characteristics of TLP-1.2 including mud contents (%), mean grain size, sorting, skewness and kurtosis. The vertical scale is depth in cm, while horizontal scale is grain size in phi (ϕ) scale. ... 100

Figure 4.19 Diatoms found in storm (TS-Pabuk) deposits in BTN, TTK and TLP including 9 Marine species: *Coscinodiscus radiatus*, *Lyrella hennedyi*, *Lyrella spectabilis*, *Odontella aurita*, *Odontella sp.*, *Paralia fenestrata*, *Paralia sp.*, *Thalassionema nitzschioides* and *Trachyneis sp.*, 5 Brackish to marine species: *Cyclotella litoralis*, *Diploneis weissflogii*, *Fallacia forcopata*, *Grammatophora oceanica* and *Tryblionella granulate* and 2 Freshwater to brackish species: *Luticola mutica* and *Luticola sp.*..... 103

Figure 4.20 Diatoms found in storm (TS-Pabuk) deposits in BTN, TTK and TLP including 1 Freshwater specie; *Hantzschia amphioxys*, 2 Freshwater to marine species: *Navicula sp.* and *Nitzschia sp.* and 3 Unknown habitat species; *Coscinodiscus or Thalassiosira sp.*, *Naviculaceae sp.* and *Pinnuavis (?) sp.*..... 104

Figure 5.1 (A) The western coast of the Gulf of Thailand showing study sites including BTN in Prachuap Khiri Khan, TTK in Chumphon and TLP in Nakhon Sri Thammarat (red dot). (B) GPR line transect perpendicular to the shore with 1 line ant BTN, 3 lines at TTK and 2 lines at TLP. (C) Washover deposits found at back dune environments on the coastal area in BTN, TTK and TLP. 106

Figure 5.2 Radar Surface (RS) and Radar facies (RF). Radar image from 900 MHz antenna, reflection tracing, description and interpretation.....	108
Figure 5.3 GPR profile of BTN-1 from 3 frequencies; 200, 400 and 900 MHz (a) 200 MHz profile with about 5 m depth (b) 400 MHz profile with about 2.5 m depth (c) 900 MHz with almost 75 cm depth and (d) 900 MHz with interpretation of TS-Pabuk deposits (yellow area) and sedimentary logs from 4 shallow pits (BTN-1.1 to 1.4).....	110
Figure 5.4 GPR profile of TTK-1 from 3 frequencies; 200, 400 and 900 MHz (a) 200 MHz profile with about 5 m depth (b) 400 MHz profile with about 2.5 m depth (c) 900 MHz with almost 75 cm depth and (d) 900 MHz with interpretation of TS-Pabuk deposits (yellow area) and sedimentary logs from 6 shallow pits (TTK-1.1 to 1.6).....	112
Figure 5.5 GPR profile of TTK-2 from 3 frequencies; 200, 400 and 900 MHz (a) 200 MHz profile with about 5 m depth (b) 400 MHz profile with about 2.5 m depth (c) 900 MHz with almost 75 cm depth and (d) 900 MHz with interpretation of TS-Pabuk deposits (yellow area) and sedimentary logs from 5 shallow pits (TTK-2.1 to 2.5).....	113
Figure 5.6 GPR profile of TTK-3 from 3 frequencies; 200, 400 and 900 MHz (a) 200 MHz profile with about 5 m depth (b) 400 MHz profile with about 2.5 m depth (c) 900 MHz with almost 75 cm depth and (d) 900 MHz with interpretation of TS-Pabuk deposits (yellow area) and sedimentary logs from 5 shallow pits (TTK-3.1 to 3.5).....	114
Figure 5.7 GPR profile of TLP-1 from 3 frequencies; 200, 400 and 900 MHz (a) 200 MHz profile with about 5 m depth (b) 400 MHz profile with about 2.5 m depth (c) 900 MHz with almost 75 cm depth and (d) 900 MHz with interpretation of TS-Pabuk deposits (yellow area) and sedimentary logs from 6 shallow pits (TLP-1.1 to 1.6).....	117
Figure 5.8 GPR profiles of TLP-2 from 3 frequencies; 200, 400 and 900 MHz (a) 200 MHz profile with about 5 m depth (b) 400 MHz profile with about 2.5 m	

- depth (c) 900 MHz with almost 75 cm depth and (d) 900 MHz with interpretation of underlying structures and sedimentary logs from 6 shallow pits (TLP-2.1 to 2.6). However, the TS-Pabuk deposits cannot be identified in this location both in the field shallow pit walls and in the sedimentological analysis logs..... 118
- Figure 6.1 The intensity of storm events (water height) is the combination between high tide, storm surge height and wave height 120
- Figure 6.2 Schematic model of washover terrace generated during inundation regime (a) Storm tide level and wave runup at Phetchaburi compared with beach topography generated washover terrace behind the ridge (b) inundation regime that the water level is higher than beach ridge and fully cover back-barrier environment causing washover terrace (Goslin & Clemmensen, 2017)..... 121
- Figure 6.3 Pak Khlong Taling channel inlet (site 19) at Tha Chana district, Suratthani (a) satellite image of the channel and surrounded environments (b) the channel lying parallel to the shore and beach ridge with the inlet that were covered by washover deposits after the TS-Pabuk event (c) photo of washover perched fan penetrated into the channel for 45 m distances with average 30 cm depth. 122
- Figure 6.4 Schematic model showing patterns of sediment stratification at distal part, near distal to middle to near proximal and proximal part of the TS-Pabuk deposits. Unit A is horizontal lamination of fine grains which always found at base of the storm deposits and over the sharp erosional surface. Unit B is massive coarse grain layer with or without landward inclined stratification. Unit C is semi-massive layer of fine grains. 127
- Figure 6.5 Details of transect TTK-1 (a) a satellite image showing storm deposits along the coastal area of TTK where are mudflat environments with swale behind beach ridge along the shore (b) washover terrace invading coastal area (c) beach topography cross-section (A-A') with mean tide level (MTL), high tide level (HT) and storm tide lever at 1.7 m above mtl..... 129

- Figure 6.6 Details of transect BTN-1 (a) a satellite image showing storm deposits along the coastal area of BTN with the inundation limit line (b) inundation zone (brown grass) separated from non-inundation zone (green grass) (c) washover perched fan penetrating into the coastal area within inundation zone (d) beach topography cross-section (A-A') showing steep slope of the beach with mean tide level (MTL), high tide level (HT) and storm tide level of 1.6 m above mtl. 130
- Figure 6.7 Details of transect TLP-1 (a) a satellite image showing the TS-Pabuk deposits over old deposits along the coastal area of TLP where (b) washover perched fan behind artificial seawall (c) beach topography cross-section (A-A') with mean tide level (MTL), high tide level (HT) and storm tide level at 1.5 m above mtl. 132
- Figure 6.8 Foreset stratification and horizontal lamination in washover deposits (a) GPR signal from 900 MHz antenna at TLP-2 of this study (b) schematic cross-section through washover fans deposited into standing water and cause delta foreset stratification at the landward edge of fans (c) schematic cross-section through washover fans resulting from flow across a subaerial surface showing horizontal stratification. Details of numbers and all marks in (b) and (c) are shown in (Schwartz, 1975)..... 138
- Figure 7.1 Summary details of three dominant stratigraphy of the TS-Pabuk deposits in trench scale (vertical) with depositional conditions (interpretation)..... 141

CHAPTER 1

INTRODUCTION

1.1 Rationale (Pabuk importance)

Washover deposits are one proxy commonly used to identify palaeostorms. They are generated when waves overtop barrier beaches and bring sediments from seaward side to deposit in back-barrier environments. However, washovers may be caused by other high intensity events such as strong monsoon and tsunami. Nowadays, the differentiation of storm and tsunami deposits is still questionable because their criteria are indistinct. To be better understand in sediments left by storms, recent storm deposits should be studied both regional and local scale.

Thailand have been attacked by several storms over about last 70 years. However, only few geological reports were published. Two studies (Kongsen, 2016; Williams et al., 2016) were set up for palaeostorm deposits and other studied recent sediment induced by strong monsoon (Phantu Wongraj, 2012; Sumet Phantu Wongraj et al., 2008; Phantu Wongraj et al., 2013). The tropical storm Pabuk which made landfall on 4th January 2019 at Nakhon Si Thammarat coast is the latest one of intense storms in Thailand. Their sedimentological characteristics can be modern analogues for evaluating palaeostorms in this region.

This study aims to analyze sedimentological characteristics of Pabuk deposits from different geological settings along with ground penetrating radar (GPR). Preservation areas of washover deposits are also determined. Study areas are located on the western coast of the gulf of Thailand. Four main sites are at Nakhon Si Thammarat where the eye of storm made landfall, Chumphon, Prachuap Khiri Khan and Phetchaburi.

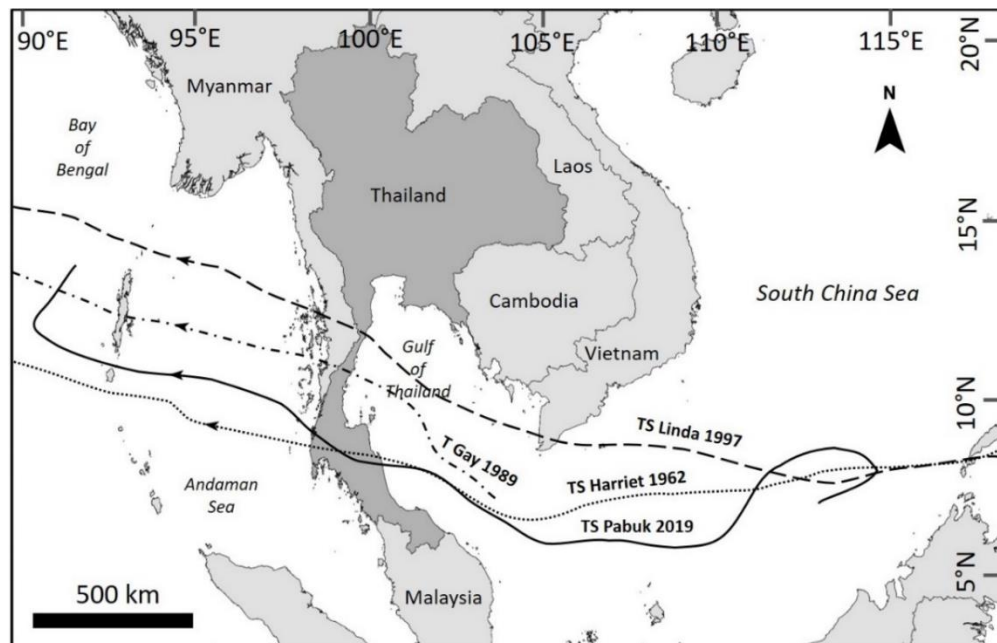


Figure 1.1 Map showing tracks of recent tropical cyclones made landfall at the western coast of the Gulf of Thailand (TS: Tropical Storm, T: Typhoon) (modified from Williams et al., 2016 and Kongsen et al., 2021)

1.2 Study Area

Gulf of Thailand (GOT) is located at the eastern side of the Thai-Malay peninsula which is oriented roughly north-south between Indian and South China Sea (SCS). The western coast of GOT was attacked by the tropical storm Pabuk in 2019. This storm is a cyclone developing in the South China Sea (SCS) before moving to the Gulf of Thailand (GOT). The storm sustained maximum wind speeds of 80 km/h during making landfall at Pak Phanang coast of Nakhon Si Thammarat, Thailand on January 4th, 2019. Pabuk generated ~5 m maximum wave heights near the landfall site which cause storm surge along the western coast of the Gulf of Thailand. In general, the effect of storm wave and tidal level is relieved in descending order to distances from the landfall site.

The study on four specific sites are focused, CSR, BTN, TTK and TLP (Figure 1.2), where the washover deposits were found to be well preserved (Figure 1.2c). All four locations are in descending order to the distance from landfall location of TS-Pabuk from south to north. CSR is located at the innermost part of the Gulf of

Thailand which experienced least hydrodynamic conditions such as windspeeds and wave heights during the storm event. The coast is also protected by several artificial offshore breakwaters. The sandy shore lies straightly between 2 canals in the northern and southern part. BTN is a pocket sand beach between two headlands located a bit southward from CSR. The headlands consist of Permian limestone interbedded shale, phyllitic shale, sandstone and siltstone with Quaternary beach sand lying between them. TTK is semi-bay of mudflat with very gentle slope (less than 0.01) located at the central part of the W-GOT. TLP is the nearest location to the landfall site of the storm's eye. This beach experienced the most intense hydrodynamic conditions during surge. Although there are 1.4 m height seawall along the shore to prevent coastal erosion problem, storm surge can come across them and left washover sediments on the back beach environments.

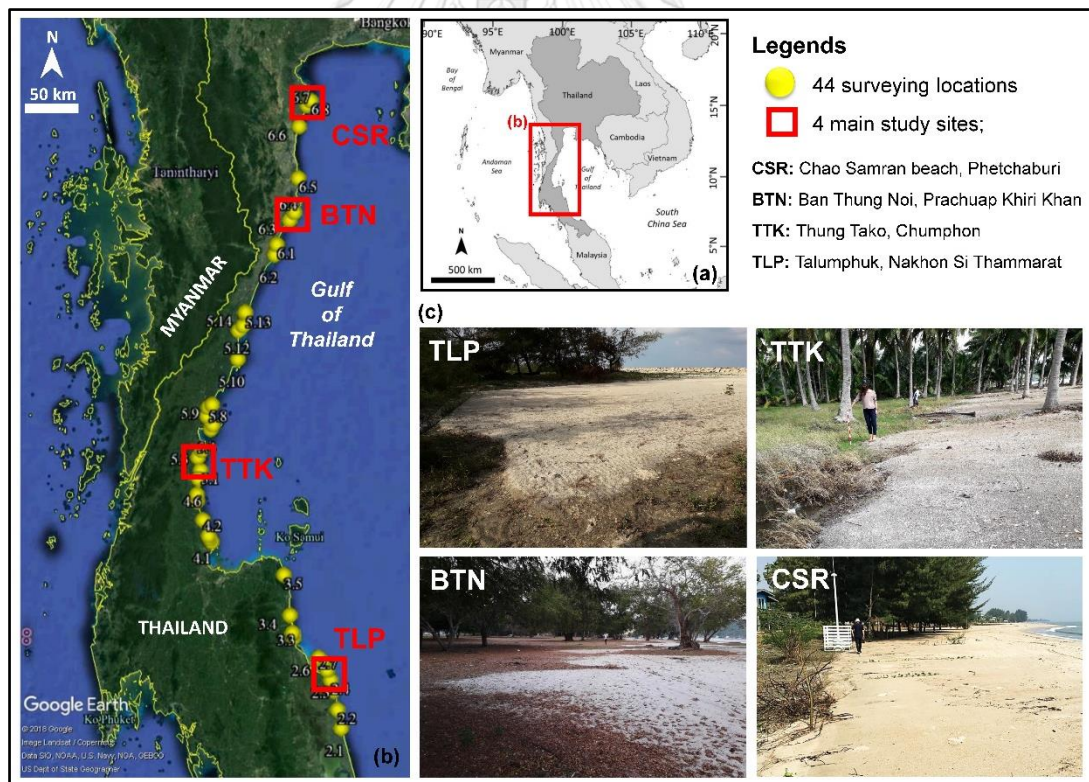


Figure 1.2 Study area (a) Location of the western coast of the Gulf of Thailand (W-GOT) (b) Satellite image showing the W-GOT and surveying point (yellow circles) and the 4 main study sites (red square) including CSR, BTN, TTK and TLP (c) Photos of washover deposits induced by the TS-Pabuk found in the 4 main study sites.

1.3 Objectives

- 1) To determine sedimentological characteristics of storm deposits induced by the tropical storm Pabuk.
- 2) To determine characteristics of GPR signals from storm deposits induced by the tropical storm Pabuk.
- 3) To investigate preservation areas of storm deposits.

1.4 Output

- 1) Obtained preservation areas of storm deposits.
- 2) Obtained sedimentological and GRP signals characteristics of storm deposits induced by the tropical storm Pabuk.

1.5 Methodology

The first field survey was conducted within 3 weeks after the storm and finished data collection within 7 months after the event. Effects of storm were observed both erosion and deposition for 44 localities and selected only 4 specific sites ranged from the farthest site from landfall location down to the nearest site (From northern to southern part of GOT) including Chao Samran beach (CSR) in Phetchaburi, Ban Thung Noi (BTN) in Prachuap Khiri Khan, Thung Tako (TTK) in Chumphon and Talumphuk (TLP) in Nakhon Si Thammarat, respectively. All locations provided well-preserved washover deposits that are suitable for studying in sedimentary detail. Several methods were applied including sedimentology, geophysics, topographic survey and microfossil technique to investigated to analyze diagnostic characteristic, depositional process and significant local factors controlling these storm deposits (Figure 1.3).

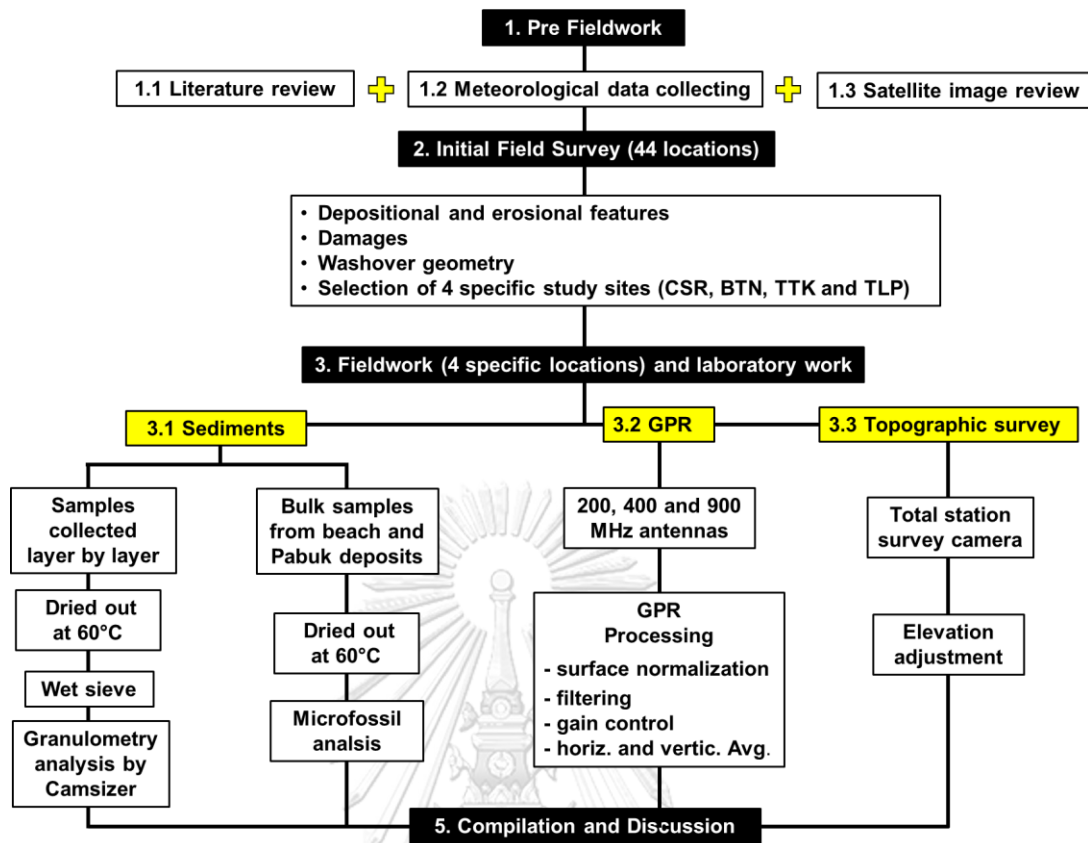


Figure 1.3 Flow chart of methodology using for this research

1.5.1 Collecting samples and sedimentary analysis

To study the sedimentary detail of the storm deposits, 57 shallow pits were excavated for 9 transect lines which are oriented perpendicular to the shore in all 4 sites including 12 pits 1 long trench at CSR, 17 pits 3 lines at BTN, 16 pits 3 line at TTK and 12 pits 2 lines at TLP (Figure 1.4a and b).

Surface and internal structures were investigated including inclined lamination, sub-horizontal to horizontal lamination, grading, shell fragments, lower contact between storm and pre-storm layers, color and other visible characteristics. For each pit, sediments were collected as layer-by-layer but not specific interval except at CSR which all samples were collected with 1 or 0.5 interval for grain geometry analysis. Most samples from a pit are from Pabuk layer and only one from pre-Pabuk layer. Firstly, these 626 samples were dried at 90 °C for 24 hours and removed mud contents using wet sieve analysis (Figure 1.4c and d). The percent weight of removed mud was calculated in percentages. Digital imaging technique

then was applied to measure grain size and geometry using a Retsch Technology Camsizer supported by University of Tsukuba (Figure 1.4e). Statistical parameters including logarithmic mean grain size, sorting, skewness and kurtosis were calculated based on the method of Folk and Ward, 1957.

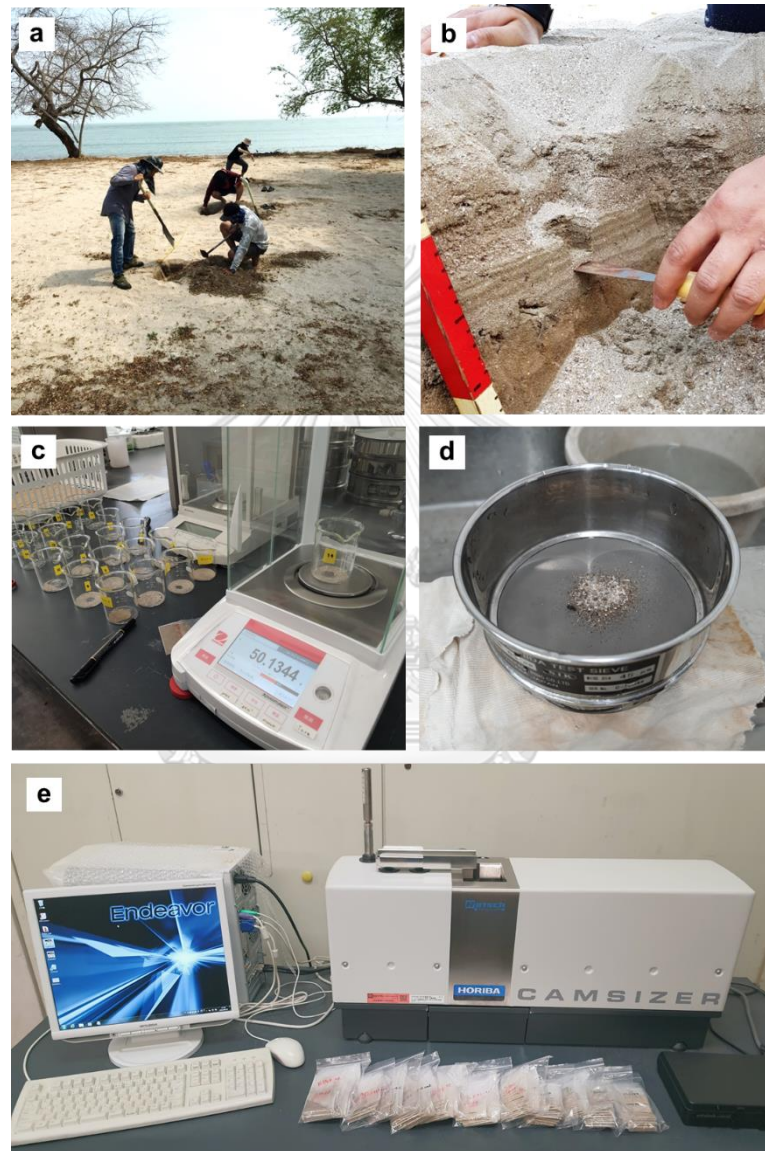


Figure 1.4 Images illustrate the process of collecting sediment samples. (a) Several shallow pits were excavated in a transect line perpendicular to the shore. The pits are about 50 cm width. (b) Collecting layer-by-layer sediment samples for grain size analysis. (c) Weighting sediment samples for 1 g before wet sieve (d) 63 μm sieve mesh for wet sieve technique and (e) Camsizer for grain size analysis

Another part of sediment samples is bulk sediments collected from surface of the storm deposits at BTN, TTK and TLP. The samples were prepared for diatom analysis using detergent solution technique (Figure 1.5). 1 g of sediments was put into the glass tube. Then, the detergent solution was dropped into the sediments and left for 10-20 minutes. Distilled water was put on top of the solution and placed the tubes into the centrifuge with 130 rpm for 10 minutes to allow the hard particles including diatom settled down. The on-top solution wastes were then removed. Put the new distilled water into the tube again and repeat the centrifuge and this step for 5 times. After removing the last waste in the tube, drop the solution on top of sediments on the glass slide above hotplate, heat the plate for 1-2 h to remove the solution. Finally, a drop of glue was put on the slides and stick the slide to the cover slide, heat the slides on the hotplate to melt the glue and wait for the glue to cover all areas. The slide for diatom analysis is ready for investigation under microscope. The microscope with 1000x magnification with immersion oil was used for diatom analysis.



Figure 1.5 Diatom analysis using detergent solution for step 1.

Line names (Area-line no.)	Analysis				
	Grain Size analysis	GPR 200 MHz	GPR 400 MHz	GPR 900 MHz	Diatoms
CSR	✓	-	-	-	-
BTN-1	✓	✓	✓	✓	✓
BTN-2	✓	-	-	-	
BTN-3	✓	-	-	-	
TTK-1	✓	✓	✓	✓	✓
TTK-2	✓	✓	✓	✓	
TTK-3	✓	✓	✓	✓	
TLP-1	✓	✓	✓	✓	✓
TLP-2	✓	✓	✓	✓	

Table 1.1 Summary table of analysis technique using for each transect line in 4 areas; CSR, BTN, TTK and TLP.

1.5.2 Ground Penetrating Radar (GPR)

SIR-20 GPR system with 200, 400 and 900 MHz shield antenna has been applied on the same transect profile line (Figure 1.6). The antenna attached with survey wheel to measure distances was dragged continuously along the transect to collect GPR data. The measurements were accomplished with sample rate of 512 samples/scan. Six profile lines were set up perpendicular to the shore including 1 line at BTN, 3 lines at TTK and 2 lines at TLP. However, only three best profiles of them are discussed here to be a representative of each location. The GPR profile lines were set up as close as possible to the shallow pit transect lines to ground truth. However, there are approximately 50 cm shift distances between them. As a result, the GPR signals and sediment results may not absolutely fit because of this limitation.

The length of transect lines ranges from 23 m at BTN and TTK to 65 m at TLP covering the distribution of washover deposits and nearby environments. The collected data then was processed using Radan software following the standard procedures (Figure 1.6) including position correction, topographic correction, horizontal and vertical averaging and gain adjustment for clarifying low-amplitude signals.

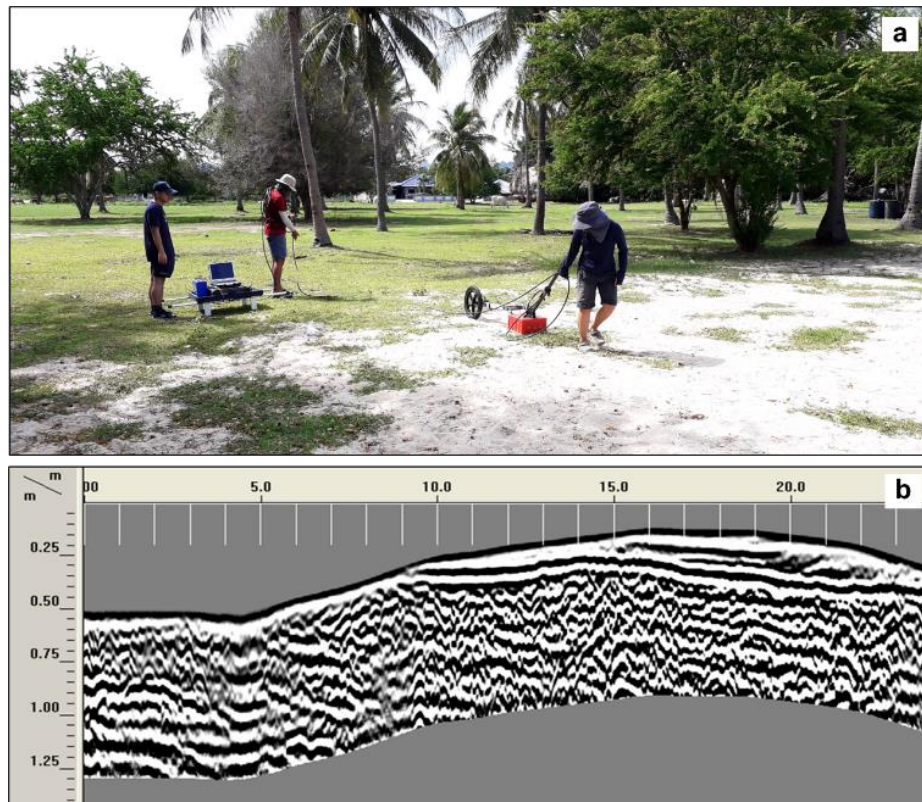


Figure 1.6 Process of collecting GPR data. (a) Dragging GPR antenna on the surface of washover lobes to collect GPR signals. (b) GPR profile signal recorded from the field that was processed by RADAN 6.0 software.

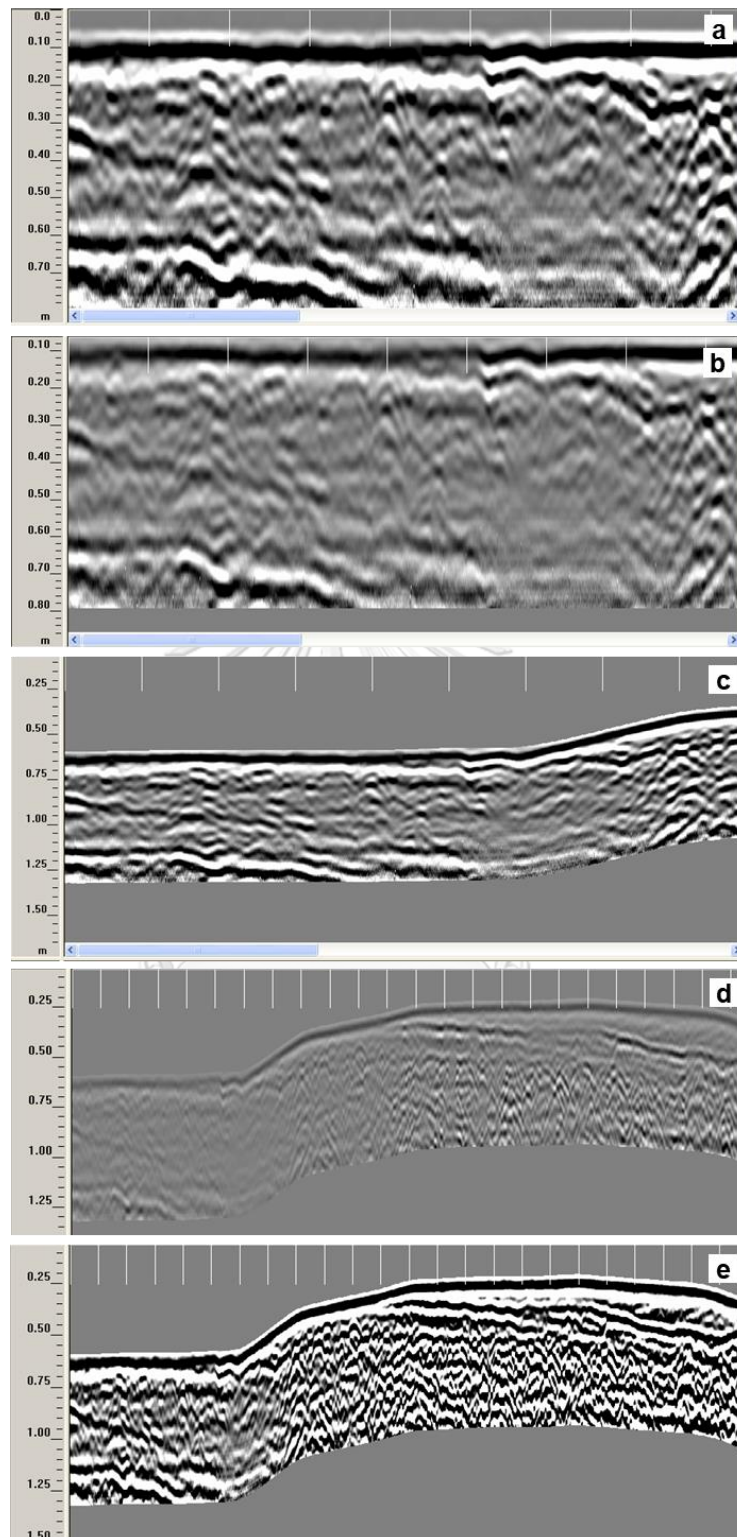


Figure 1.7 Example of processing GPR raw data from TTK-1 900 MHz signals. (a) raw data (b) after position correction (c) after elevation adjustment (d) after stacking and (e) after gaining.

1.5.3 Topographic survey and Hydrodynamic parameters

Topographic elevation profiles were applied for all transect lines using a SOKKIA total station survey camera. All reference points are located by handheld GPS. The elevation of each profile was eventually referenced to the mean tide level (MTL), mean high tide level (HT) and storm tide level obtained from tide gauge stations along the GOT supported by the Marine Department (2019) and Hydrographic Department (2019) of the Royal Thai Navy. These parameters are specific to the location. Consequently, the tidal data from tide gauge stations that are closest to our 4 study sites was determined to simulate hydrodynamic conditions that each site have experienced as close to the real situation as possible.



CHAPTER 2

LITERATURE REVIEW

2.1 Paleotempestology

Tropical storms are one of the major geohazard impacted on beaches. Their strong wind, heavy rain and storm surge can cause several damages on coastal area. Historical records of storm tracks and intensities may help evaluating recurrence intervals of storms. However, many regions lack long-term records of tropical storms. This results in a study of paleostorm called Paleotempestology.

Paleotempestology was defined by Nött (2004) as the study to “reconstruct past extreme events from sedimentary or erosional evidence left in the landscape as a result of storm surge and wave action. One technique that is commonly used to study paleostorm is overwash deposits which is generated when waves overtop barrier beaches and bring sediments from seaward side to deposit in back-barrier environments. Although overwash sediments can be evidence of storm, they may be caused by other high intensity events such as strong monsoons and tsunamis (Donnelly et al., 2004; Phantuwongraj et al., 2013). The differentiation of storm and tsunami deposits is still challenge especially in areas affected by both storm and tsunami. Sediments from both events can be recorded in the same site making it difficult to classify which events cause each layer. The evaluation of frequencies and intensities of major events then may not be effective. In order to distinguish overwash deposits induced by these two events, many criteria were considered. Sedimentological method is employed to study washover’ s sedimentological characteristics such as grain size, grain shape, grading, sorting, sedimentary structure, composition, basal contact, extent and thickness.

The recent storms with known track and intensity are greatly valuable for paleotempestology because their sedimentological characteristics can be modern analogues for identifying and analysing older storm deposits in the same region.

2.2 Regional of washover deposits

2.2.1 Overwash regimes

Overwash is the process generating washover sediments to deposit in back barrier environment. However, differences in surge intensity can cause differences in coastal vulnerability and characteristics of washover deposits. Sallenger (2000) proposed conceptual model of coastal impacts depending on topographic elevation of coastal barrier. Figure 2.1 shows parameters used in scaling the impact of storms on barrier island. R_{high} and R_{low} represent storm-induced swash elevation which include astronomical tide, storm surge and wave runup. D_{high} and D_{low} represent elevation of dune crest and dune base, respectively. Using these variables, storm impacts can be divided into four regimes including swash, collision, overwash and inundation. These are also studied in detail by Masselink and Heteren (2014) and can be briefly defined as follows:

1) Swash regime: $R_{high} < D_{low}$, maximum water level is confined to foreshore and the swash generally transports foreshore sediment to offshore zone causing. After the storm, eroded sediments can be replaced (Figure 2.2a).

2) Collision regime: $D_{high} > R_{high} > D_{low}$, maximum water levels exceed dune base but is not higher than dune crest causing the collision at foredune ridge and the following dune scarp. Foredune sediments then are transported offshore. This result may be more long-lasting than that of the swash regime (Figure 2.2b).

3) Overwash regime: $R_{high} > D_{high}$, water levels overtop dune or berm crest leading to breaching and seawater intrusion in the back barrier area. Sediments are transported landward (tens to hundreds of meters) and deposited as 'washover' (Figure 2.2c).

4) Inundation regime: $R_{low} > D_{high}$, elevation of the swash base exceeds the elevation of dune crest. Consequently, beach and dune system are subaqueous and are flatten. Massive sediments are transported and deposited landward (Figure 2.2d).

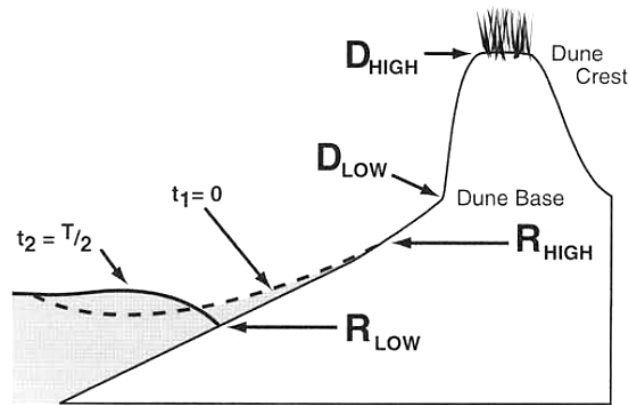


Figure 2.1 Model showing variables used in scaling the impact of storms on beach barrier. R_{high} and R_{low} represent elevations of swash. D_{high} and D_{low} represent elevations of dune. (Sallenger, 2000)

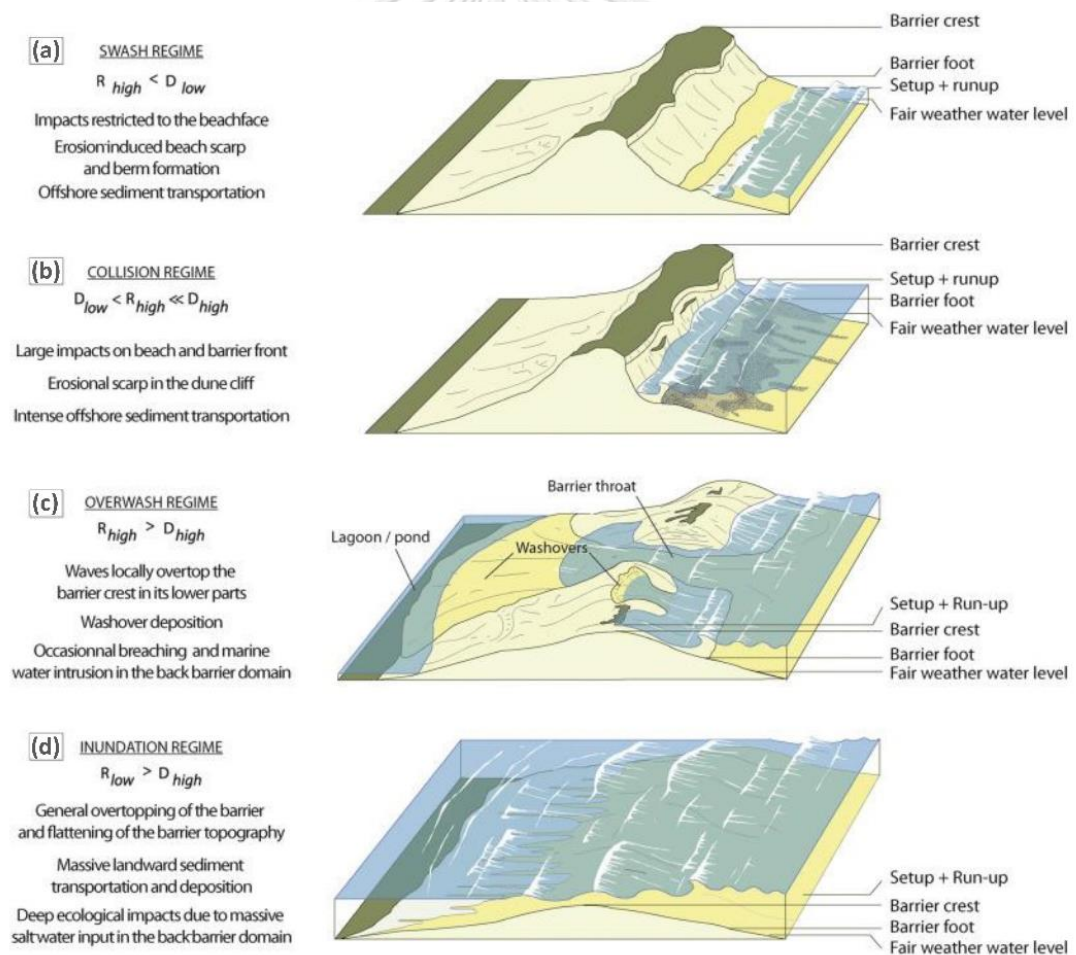


Figure 2.2 Schematic illustration of the Four storminess regimes developed under the conceptual model of Sallenger (2000) consisting of swash, collision, overwash and inundation (Goslin & Clemmensen, 2017).

Although storm wave behaviors can be controlled by dune elevations, they are also vulnerable to other physical factors such as location relative to the storm center, flooding duration, wind speeds, source materials, type and density of vegetation and human activity on the coast. These factors are responsible for influencing the intensity and type of storm impacts (Morton, 2002).

2.2.2 Beach morphology changes

Storm plays an important role in reshaping the coastal morphology. Large storms with high intensity can cause the great changes and destruction on the coast. In addition to destructive or erosional features, depositions are also found as a result of storm impacts. Morton and Sallenger (2003) differentiated coastal landform changes after storm into 2 major types, erosional and depositional.

1) *Erosional features*

Dune erosion: total wave height that is significantly higher than back beach but not exceed dune crest can collide and cause an erosion of dune. This feature is also known as 'dune scarp' (Figure 2.3A).

Channel incision: storm wave heights are higher than the primary dunes causing the inundation over the barrier island and headland. The sheetwash can be formed. Moreover, the incision of channels can also occur in barrier islands (Figure 2.3B).

Washout: an erosion of channel occurring in the condition that lagoon elevation is higher than the ocean. As a result, the lagoon water flows seaward across the barrier and form channels with landward erosion. In the late stage of water draining, dendritic drainage patterns occur in the head of the channels due to water sapping (Figure 2.3C).

2) *Depositional features*

Perched fans: one type of washovers that deposits as lobate or elongate features landward. Fans occur when total water levels during storm events exceed

the lowest dune crest, but elsewhere the surge is not higher than dune elevations (Figure 2.3D).

Washover terrace: long features of sediments stretching out landward and oriented parallel to the shore. This feature always forms in the condition that land elevations are lower than maximum water levels and relatively uniform (Figure 2.3E).

Sheetwash lineations: narrow lined erosional and depositional features forming in the same direction of the flow. The feature is involved unconfined flow (Figure 2.3F).

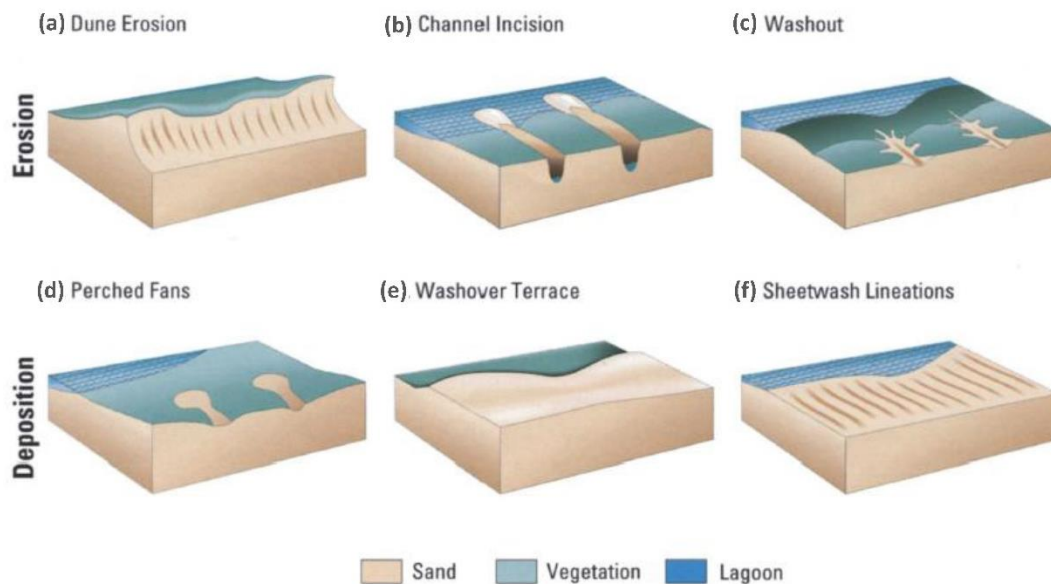


Figure 2.3 Erosional and depositional features induced by storms including a. Dune Erosion, b. Channel Incision, c. Washout, d. Perched Fans, e. Washover Terrace and f. Sheetwash Lineations. (Morton & Sallenger, 2003)

According to three types of depositional features including perched fans, washover terrace and sheetwash lineations (Phantu Wongraj et al., 2013), beach configurations are the major factors controlling these washover types and were defined them into 2 styles; uniform and non-uniform (Figure 2.4). A uniform beach configuration contributed to unconfined flow condition supports the formation of washover terrace. Whereas, a non-uniform beach configuration promoted confined flow is suitable for perched fan deposits.

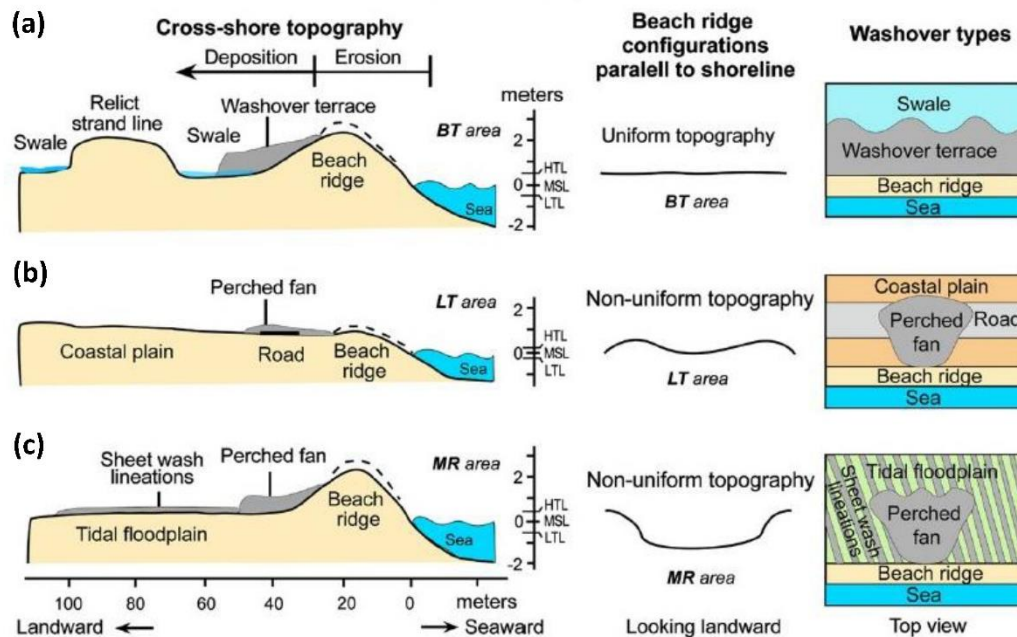


Figure 2.4 Cross-shore topography and beach ridge configurations parallel to shoreline of three areas; BT, LT and MR that control washover types. (a) A uniform beach configuration with large back-ridge swale inducing washover terrace at BT area. (b) A non-uniform beach configuration with flat and high coastal plain inducing perched fan at LT area. (c) A non-uniform beach configuration with low-lying tidal floodplain inducing sheetwash lineation superimposed by perched fan at MR area. (Phantu Wongraj et al., 2013)

2.2.3 Sedimentary characteristics of washover sediments

Internal and surficial structures found in storm-induced washover sediments include planar stratification, subhorizontal and horizontal bedding/lamination, foreset bedding, wavy bedding, coarsening and fining upward sequence, inclined sigmoid bedding, sharp upper and lower contact, erosional contact, mud drape and mud rip-up clasts (Brandon et al., 2014; Brill et al., 2016; Donnelly et al., 2001; Donnelly & Woodruff, 2007; Hong et al., 2018; Kongsen, 2016; Phantu Wongraj & Choowong, 2012; Phantu Wongraj et al., 2013; Phantu Wongraj et al., 2010; S. Phantu Wongraj et al., 2008; Pilarczyk et al., 2016; Soria et al., 2017; Switzer & Jones, 2008; Williams et al., 2016)

Storm surge washover deposits induced by 2007-2010 NE monsoon and 2011 Low-pressure system were studied by Phantu Wongraj et al. (2013) at 3 locations along the western coast of the Gulf of Thailand including Khao Mai Ruak (Prachuap Khiri Khan), Ban Takrop (Surat Thani) and Laem Talumphuk (Nakhon Si Thammarat).

The modern deposits present as washover terrace, perched fan and sheetwash. Additionally, they were characterized into 2 types 1) a thick-bedded sand of multiple reverse grading layers with the presence of foreset bedding, wavy bedding and sub-horizontal bedding and 2) a medium-bedded sand of normal grading layers with dune structures and horizontal bedding (Figure 2.5 and Table 2.1). Deposit thickness ranges from 15 to 80 cm. The maximum thickness was found in backshore swale area of Ban Takrop. Sharp and erosional basal contacts are common. Bedding structure shows landward inclined trend. Besides the deposition, erosional features including beach erosion, beach scarp, scour and breached can be observed from these sites.

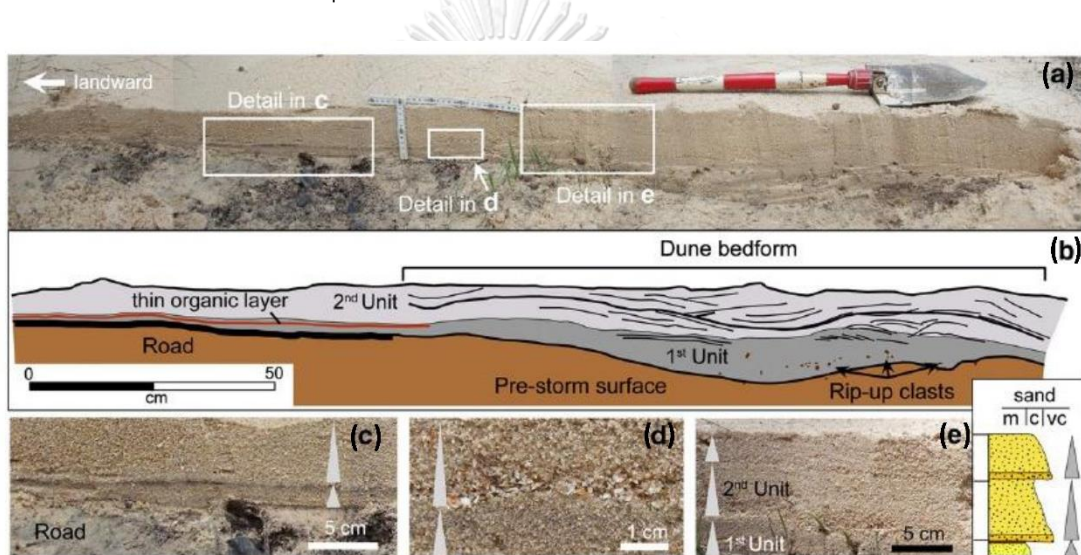


Figure 2.5 (a) Washover deposits induced by 2010 NE monsoon at Laem Talumphuk, Thailand. (b) Illustrated image of the deposits showing two sediment units and thin organic layer at distal part between the two units. (c) Thin organic layer. (d) Shell base of unit 2 and (e) Normal grading in both units (Phantuwoongraj et al., 2013).

Table 2.1 Comparison of geomorphic setting, washover type, flow condition, and sedimentary characteristic in washover deposits induced by monsoons and low pressure systems from many locations in the western coast of the Gulf of Thailand (Phantuwoongraj et al., 2013).

Features	Ban Takrop	Laem Talumphuk	Khao Mai Ruak 1st event	Khao Mai Ruak 2nd event
Topographic setting	Prograded shoreline	Sand spit	Beach barrier	Beach barrier
Backshore topography	Swale lower from beach ridge 2 m	Flat coastal plain higher than beach ridge	Tidal flood plain lower from beach ridge 2.5 m	Tidal flood plain lower from beach ridge 2.5 m
Erosional features	Beach erosion	Beach erosion, scour	Beach scarp, Breached barrier	Beach scarp
Storm impact regime	Overwash regime*	Overwash regime*	Inundation regime**	Overwash regime*
Flow confinement	Unconfined flow	Confined flow	Unconfined flow	Confined flow
Washover type	Washover terrace	Perched fan	Sheetwash	Perched fan
Deposit thickness	60–80 cm	15–20 cm	30 cm at crest of sand lineations	50–30 cm
Number of layers	11	3	–	12
Vertical grading in layer	Reverse grading	Normal grading	–	Reverse grading
Sedimentary structure	Lamination, foreset bedding, sub-horizontal bedding, wavy bedding	Horizontal bedding, dune bedform	–	Lamination, foreset bedding, sub-horizontal bedding
Bedding Inclination	Landward	Landward	–	Landward
Rip-up clasts	None	Present at bottom unit	None	None
Basal contact	Sharp contact	Sharp contact, erosional contact	Sharp contact	Sharp contact
Shell laminae	None	Common	None	None
Geometry	Sand sheet, lobate sand, thickness increasing in the depression	Lobate sand, landward thinning	Elongate narrow parallel to flow direction	Lobate sand, thickness increasing in the depression
Lateral deposition	Extensive	Patchy	Discontinuous	Patchy

* Overwash regime occurring when wave run up superimposed on the water level exceeds the beach or dune crest.

** Inundation regime occurring when the barrier or beach is completely flooded by seaward running water body.

Washover sediments of Typhoon Haiyan 2013 in Leyte Gulf of the Philippines were also studied (Brill et al., 2016; Soria et al., 2017). Consistent with those of Phantuwongraj et al. (2013), Haiyan deposits were classified based on sedimentary structure into 2 units. Unit 1 is massive to horizontal planar lamination with scour marks at the base and Unit 2 is subhorizontal planar laminae or inclined lamination (10–15°). Thickness ranges from a few mm to 80 cm. Common structures is sharp and erosional contact as well as landward fining trend. Sediment sorting is varied from poor to well (Figure 2.6 and Table 2.2).

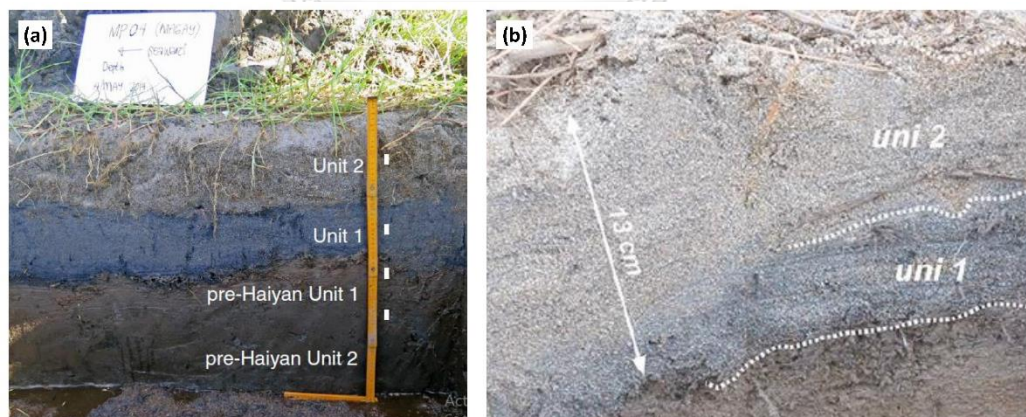


Figure 2.6 (a) Sediment units of Typhoon Haiyan deposits in Philippines overlie pre-Haiyan unit with sharp contact. unit 1 is magnetite-rich medium sand with coarsening upwards trends and unit 2 is light grey coarse sand with fining upwards trend (Soria et al., 2017). (b) Haiyan deposits showing massive sand of unit 1 and laminated sand of unit 2 (Brill et al., 2016).

Table 2.2 Comparison of local geomorphic setting, hydrodynamic conditions and sedimentary textures and structures of Typhoon Haiyan deposits in many locations of Philippines coasts (Soria et al., 2017).

Local setting	Locality	Tanauan, Leyte	Basey, Samar	Tanauan, Leyte	Tolosa, Leyte	Tolosa, Leyte	
	Coastal geomorphology	Sandy beach, coastal plain	Narrow sandy beach on carbonate platform	Sandy beach	Sandy beach	Beach-ridge plain	
Ground surface elevation, m (asl)	1.5 to 2m	2 to 3m	0 to 5m	0 to 3m	0 to 2.5 m		
Hydrodynamic conditions	Flow depth, m	3 to 4m	3 to 4m	3.6 m	3.8 m	3.5 m	
	Inundation distance, km	2 km	0.8 km	3.1 km	1.4 km	0.8 km	
	Distance from storm eye (zone of max winds)*	15 km	30 km	15 km	5 km	5 km	
References	Soria et al., 2016	Soria et al., 2016	Abe et al., 2015	Abe et al., 2015	Brill et al., 2016		
Sedimentary textures and structures	Trench scale	Thickness	10–20cm (proximal); 2cm (distal)	2 to 8cm	0.1 cm to 10 cm; 40 to 80 cm very close to shore	0.1 cm to 10 cm	10 to 20 cm (proximal); few mm, 2 to 5 cm (distal)
		Vertical grading of entire deposit	Unit 1 (sand sheet to mud): coarsening upward Unit 2 (washover terrace): coupled fining and coarsening upward	No analysis	No analysis	No analysis	Unit 1 (sandsheet): fining upward Unit 2 (washover terrace): repeated coarsening fining sequences
		Sorting	Moderate to well-sorted	Poorly sorted	No analysis	No analysis	Well-sorted
		Sedimentary structures	Unit 1: massive to horizontal planar lamination Unit 2: subhorizontal planar laminae	Massive	No analysis	No analysis	Unit 1: planar lamination; scour marks at the base Unit 2: inclined lamination (10–15°)
		Basal contact	Sharp, depositional	Sharp, depositional	No analysis	No analysis	Sharp, erosional and depositional
	Transect scale	Cross-shore geometry	Washover terrace (proximal); sand sheet to mud (distal) with varying thickness landwards but generally thick in depressions	Overall but not systematic landward thinning	Landward thinning	Landward thinning	Washover terrace (proximal); sand sheet (distal) exhibiting landward thinning
		Lateral grading	Overall landward fining	Overall landward fining	No analysis	No analysis	Landward fining
		Inland extent	1.6 km	350 m	150 m to 80 m (sandsheet)	130 m to 150 m (sandsheet)	250 m (sandsheet)
		References	This Study	This Study	Abe et al., 2015	Abe et al., 2015	Brill et al., 2016

* Estimated based on the storm eye location of Morigerman, 2014.

As shown in Table 2.3, sedimentary signatures related to local setting and hydrodynamic conditions of Typhoon Haiyan are also compared with others of comparable intensity including Cyclone Yasi (2011), Hurricane Ike (2008), Hurricane Rita (2005), Hurricane Katrina (2005), Hurricane Isabel (2003) and Hurricane Caria (1961). Although storms are in comparable intensity, there are differences in occurring effects such as inundation area, maximum water level, inundation duration and thickness of washovers. However, the common properties are preserved in overwash deposits. Sharp and erosional contact is notable character found in all storms. Two units of the deposits can be classified in sediments from Typhoon Haiyan and Hurricane Rita. Unit 1 exhibits massive or planar lamination, while unit 2 shows subhorizontal and foreset laminae. Fining and thinning landward is also common lateral grading type.

Table 2.3 Comparison of local setting, meteorology, hydrodynamic conditions and sedimentary signatures in transect and trench scale of the Typhoon Haiyan and other recent storms of comparable intensity (Soria et al., 2017).

Storm type	Tropical cyclone ID	Typhoon Haiyan	Typhoon Haiyan	Cyclone Yasi	Hurricane Ike	Hurricane Ike	Hurricane Rita	Hurricane Katrina	Hurricane Isabel	Hurricane Carla	
	Event Date	November 2013	November 2013	February 2011	September 2008	September 2008	September 2005	August 2005	September 2003	September 1961	
Local setting	Locality	Tanauan, Leyte	Bawey, Samar	South of Cairns, northeast Queensland, Australia	Galveston and San Luis Islands, Texas	McFaddin National Wildlife Refuge, Texas	Constance Beach, Louisiana	Ocean Spring and St. Andrews, Mississippi	Hatteras Is., North Carolina	Matagorda Peninsula, Texas	
	Coastal geomorphology	Sandy beach, coastal plain	Sandy beach	Sandy beach ridge plains	Barrier islands (ridge and swale topography)	Palustrine marshes and brackish lakes, sandy beach with low foredunes	Beach ridges separated by low-lying, muddy marshes	Salt marsh	Barrier island with dunes	Barrier island	
Meteorology	Ground surface elevation, m (asl)	1.5 to 2 m	2 to 3 m	Ridge crests at higher than 4 to 5 m	0.75 to 2.2 m	1 to 2 m	0.5 to 1 m (ridges)	1.7 to 5 m	Dunes at 3 to 4 m		
	Peak intensity	Cat 5 (895 hPa; -314 kph)	Cat 5 (895 hPa; -314 kph)	Cat 5 (929 hPa; -205 kph)	Cat 4 (231 kph)	Cat 4 (231 kph)	Cat 5 (897 hPa; 288 kph)	Cat 5 (902 hPa; 280 kph)	Cat 4 (> 270 kph)	Cat 5 (280 kph)	
	Intensity at landfall	Cat 5 (-296 kph)	Cat 5 (-296 kph)	Cat 5	Cat 2 (175 kph)	Cat 2 (175 kph)	Cat 3 (190 kph)	Cat 3 (920 hPa; 200 kph)	Cat 2	Cat 5 (280 kph)	
	Translation speed	41 kph	41 kph	41 kph	20 kph	20 kph	19 kph	24 kph	24 kph		
	References	Takagi et al., 2015	Takagi et al., 2015	Boughton et al., 2011	Doran et al., 2009; Morton & Barras, 2011	Doran et al., 2009; Morton & Barras, 2011	Williams, 2009; Morton & Barras, 2011	Morton & Barras, 2011	Morton et al., 2007	Morton et al., 2007	
Hydrodynamic conditions	Maximum water level, m (asl)	5 to 6 m	5 to 6 m	3 to 6 m	3-4 m	> 3 m	4 to 5 m	-7 m	2.7 m (open-coast) > 3 m to 4 m	3 to 4 m	
	Flow depth, m (above ground surface)	3 to 4 m	3 to 4 m		1 to 4 m		At least 3 m	5 to 6 m	1.28 m (landward limit overwash deposition)	1 to 1.5 m	
	Inundation duration	-1 hour	-1 hour	12 hrs (peak inundation lasting for 2 hrs)	2 days of flooding	2 days of flooding	6 hours	-24 hrs	9 hrs (with peak inundation lasting for 5 hrs)	24 hrs	
	Inundation distance	2 km	800 m	500 m		25 km		725 to 780 m (< 1 km)	15 to 30 km	15 to 35 km	
	Distance from storm eye (zone of max winds)	15 km	30 km	20-40 km	25 to 50 km	-70 km	35 km	40-50 km	55 km	60 km	
	References	Soria et al., 2016	Soria et al., 2016	Boughton et al., 2011; Nott et al., 2013	Hawkes and Horton, 2012; Doran et al., 2009	Williams, 2010; Horton et al., 2009	Williams, 2009; McGee et al., 2013	Fritz et al., 2007; Horton et al., 2009	Morton et al., 2007	Morton et al., 2007	
Sedimentary patterns and grain sizes	Thickness	2 cm (distal) 10-20 cm (proximal)	2 to 8 cm	5 cm (87 m from shore); 20-50 cm (50 m from the shore)	2 cm to 28 cm	51-64 cm (within 200 m); 3-10 cm (> 200 m)	2 to 50 cm	9 to 13 cm	40-57 cm (2 m thick overwash terrace)	At least 25 to 30 cm	
	Vertical grading of entire deposit	Unit 1 (sand sheet to mud); coarsening upward Unit 2 (washover terrace); coupled fining and coarsening upward	No analysis	Fining upward with fine-sloped trends	Coarsening upward; alternate coarsening and fining upwards	No analysis	Unit A (sand sheet): coarsening upward Unit B (washover terrace): coarsening upward	Massive	Cycles of upward coarsening or upward fining	Upward fining	
	Sorting	Moderate to well-sorted	Poorly sorted	Not reported	Not reported	Not reported	Well sorted	Not reported	Well sorted	Poorly sorted (proximal) to well sorted (distal)	
	Sedimentary structures	Unit 1: massive to horizontal planar laminae Unit 2: subhorizontal planar laminae	Massive	Horizontal planar laminations; basal coarse grained sediments	Not reported	Ripple marks on the surface	Unit A: planar laminae Unit B: foreset laminae	Not indicated	Subhorizontal planar stratification	Planar parallel laminae	
	Basal contact	Sharp, depositional	Sharp, depositional	Sharp, erosional	Sharp, depositional with little or no erosion	Sharp	Sharp, erosional	Sharp, erosional	Sharp	Sharp, erosional and depositional	
	Cross-shore geometry	Washover terrace (proximal); sand sheet to mud (distal) with varying thickness landwards but generally thick in depressions	Overall but not systematic landward thinning	Highly variable thickness	Landward thinning; thicker deposits on the swales	Fining and thinning landward	Landward thinning	No transect data	Narrow thick terrace deposits terminating in avalanche faces	Narrow thick terrace deposits, moderately thin broad fans, landward thinning	
	Lateral grading	Overall landward fining	Overall landward fining	Landward fining in one site, no systematic trend in another site	Not reported	Thinning and fining inland	Inland fining only on the distal deposit			Landward fining	
	Inland extent	1.6 km	350 m	Up to 87 m	110 to 320 m	2700 m	400 to 500 m		Up to 250 m	Average at 190 m, up to 320 m	
		References	This Study	This Study	Nott et al., 2013	Hawkes and Horton, 2012	Williams, 2010	Williams, 2009	Horton et al., 2009	Morton et al., 2007	Morton et al., 2007

The typical physical characteristics of storm and tsunami deposits as shown in Figure 2.7 have been proposed in 2007 (Morton et al., 2007). The storm deposits display as planar stratification with some foresets, troughs and climbing ripples. The thickness is about 25-200 cm with abrupt and erosional lower contact. Shell fragments are common, while mudcap and mud rip-up clasts are rare. The tsunami deposits are thinner in total thickness which are about 5-25 cm. Mudcap and rip-up clasts are always preserved but shell laminations are not likely. The lower contact is sharp with some erosion. However, the overwash sediments generated by Typhoon Haiyan 2013 striking Philippines coast show hybrid characteristics between storm and tsunami (Soria et al., 2017). The Haiyan deposits are thinner than other deposits from modern storms and extend up to 1 km inland while many of storm deposits extend only less than 100 m. In addition, the deposits are also found as a massive lamination. Consequently, the differentiation between storm and tsunami deposit is still questionable and their sedimentary characteristics are needed to be studied.

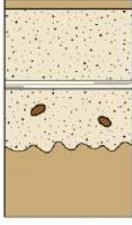

Typical tsunami deposit	Typical storm deposit
 <ul style="list-style-type: none"> • mudcap • lamina sets may be separated by thin mud or heavy mineral lamina • often normally graded • rip up clasts • 5-25 cm thick • abrupt lower contact 	 <ul style="list-style-type: none"> • mudcap rare • may have foresets, troughs, climbing ripples • planar stratification • many laminae and laminasets • 25-200 cm thick • abrupt lower contact

Figure 2.7 Sedimentary characteristics of tsunami and storm deposits. (Morton et al., 2007)

2.3 Analytical techniques for washover sediments

2.3.1 Grain size analysis

Grain size is a physical characteristic of particles directly depending on settling environments. Consequently, it is a useful environmental proxy that is fundamentally measured to obtain depositional conditions such as transport agents, flow energy and transportation time and length.

Several techniques can be applied to measure grain sizes such as sieving analysis, sedimentation or settling, laser diffraction analysis (Mastersizer) and digital image analysis (Camsizer). However, the results of each technique may be different due to the physical property that is measured. Details of each technique is explained as follows (López, 2016; Switzer & Pile, 2015; Syvitski, 1991)

1) Sieving

There are two types of sieving; dry and wet applications. However, both of them are primarily applied for sand-sized particles or greater rather than silt size. The instrument used in this method is a series of stacked mesh. Each mesh will trap sediments that are larger than mesh sizes. So, the coarsest particles will be placed on the top of the stack. For dry sieve, sediments pass through a series of sieves and are agitated shaker for about 15-20 minutes. The sediments braked up and retained in each mesh will be weighed to calculate the percentages. For wet sieve which is suitable for fine particles, the samples will be dried at ~110°C. Dry samples are

resaturated in water with a dispersant (usually sodium hexametaphosphate) and stirred in water for ~1 hour. Then, the samples are washed through a stack of sieves until the draining water from the stack base is clear.

This method is cheap, user friendly and suitable for very coarse samples. However, there are some limitations as mentioned by (Switzer & Pile, 2015) that dry sieving can confront particle aggregation which is larger than a single grain, unclean mesh and overloading of sieves which can cause mesh distortion. These can cause error. Nevertheless, solutions are proposed to relieve these problems; the particle aggregation can be checked by binocular microscope and the samples should not be more than 100 g to avoid overloading.

2) Sedimentation or Settling

The concept of this method is considering the sedimentation rate of particles suspended in fluids based on Stokes' law. It is applicable to very fine sediments such as silt, clays and soils. The equivalent grain diameters can be calculated from the settling velocities. Although this method is relatively low cost, the limited range of grain sizes and grain-shape sensitivity are disadvantage. Settling tubes are also used to investigate grain size of washover deposits induced by 2004 Indian Ocean Tsunami in Thailand (Choowong, Murakoshi, Hisada, Charusiri, et al., 2008).

3) Laser Diffraction Analysis (Mastersizer)

Laser Diffraction Analysis (LDA) measures the diffraction angle of laser light scattered by whole suspended particles. An intensity of laser light will be then converted to a volume distribution. In the processing, suspension medium which is usually water is measured for background. After that, sediments are put into the instrument and agitated by ultrasound until the laser obscuration is appropriate. Too high obscuration can cause the inter-particle interference and too low obscuration causes bad signal and noise ratio. Finally, the output will be grouped based on standard. The instruments are available by many manufacturers including Malvern, Beckman-Coulter, Retsch and Horiba.

This technique can deal with a wide range of particle sizes which cover < 100 nm to 2-3 mm (López, 2016). Many researches apply LDA for material < 2 mm (Brill et al., 2016; Soria et al., 2017).

4) Digital image analysis (Camsizer)

This method is high speed camera-based measurement produced by Retsch of Germany capable for determining grain size over 30 µm to 30 mm. The camsizer captures falling sediments at 25 Hz and measures cross-sectional area of the sediment. Then, the equivalent spherical diameter is reported.

Table 2.4 Particle size ranges with optimal analytical techniques. (López, 2016)

Particle Size Range	0.1 nm	1 nm	10 nm	100 nm	1 µm	10 µm	100 µm	1 mm	10 mm
Applicable Analytical Technique									
Sieving									
Laser Diffraction									
Settling									
Dynamic Light Scattering									

2.3.2 Microfossil analysis

Washover deposits contain not only sediments but also microfossils and shell fragments from coastal and marine environments. These can reveal the provenance of sediments and depth of storm wave base. Microfossil assemblages, hence, are necessary criteria used to distinguish washover deposits and those sediments from inland processes. Foraminifera, for example, is marine microfossil always found in washover sediments owing to being transported landward by storm surge. Freshwater fauna such as testate amoebae can indicate the terrestrial scouring.

Washover deposits induced by monsoon and low pressure system in Thailand contain Mollusca (bivalve; *Vepricardium*, gastropod; *Cerithidea cingulata* and scaphopods) and foraminifera (*Elphidium crispum*) indicating shallow water transitional zone (mangrove to shoreface) as shown in figure 2.8 (Phantu Wongraj, 2012).

Pilarczyk et al. (2016) study microfossils in Typhoon Haiyan deposits in the Philippines. The intertidal, marine and freshwater organisms were considered along

with their concentration (per 5 cm³), abundances of each foraminifera species, taphonomic conditions and test size. The washover deposits were distinguished from underlying sediments based on the presence of intertidal and subtidal benthic and planktic foraminifera. They contain much of shallow benthic and planktic calcareous foraminifera, whereas underlying substrates are abundant of testate amoebae with an absence of calcareous foraminifera (Figure 2.9). This is conform to back-barrier deposits in South Carolina Atlantic Coastal Plain, total calcareous foraminifera tends to be found more in washovers than background marsh samples (Hippensteel & Martin, 1999). Moreover, classification of fossil species represents three source zones: terrestrial, intertidal and subtidal zones. In addition, unaltered deeper-dwelling species found in Haiyan deposits including *E. repandus* and *C. tabaensis* indicate subtidal zone deeper than 5 m.

Diatoms were also studied in storm deposits induced by the 2007 cyclone Sidr at Kuakata coast, Bangladesh (Haque et al., 2021). Sediments from the core B-1 were collected with 5 cm intervals and prepared for diatom analysis. The diatoms, then, were identified by a 1000x magnification microscope. The result shows that storm deposits contained both freshwater and marine diatoms (Figure 2.10) which can be inferred that intense precipitation caused river flooding and inundated the area coupled with seawater storm surge. Consequently, the mixing of freshwater and marine diatoms was presented in the storm deposits. Moreover, brackish-freshwater diatoms are relatively higher than marine diatom at the upper part of deposits. This also insists the inundation of inland water during the late stage of the storm event.

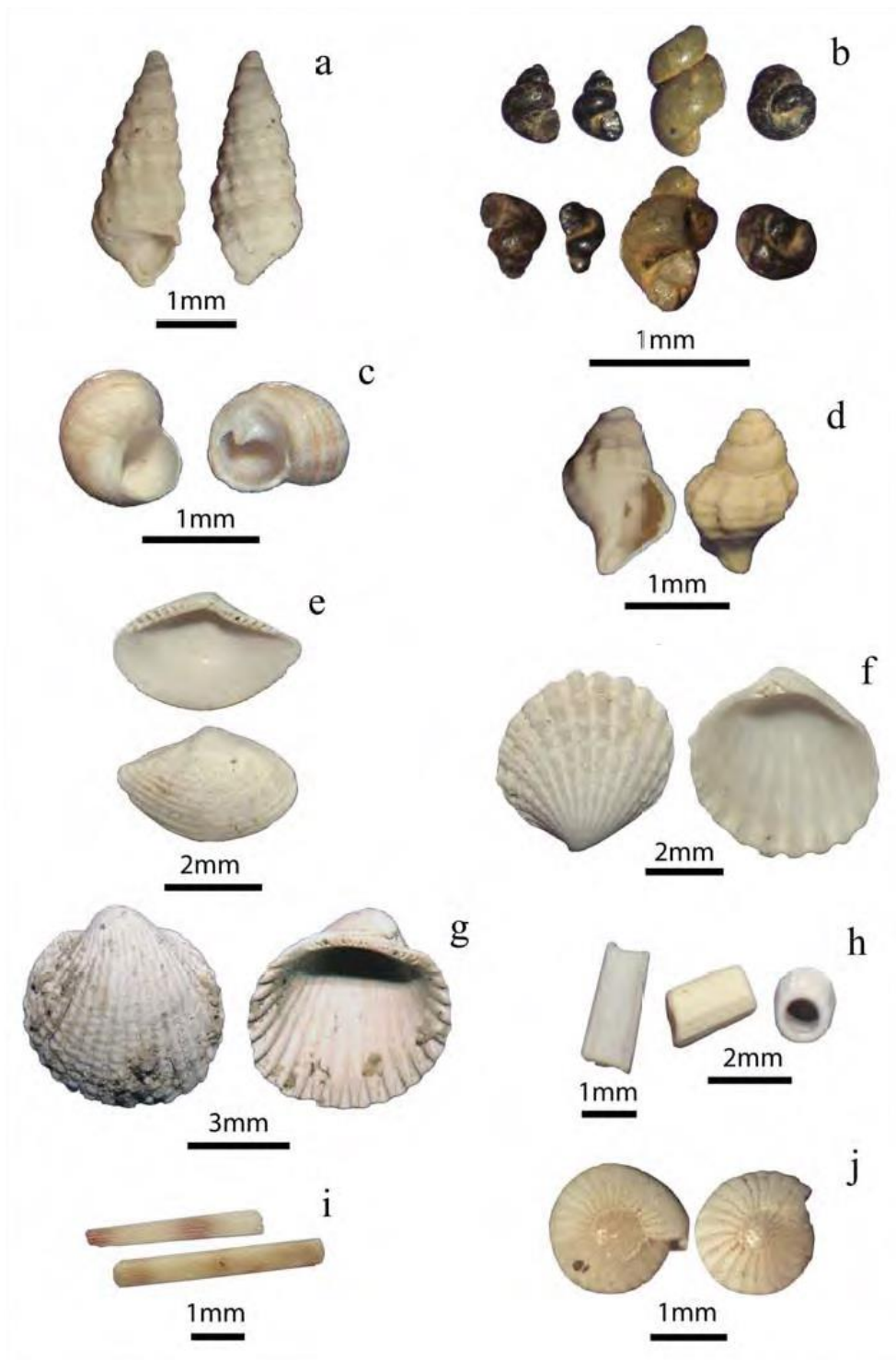


Figure 2.8 Mollusca and foraminifera found in washover deposits induced by NE monsoon and low-pressure system during the years 2007 to 2011 in the Gulf of Thailand coast. a) *Cerithidea cingulate*. b) *Siliquaria*. c) *Natica*. d) *Pseudoneptunea varicose*. e) *Nuculana* (*Thestyloda*) *soyaoe*. f) *Vepricardium*. g) *Anadara*. h) *Antalis dentalis*. i) *Antalis vulgaris*. j) *Elphidium crispum*. (Phantu Wongraj, 2012)

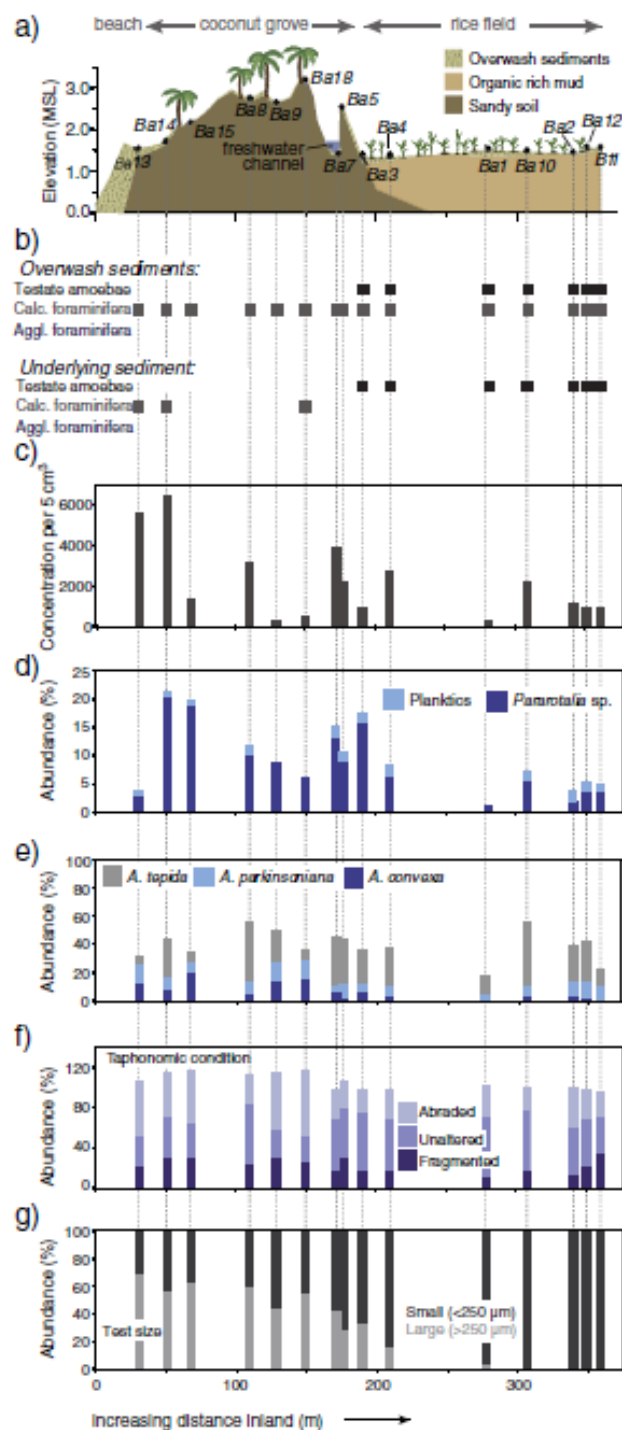


Figure 2.9 An example of microfossil assemblage changes in Typhoon Haiyan deposits in Philippines (Basey). (a) Elevation profile, sampling locations (black circle) and washover thickness. (b) Presence of testate amoebae (freshwater organisms), calcareous and agglutinated foraminifera (intertidal and marine organisms). (c) Foraminifera's concentration per 5 cm³. (d,e) Abundances of dominant foraminifera species. (f) Taphonomic condition of calcareous foraminifera. (g) Abundances of small and large tests. (Pilarczyk et al., 2016)

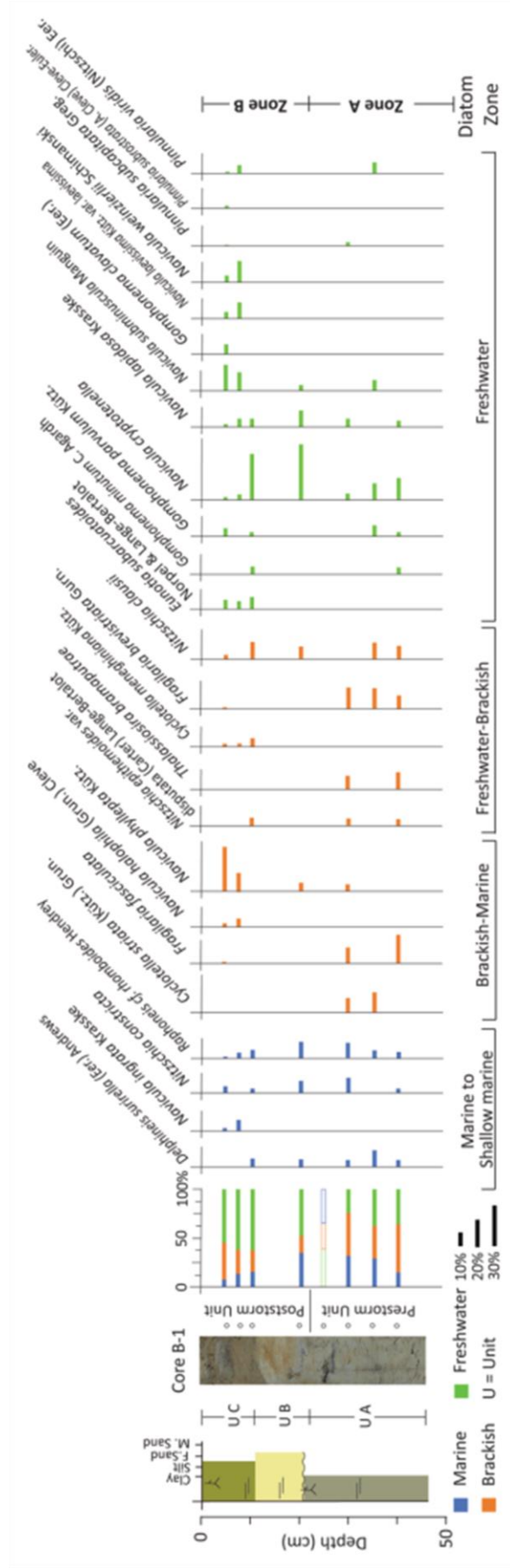


Figure 2.10 Fossil diatom assemblages of core B-1 induced by the Cyclone Sidr from Kuakata coast, Bangladesh (Haque et al., 2021).

2.3.3 Ground Penetrating Radar (GPR)

Ground Penetrating Radar (GPR) is a non-destructive geophysical technique widely used to investigate the shallow-subsurface underground. Electromagnetic energy was emitted into the ground. When the waves encounter contacts between materials having different electrical and magnetic properties, it will be reflected or refracted or scattered back to the surface. The receiver then can record the reflected signal. The more differences in dielectric properties or permittivity of boundaries, the more strength of reflected signals. Thereby, the low contrast in dielectric properties can cause no distinct reflections.

Many frequencies of GPR antennas can provide differences in depth and resolution of the signals. Lower frequency can penetrate into the ground deeper than higher frequency but causes less resolution. In Phra Thong islands, Thailand, GPR was applied both low (100 MHz) and high (500 and 1000 MHz) frequency GPR to investigate thin-bed washovers of modern and paleotsunami in 2 swales (Gouramanis et al., 2015). Along with this method, the auger cores were set up to ground truth. The results show that 500 MHz GPR antennas provide the best images of internal stratigraphy and upper-lower contacts of tsunami layers (Figure 2.11). Whereas the 1000 MHz antennas provide poor depth and poor resolution in deeper zone. However, they are suitable for the environments having uniform grain size sediments such as siliciclastic coasts with heavy minerals. The lowest frequency, 100 MHz antennas, cannot differentiate internal stratigraphy of thin bed sediments (Gouramanis et al., 2014; Gouramanis et al., 2015).

Owing to thin layers, storm-induced washover sediments are also investigated by many frequencies of GPR. Wang and Horwitz (2007) used 250 MHz GPR to examine erosional and depositional characteristics of washovers caused by 4 storms including Ivan (2004), Dennis (2005) Frances (2004) and Jeanne (2004) which made landfall on the Florida coast of USA. The examination was set up in dune field, wetland with vegetation cover and back-barrier bay. The truncated dune can be shown in GPR reflection as a bi-directional inclination together with the subhorizontal stratification which represent the washover deposition on the dune interior platform. Moreover, inclined tabular foresets are also captured in landward side emphasizing the

progradation of washovers into the back-beach bay environments (Figure 2.12). Steep tabular bedding was found in the vegetated wetland environments and sigmoidal bedding is found in back-barrier bay.

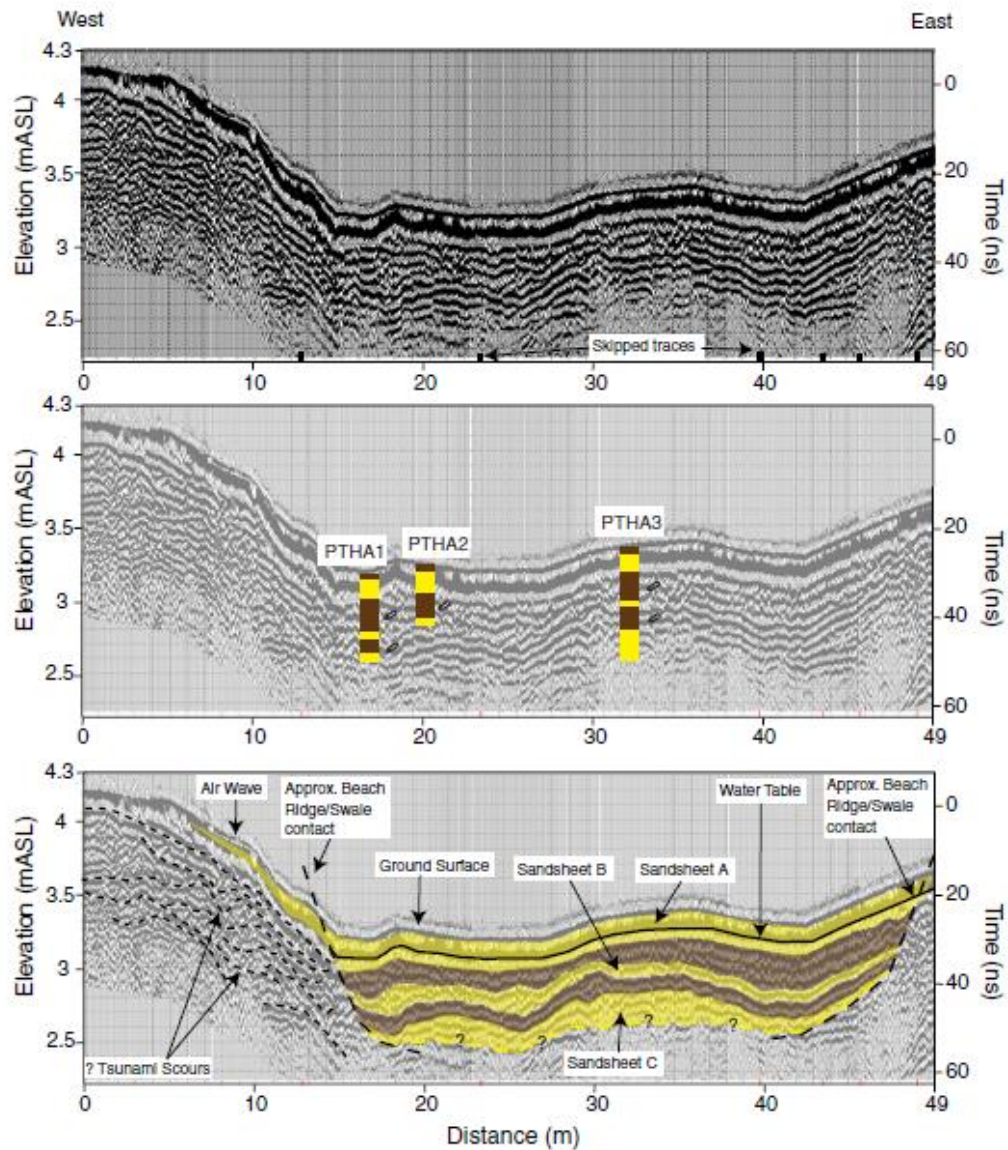


Figure 2.11 An example of 500 MHz GPR reflection showing contacts between tsunami, paleotsunami and non-tsunami layers. (Gouramanis et al., 2015)

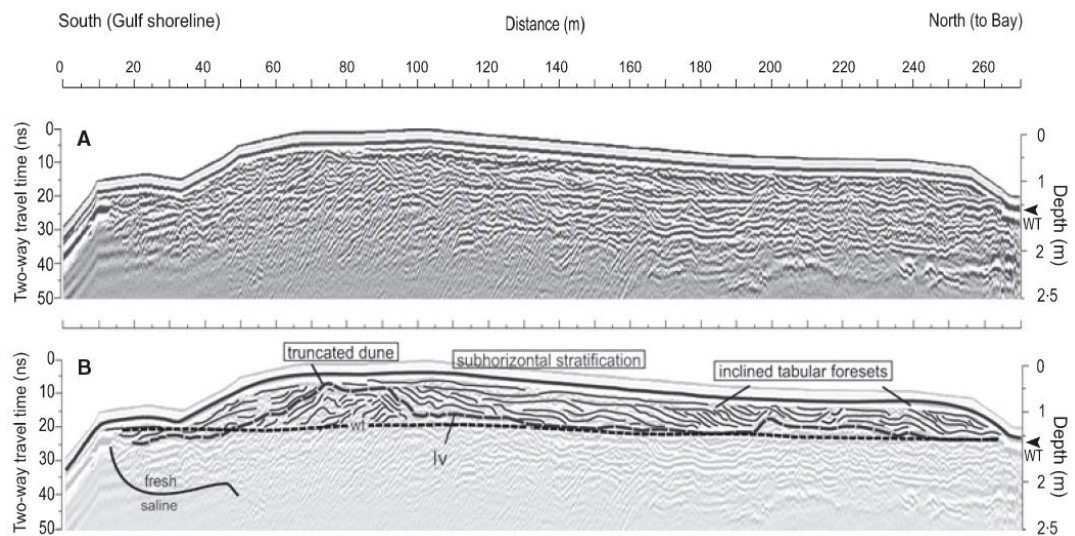


Figure 2.12 The 250 MHz GPR signals and interpretation of BP area located at the northern part of Florida and confronting Ivan (2004) and Dennis (2005) Hurricane. The GPR profile shows truncated dune, subhorizontal stratification, inclined tabular foresets formed when washover prograded into the bay on the land, water table (wt) and radar surface interpreted as the base of Hurricane Ivan deposits (lv). (Wang & Horwitz, 2007)

The 100 MHz antennas (Low frequency) GPR is also used to investigate the volcanoclastic barrier dune system in the central Philippines which undergoes Typhoon Durian in 2006 (Pile et al., 2016). The cross-shore profiles as shown in Figure 2.13 present an erosional surface of Typhoon Durian and two lines of pre-Durian events (red), shoreward dipping reflections (yellow) were interpreted as beach progradation. Whereas landward dipping and subhorizontal reflections were interpreted as overwash deposits (green). The continuous horizontal line (blue) is water table.

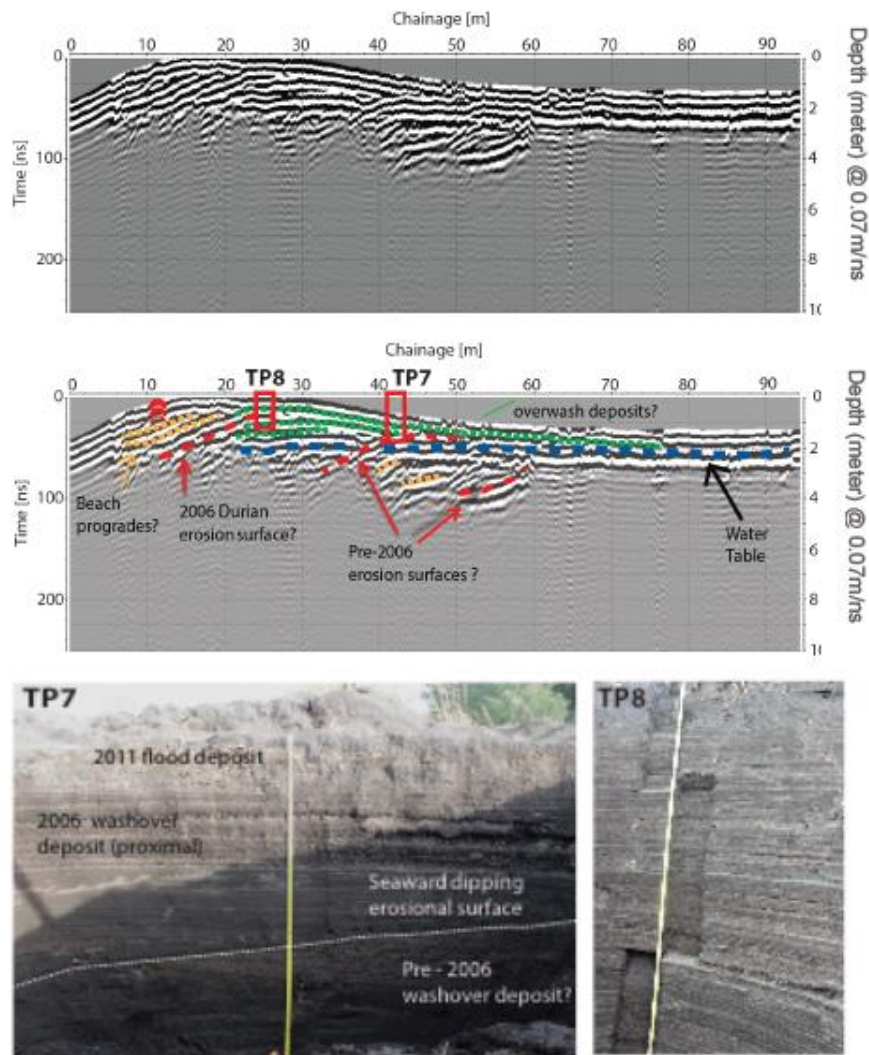


Figure 2.13 An example of 100 MHz antenna frequency GPR profile on the Bay-Bay Spit, Bicol, Central Philippines. Red lines show erosional surfaces induced by Typhoon Durian and Pre-Durian events. Yellow lines are interpreted as beach progradation. Green lines represent overwash deposits and the continuous blue line is water table. (Pile et al., 2016)

2.4 Washover deposits in Thailand

Overwash events in Thailand are influenced by both storm and tsunami. The western coast of Thailand peninsular (Andaman coast) encountered 2004 tsunami resulted from 9.2 magnitude earthquake of Sumatra-Andaman catalogue and the bedform structures and washover sediments are preserved (Choowong et al., 2007; Fujino et al., 2010; Fujino et al., 2008). In addition, the remains of sand sheet were found in marshy swales which are interpreted as tsunami overwash sediments

(Jankaew et al., 2008). Whereas the eastern coast (Gulf of Thailand coast) experienced storms frequently with no tsunami records. The absence of tsunamis in the region can be advantages for characterizing storm deposits because it insists that washover layers observed in the area tend to be induced by storms rather than tsunamis (Wallace et al., 2014).

An initial study of storm deposits in the Gulf of Thailand was set up along the western coast (Phantuwongraj et al., 2013; Phantuwongraj et al., 2010; S. Phantuwongraj et al., 2008). They describe sedimentological characteristics of storm deposits which are induced by modern strong northeast monsoon winds and low-pressure systems. Subsequently, paleostorm was studied on the same coast by (Williams et al., 2016). Using the criteria of sharp upper and lower contacts between coarser and finer grain sediments, the 19 typhoon layers are classified. The results show that eleven typhoons strike at Cha-am site and the others strike at Kui Buri site within the last 8,000 years. The Bayesian age-depth model reveals that typhoons are more frequent and intense in the mid-Holocene. Moreover, ancient storm sediments have been found up to 27 layers at Prachuap Khiri Khan area by (Kongsen, 2016). Four layers formed in the late-mid Holocene, while twenty-three layers are older.

Thailand have been attacked by several intense storms (Figure 2.14); Tropical storm Harriet (1952), Tropical storm Ruth (1970), Typhoon Gay (1989) and Typhoon Linda (1997) which made landfall in Thailand as the tropical storm. Nevertheless, the records of sedimentological characteristics are very little. This is a problem for evaluating intensity of paleostorms generated each layer of overwash deposits. The latest tropical storm Pabuk landfalling in Thailand in 2019 gives an opportunity for sampling and analysing the sedimentary characteristics of modern intense storm. These will provide a modern analog that can be beneficial to evaluate intensity of paleostorms in Thailand.

In December 31th, 2018, the tropical storm Pabuk developed from low pressure system at the South China Sea and moved to the lower Gulf of Thailand in January 2nd, 2019 causing heavy rainfall in southern Thailand. Pabuk made landfall as a category of tropical storm on January 4th, 2019 at Laem Talumphuk, Pak Phanang

district, Nakhon Si Thammarat province before crossing the peninsular into the Andaman Sea on January 5th, 2019 (Figure 2.15).

Due to moving counter clockwise, the front right of the Tropical storm Pabuk threatens the northern part of Nakhon Si Thammarat province along the western coast of the Gulf of Thailand. Maximum wind speeds of 95 km/h cause maximum wave runup up to 3-5 metres, especially on the coast of Nakhon Si Thammarat and Surat Thani (Hydro-Informatics Institution Thailand, 2019).

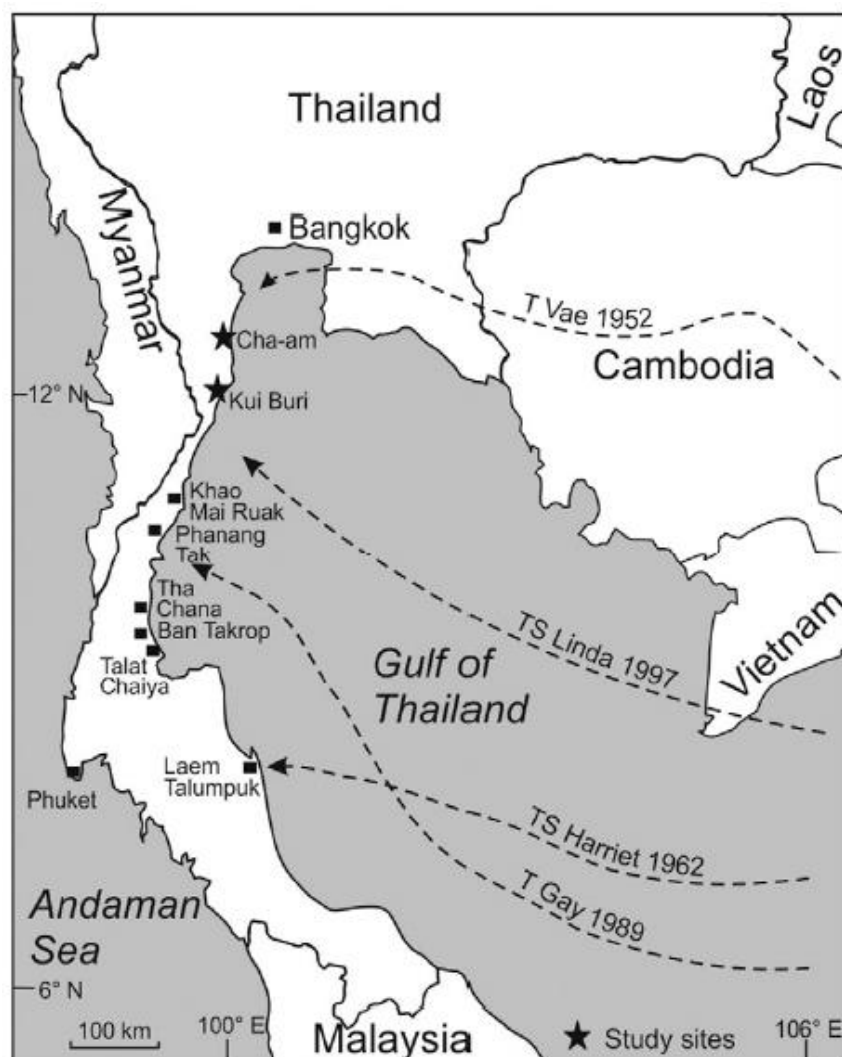


Figure 2.14 Tracks of recent tropical cyclones landfalling in the Gulf of Thailand. (Williams et al., 2016)

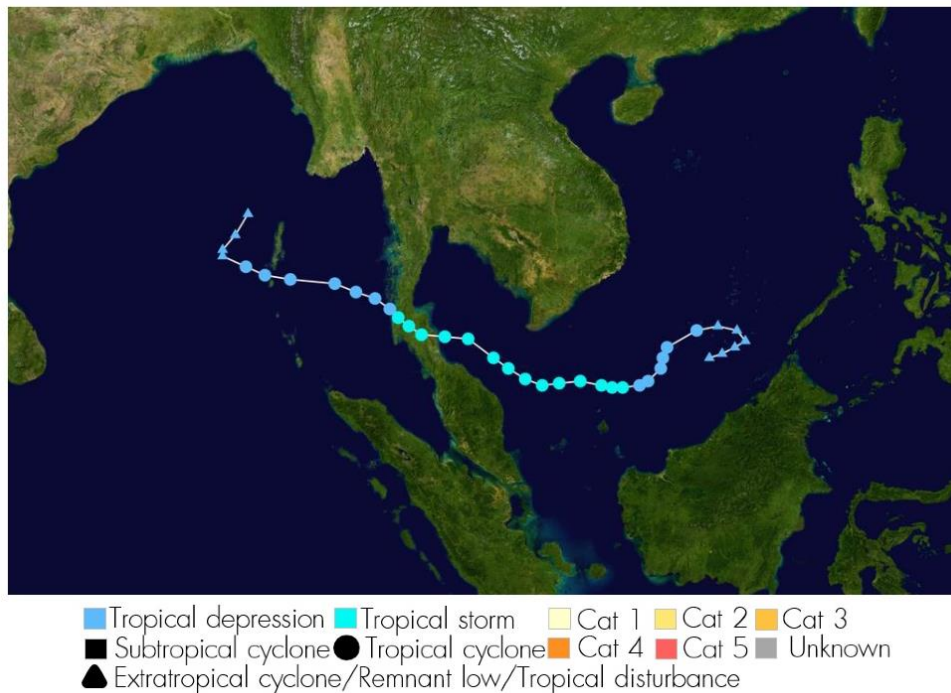


Figure 2.15 Map showing track and intensity of the tropical storm Pabuk on the 4th of January 2019 (Wikipedia, 2019)

About two weeks after the landfall of Pabuk on January 4th, 2019, a primary survey was set up along the eastern peninsular of Thailand from Phetchaburi to Nakhon Si Thammarat confronting the front right of the storm. Evidences of storm surge can be seen clearly. Erosional features such as beach erosion and beach scarp are also found along with failure of onshore vegetation and electric pole. Furthermore, washover deposits can also be observed in back-barrier environments with some sedimentary structures on the surface such as current ripples. The deposits exhibit two types; perched fan and washover terrace. These can be useful for the study of recent storm's sedimentary characteristics. In this research, the hydrological data were collected including wind speeds, wave height and tidal range recorded along the W-GOT and also applied sedimentological techniques, ground penetrating radar (GPR) and microfossils analysis on the storm deposits.

CHAPTER 3

HYDRODYNAMIC CONDITIONS AND WASHOVER MORPHOLOGY

3.1 Hydrodynamic conditions

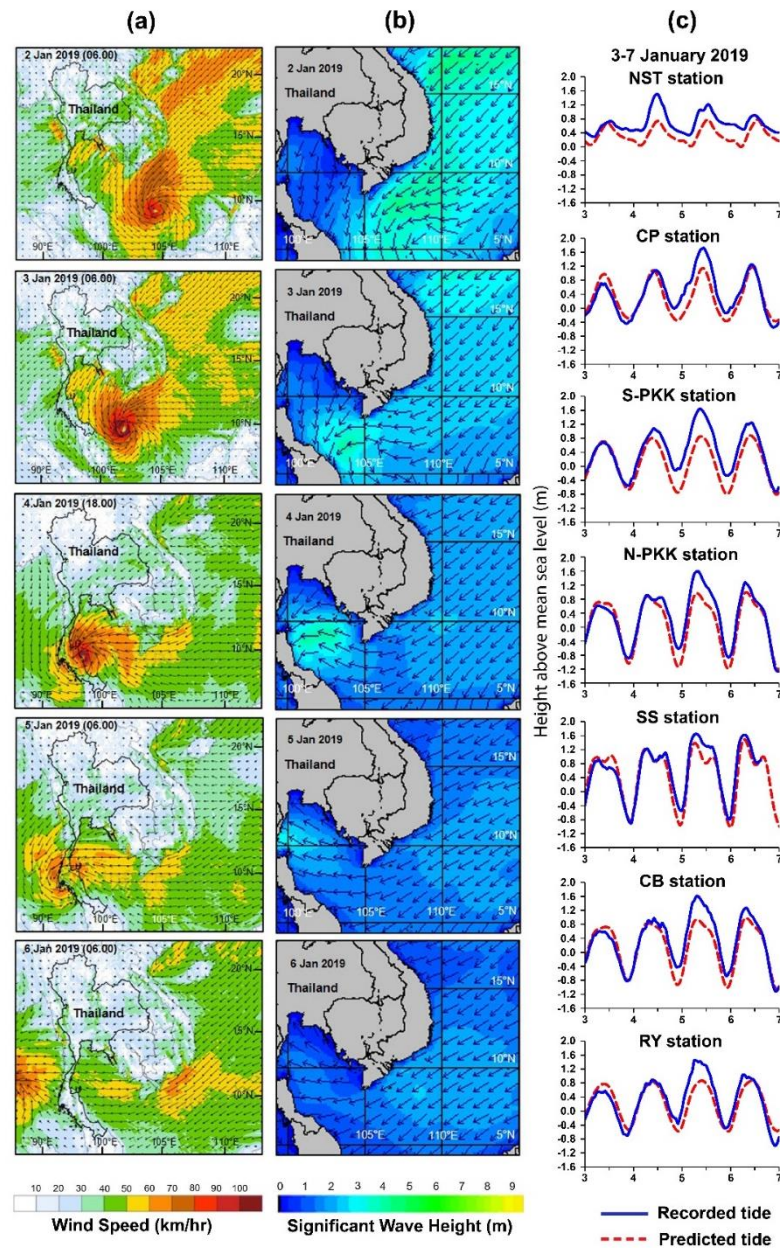


Figure 3.1 (a) Wind speeds and (b) wave height during an arrival of the tropical storm Pabuk from January 2nd to 6th, 2019 obtained from WRF-ROMS (Thaigeo) model (Hydro-Informatics Institute Thailand, 2019). (c) Predicted and recorded tidal level above mean tide level (MTL) recorded by the Royal Thai Navy.

3.1.1 Wind speeds

Wind speeds at 10 m height due to tropical storm Pabuk obtained from WRF-ROMS (Thaigeo) model are shown in Figure 3.1a (Hydro-Informatics Institute Thailand, 2019). During January 2-3, widespread strong wind has maximum speeds of 80-100 km/h covering most of the SCS. Storm's left front also attacked on the southern coast of Vietnam. On January 4, the storm moved to GOT. Most parts of SCS returned to normal while wind was stronger along the western coast of GOT. The most intense area affected highest wind speeds of ~100 km/h is Nakhon Si Thammarat (NST) province where the storm's eye made landfall, with Suratthani (ST), Chumphon (CP), Prachuap Khiri Khan (PKK) and Phetchaburi (PC) (see locations in Figure 3.3) following in descending order. After the moving of Pabuk into the Andaman Sea on January 5-6, wind speeds in GOT decreased significantly until back to normal condition.

3.1.2 Wave height

Significant wave heights induced by the storm is also corresponding to wind speeds as shown in Figure 3.1b. On January 2, waves of 3-5 m height distributed widely in SCS especially near the Vietnam coast. On January 3-4, the cluster of high waves was smaller and located at southern GOT. The maximum wave height was almost 5 m appeared at Nakhon Si Thammarat offshore. Although the storm has crossed the Thai peninsular into the Andaman Sea, the remains of 2-4 wave heights still affected the coast of Chumphon and Prachuap Khiri Khan.

3.1.3 Tidal range and inundation in the GOT

Apart from higher wave height, storm wind induced tidal range higher than usual conditions. Tidal data collected by the Marine Department (2019) and Hydrographic Department (2019) of the Royal Thai Navy revealed that the recorded tide during the storm event was higher than the predicted tide as shown in Figure 3.1c (The name of stations used in the study derived from provinces, not the real name from the Royal Thai Navy index). According to 7 tide gauge stations including NST, CP, Southern PKK (S-PKK), northern PKK (N-PKK), Samut Songkhram (SS),

Chonburi (CB) and Rayong (RY), maximum differences between predicted and recorded tide or storm surge height at most stations was about 0.6-0.8 m, only SS station located at innermost of the Gulf has the maximum differences of 0.3 m. On January 4 about noon, there is only NST station showing significant differences between predicted and higher recorded tide, whereas other stations reached their peak on January 5. The maximum storm surge height of 0.8 m was at NST station, nearest station to the storm's eye, whereas those of CP, S-PKK, N-PKK, SS, CB and RY were 0.6, 0.7, 0.6, 0.3, 0.7 and 0.6 m, respectively. On the 6th January, tidal range at all stations seemed to be returned to normal. Moreover, the maximum storm surge height at most stations noticeably occurred during the midday high tide. High tide cooperated with storm surge height, hence, brought storm tide up to 1.7 m above mean sea level at CP station (Figure 3.2), about 1.6 m at S-PKK, N-PKK, SS and CB, 1.5 m at NST and 1.4 m at RY.

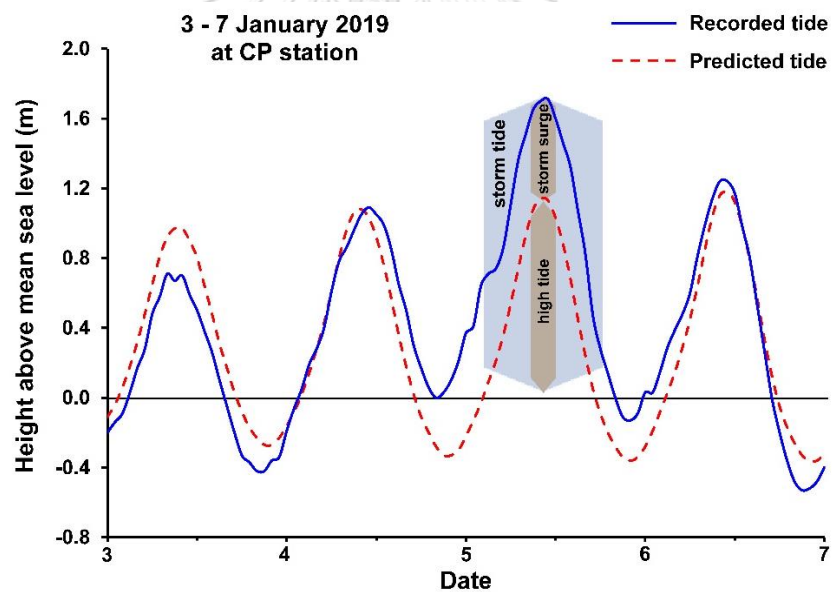


Figure 3.2 Example of predicted tide (broken red line) and recorded tide (solid blue line) from Chumphon tide gauge station (CP) showing high tide level in normal condition and recorded high tide level that is significantly higher than usual at the midday of January 5th, 2019 which is an effect of the TS-Pabuk. The difference between normal high tide and recorded tide is storm surge height, while the combination of them is storm tide level.

High storm tide and wave height induced maximum inundation to extended farthest 330 m and 210 m inland at site 3 and 4, respectively (see table.1). These two sites are located at NST the nearest location to the landfall site of storm's eye. However, the length of inundation does not in descending order to distances from the landfall site. Inland flooding at farther site, for example, site 16 can reach to 130 m from coastline. Likewise, inundation at site 39 extended 50-120 m from coastline.

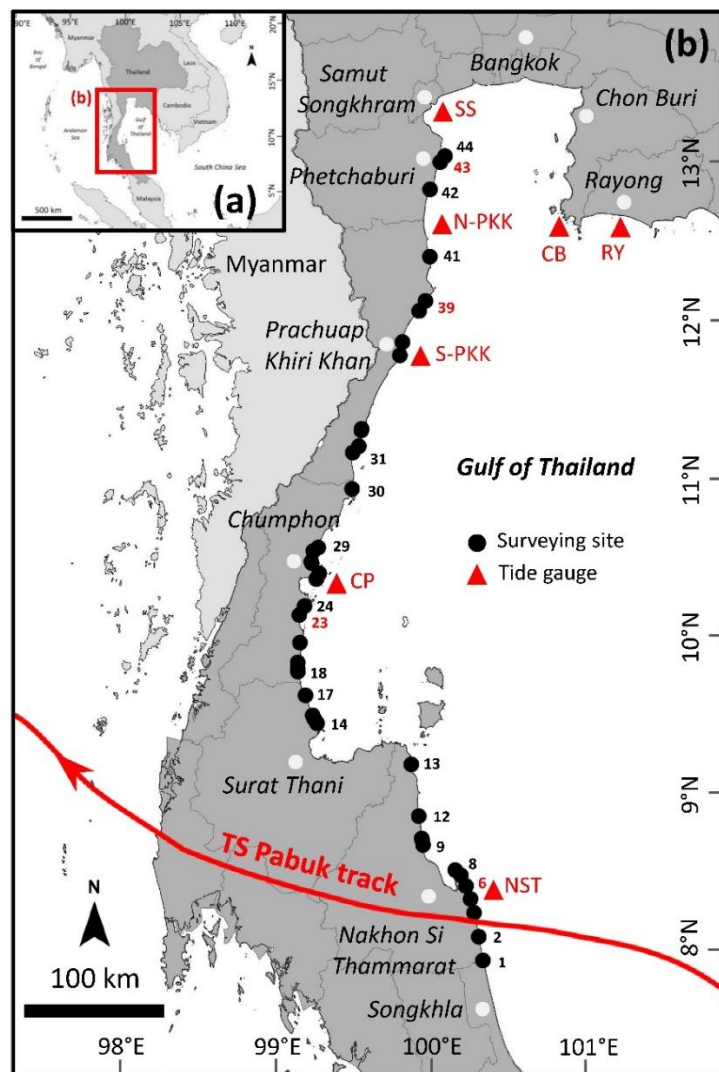


Figure 3.3 The tropical storm Pabuk track (red line), the 44 initial surveying sites (black dot) and the 7 tide gauge stations (red triangle) along the Gulf of Thailand (GOT) supported by the Marine Department (2019) and Hydrographic Department (2019) of the Royal Thai Navy including 5 stations from the western GOT; Nakhon Si Thammarat (NST), Chumphon (CP), South-Prachuap Khiri Khan (S-PKK), North-Prachuap Khiri Khan (N-PKK), Samut Songkhram (SS) and from the eastern GOT; Chonburi (CB) and Rayong (RY).

3.2 Damages and erosional features

Strong winds damaged infrastructures and natural beaches along the W-GOT coast. The most severe case occurred at Pak Phanang, NST province where many knocked down trees and electric poles were found. Seawater flooding also brought the sediments to deposit on the local road blocking transportation in the village (Figure 3.7). The common erosional feature is beach scarp that was found in many locations (Figure 3.8) with the maximum height of up to 80 cm at NST and CP.



Figure 3.4 (a), (c) and (d) Knocked down trees at Nakhon Si Thammarat and Chumphon. (b) Washover sediments covering local road were partly cleared out at Laem Talumphuk, Nakhon Si Thammarat. (e) and (f) Knocked down electric pole at Laem Talumphuk.

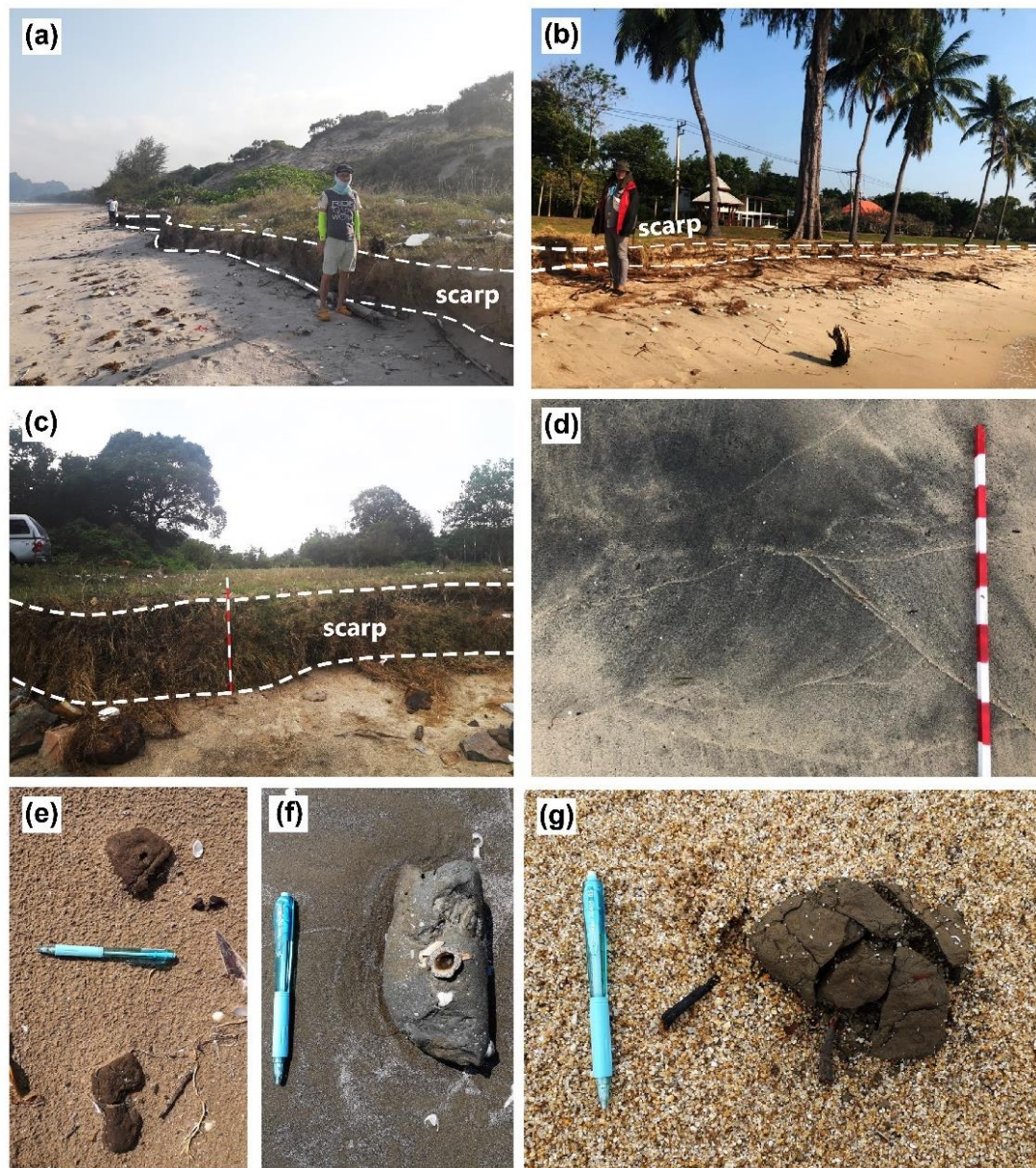


Figure 3.5 a), (b) and (c) Beach scarp Chumphon, Prachuap Khiri Khan and Nakhon Si Thammarat with the maximum height of about 80 cm. (d) Heavy mineral at Nakhon Si Thammarat. (e) and (g) mud rip-up clasts on sand beaches at Chumphon. (f) Mud rip-up clast at muddy beaches in Prachuap Khiri Khan.

Table 3.3.1 Summary of morphology setting, depositional and erosional features, sedimentary structures and inundation detail from each surveying sites. (PF: Perched Fan, WT: Washover Terrace, * Wind blowing from land to sea, Site 1 = Songkhla, Site 2-13 = Nakhon Si Thammarat, Site 14-17 = Suratthani, Site 18-31 = Chumphon, Site 32-41 = Prachuap Khiri Khan and Site 42-44 = Phetchaburi)

Site	Province	District	Morphology	Depositional feature		Damages and erosional features	Bedform surface	Inundation (m)
				Washover types	Thickness (cm)			
1	SK	Ranot	sand beach	no	-	-	-	no
2	NST	Hua Sai	sand beach	no	-	-	-	No*
3	NST	Pak Phanang	near channel inlet	perched fan	< 1	150	-	330
4	NST	Pak Phanang	sand beach with seawall	perched fan	10	-	current ripple (sinuous, straight)	210
5	NST	Pak Phanang	sand beach	perched fan	30	25-30	knocked down coconut trees, scoured depth 1 m	-
6	NST	Pak Phanang	sand beach with seawall	perched fan	-	55	current ripple (straight)	-
7	NST	Pak Phanang	sand spit	washover terrace	-	80	-	-
8	NST	Pak Phanang	sand spit	washover terrace	-	-	knocked down trees and electric poles	-
9	NST	Tha Sala	sand beach	washover terrace	-	20	-	100
10	NST	Tha Sala	sand beach with riprap	perched fan	-	10	beach scarp 80 cm height	-
11	NST	Tha Sala	sand beach with riprap	perched fan	-	10	beach scarp 50 cm height	-
12	NST	Tha Sala	sand beach	washover terrace	5-10	10	-	15
13	NST	Khanom	sand beach between headlands	no	-	-	-	no
14	ST	Chaiya	sand beach	no	-	-	-	-
15	ST	Chaiya	channel inlet	perched fan	20-60	40	beach scarp 1 m height	-
16	ST	Chaiya	sand beach	no	-	-	-	130
17	ST	Tha Chana	channel inlet	perched fan	30	45	-	-
18	CP	Lamae	sand beach	washover terrace	10	10-20	-	-
19	CP	Lamae	channel inlet	washover terrace	40	-	-	55
20	CP	Lang Suan	sand beach	perched fan	5	20	-	no
21	CP	Lang Suan	sand beach	perched fan	-	20	-	-
22	CP	Lang Suan	sand beach between headlands	perched fan	-	5-10	-	50

Table 3.1 (continued) Summary of morphology setting, depositional and erosional features, sedimentary structures and inundation detail from each surveying sites. (PF: Perched Fan, WT: Washover Terrace, * Wind blowing from land to sea, Site 1 = Songkhla, Site 2-13 = Nakhon Si Thammarat, Site 14-17 = Suratthani, Site 18-31 = Chumphon, Site 32-41 = Prachuap Khiri Khan and Site 42-44 = Phetchaburi)

Site	Province	District	Morphology	Depositional feature			Damages and erosional features	Bedform surface	Inundation (m)
				Washover types	Thickness (cm)	Distance (m)			
23	CP	Thung Tako	Mudflat	washover terrace	20	15-20	scoured depth 20 cm	rip-up clast	80
24	CP	Sawi	sand beach	perched fan	5	5	road failure	-	-
25	CP	Mueang	sand beach near headland	perched fan	5	30	scoured depth 0.5-1 m	-	35
26	CP	Mueang	headland	no	-	-	-	-	-
27	CP	Mueang	sand beach	washover terrace	20-30	20	-	-	-
28	CP	Mueang	sand beach	washover terrace	-	15	-	-	-
29	CP	Mueang	clay beach near headland	washover terrace	20-30	5-10	-	-	30
30	CP	Pathio	sand beach between headlands	washover terrace	-	9	-	-	6
31	CP	Pathio	sand beach	no	-	-	beach scarp 80 cm height	-	-
32	PKK	Bang Saphan	sand beach	washover terrace	-	-	scoured depth 30-40 cm	-	-
33	PKK	Bang Saphan	sand beach near headland	no	-	-	knocked down trees	-	25
34	PKK	Bang Saphan	sand beach	washover terrace	-	10	-	-	-
35	PKK	Bang Saphan	sand beach	no	-	-	beach scarp 20-30 cm height	-	-
37	PKK	Mueang	sand beach between headlands	washover terrace	-	7	beach scarp 50 cm height	-	-
36	PKK	Mueang	sand beach near headland	perched fan	-	-	-	-	-
38	PKK	Kui Buri	sand beach	perched fan	-	10	beach scarp 10 cm height	-	-
39	PKK	Kui Buri	sand beach between headlands	perched fan	10-20	20	-	-	50-120
40	PKK	Kui Buri	mudflat	washover terrace	-	30	-	current ripple (straight), rip-up clast	-
41	PKK	Pran Buri	sand beach	washover terrace	20	10	beach scarp 10 cm height	-	-
42	PB	Cha-aim	sand beach	washover terrace	5	15-20	-	-	-
43	PB	Mueang	sand beach	washover terrace	10	-	-	-	-
44	PB	Ban Laem	mudflat with seawall	perched fan	10-20	90	-	current ripple (straight, sinuous, linguoid)	-

3.3 Washover Morphology

3.3.1 Surface morphology

After the survey for 44 points along W-GOT the 2 points at Songkhla (SK) and NST located lower than the eye of storm has no evidence of inundation and washover deposits. Eyewitness accounts confirmed that there are no surges during the storm event, but only wind blowing from land toward the sea. The 32 points located higher than the storm's eye preserved washover deposits in coastal areas. According to the washover classification depending on shapes that was evolved by Morton and Sallenger (2003), washover deposits in the study area can be classified into 2 types; washover terrace - broaden sediments lying parallel to the shore (Figure 3.4a, b and c) and perched fans - small elongate deposits perpendicular to the shore (Figure 3.4d, e, f, g and h). The maximum inland length of washover deposits was found at NST (Pak Phanang) as shown in Table.1 (site 3) with the length of about 150 m from coastline. Eyewitnesses at this site also informed that seawater was flooded 330 m far from the coastline with its depth of about 70 cm. The maximum thickness was up to 40-60 cm mostly found at channel mouth. Thinning landward is a common feature found in many sites.

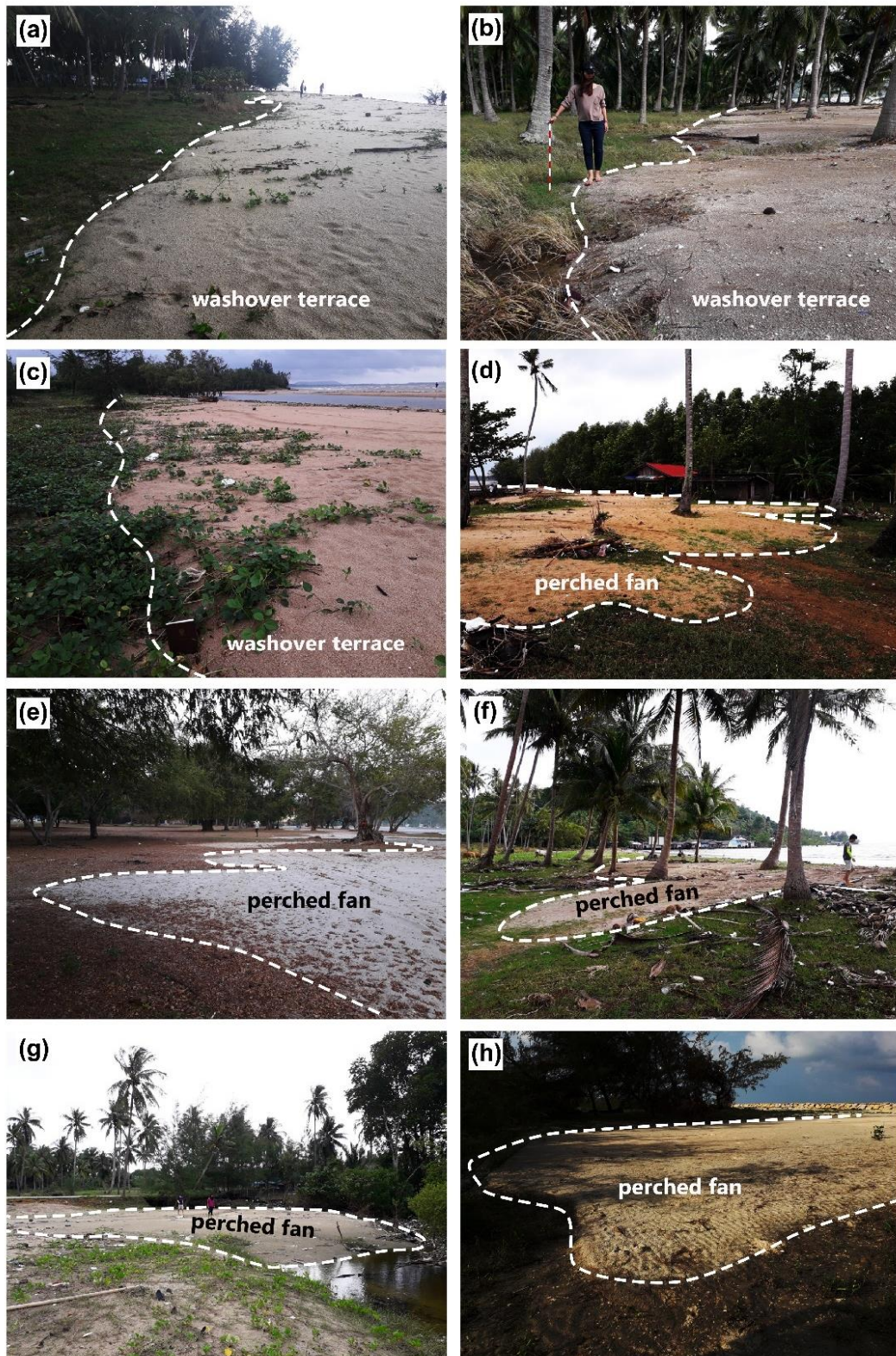


Figure 3.6 a), (b) and (c) Washover terrace at sites 12, 23 and 19, respectively. (d), (e), (f), (g) and (h) perched fans at sites 20, 39, 22, 17 and 16, respectively.

3.3.2 Sedimentary structures

Surficial sedimentary structure induced by the tropical storm Pabuk observed in the W-GOT includes current ripples and mud rip-up clasts. The current ripples were well observed at NST (sites 3, 4 and 5), PKK (site 40) and PB (site 44). Most of them were preserved as straight, sinuous and liguoid features showing seaward current direction (Figure 3.5a, b, c and d). At site 44 (Phetchaburi), the truncation of sediment lobes – the younger fan-shape sediments cutting through the older lobe or sheet (Figure 3.5e, f and g) was found. Additionally, a unique current ripple pattern appeared in the younger cutting lobes (Figure 3.5h). Mud rip-up clasts were rare but could be found in two clay beaches (sites 23 and 39) (Figure 3.8e, f and g).

Internal sedimentary structures (Figure 3.6) include planar stratification, cross stratification, foreset bedding, scouring at base, sharp contact and erosional contact. Based on their stratification, there are up to 3 distinct layers (Figure 3.6b and f). The scoured base and planar stratification were founded at the floor of washover deposits and overtopped by cross stratification dipping toward the land. All of these were covered by planar stratification again. However, some sites might preserve less than this. For instance, at NST (Figure 3.6a and d), only two distinct layers were preserved; lower planar stratification and upper cross stratification. At PKK only horizontal stratification was found overlaid on the sharp contact (Figure 3.6e). Foreset bed was found at CP (site 9) (Figure 3.6c). This site is a pond near the river mouth and will be exposed as a pond during low tide. The foreset bed was found deposit on a sloping surface with landward dipping to the pond.

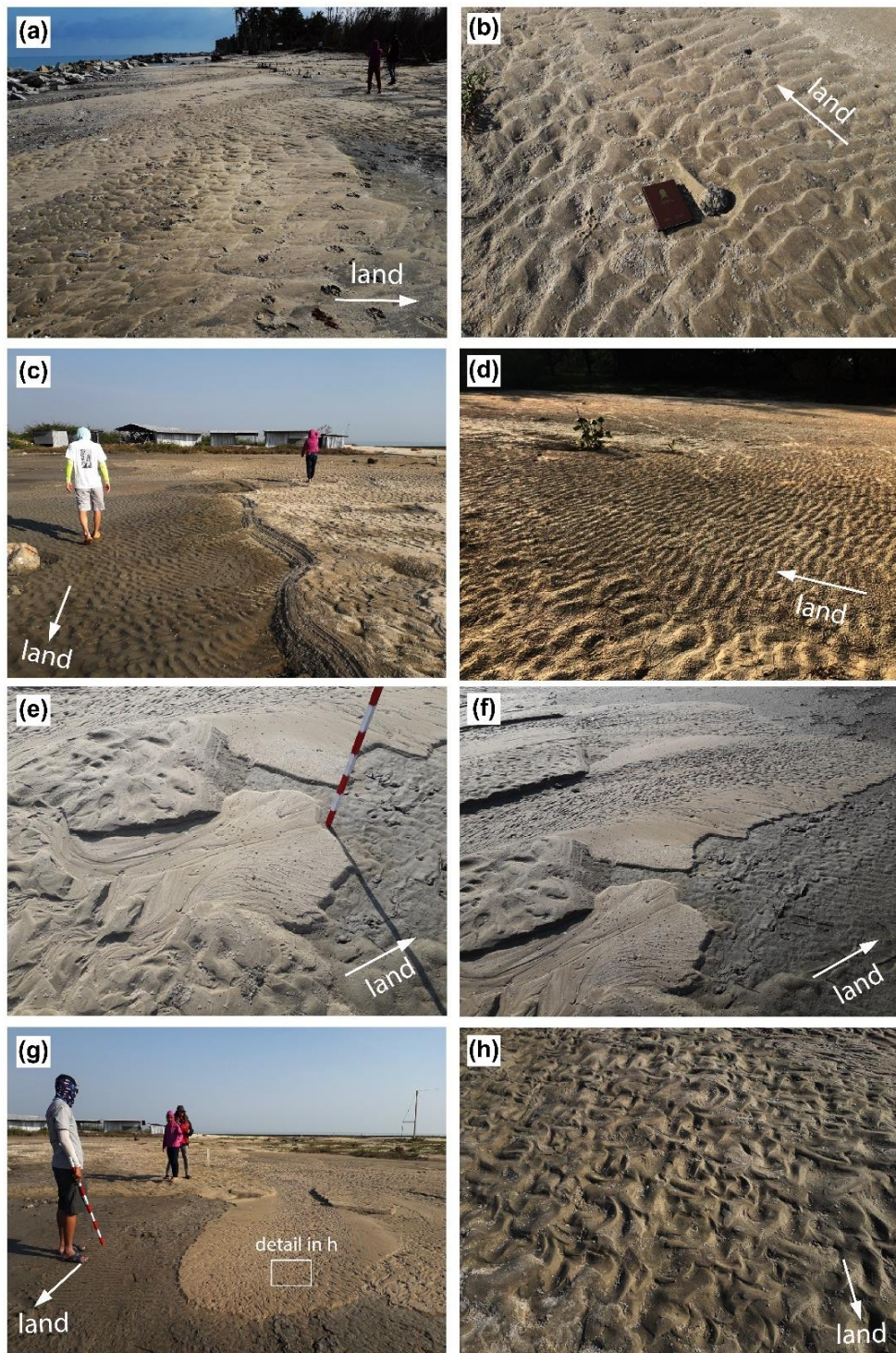


Figure 3.7 (a) Linguoid current ripple at Nakhon Si Thammarat (site 5). (b) Sinuous current ripple at Phetchaburi (site 44). (c) Straight to sinuous current ripple on pre-Pabuk mud and Pabuk sand (site 44). (d) Straight current ripple at Nakhon Si Thammarat (site 6). (e), (f) and (g) Truncation sediment lobes at Phetchaburi (site 44). (h) A unique current ripple on the surface of younger truncating lobes.

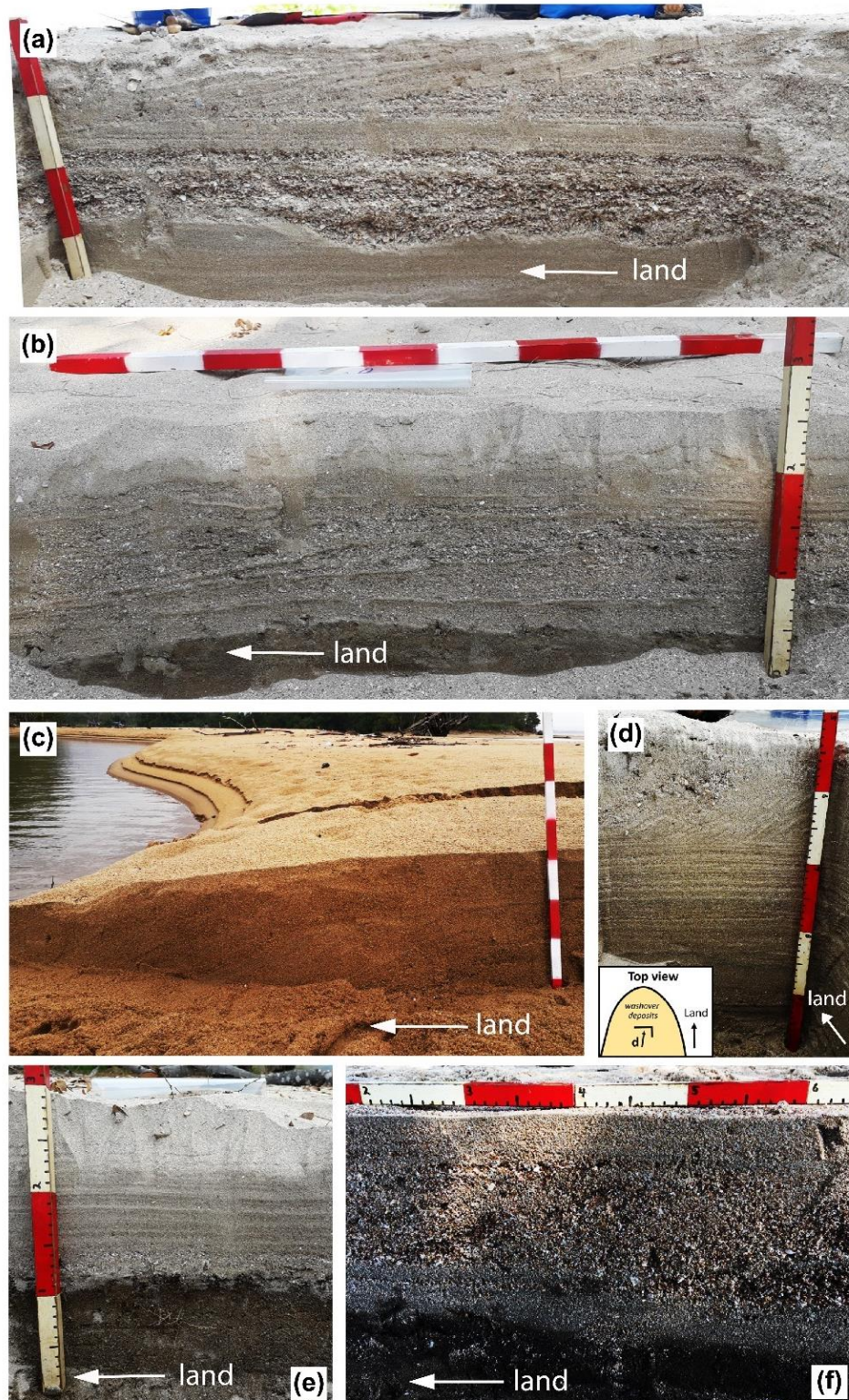


Figure 3.8 (a) Stratification at Nakhon Si Thammarat, erosional base was overlaid by shelly thick bed and horizontal sediment laminations overtopped by inclined laminations dipping landward of much shell sediments and less shell sediments. (b) Stratification at Prachuap Khiri Khan, sharp

contact located at the base overlaid by sub-horizontal bed of sands. Inclined laminations dipping landward located as a middle layer and overtopped by horizontal laminations. (c) Foreset bedding at a pond near river mouth in Chumphon. The inclined bed deposited on a sloping surface and dip landward into the pond. (d) Stratification at Nakhon Si Thammarat, this picture was looked into the land. The contact between Pabuk469 and Pre-Pabuk does not notable but the sequence start with thick planar laminations and overlaid by the inclined laminations dipping to the south. (e) Stratification at Prachuap Khiri Khan showing only sharp contact and planar laminations. (f) Three distinct layers at Phetchaburi, sub-horizontal bed over a sharp contact, cross laminations and overtopped again by horizontal laminations.



CHAPTER 4

STORM DEPOSITS AND MICROFOSSILS

4.1 Storm Deposits

4.1.1 Chao Samran Beach (CSR)

CSR is sandy beach located at the innermost part of GOT between two canals. The beach experienced the weakest hydrodynamic intensity during TS-Pabuk landfall due to the farthest distances. In addition, the coast was protected by several artificial offshore breakwaters that can relieve storm wave energy. The breakwaters are 2 m high from mean tide level and was located 250 m far from the coastline with the spaces of 150 m between each one. This structure allows the accretion of sediments between them and shoreline as tombolo during low tide and the small bay between them. However, the overwash event of TS-Pabuk occurred and leaved Pabuk deposits along the shore as washover terrace. The sampling trench (A-A') is located on the coastal line between two breakwaters (Figure 4.1a)

The Pabuk deposits extended ~16 m inland with the outer edge of distal part that preserved many long and straight current ripples showing landward direction of flow (Figure 4.1b and 4.1c). The thickest deposits are found at the proximal part or pit-5 and thinner inland to ~15 cm at the distal part (pit-2.2) and end up with the 5 cm thickness of current ripples at pit-1.1, 1.2 and 1.3 (Figure 4.1e)

In overall trend, grain size of Pabuk deposits ranges from fine to medium sand at base before grading to coarse to very coarse sand at the middle part. Most pits end up with the fine to medium sand at top. Sorting of Pabuk sediments ranged from moderately well to moderately sorted. Whereas the pre-Pabuk sediments seem to be smaller in grain size (fine to medium sand), containing higher organic matters, moderately well to moderately sorted. Sharp contact can be clearly seen.

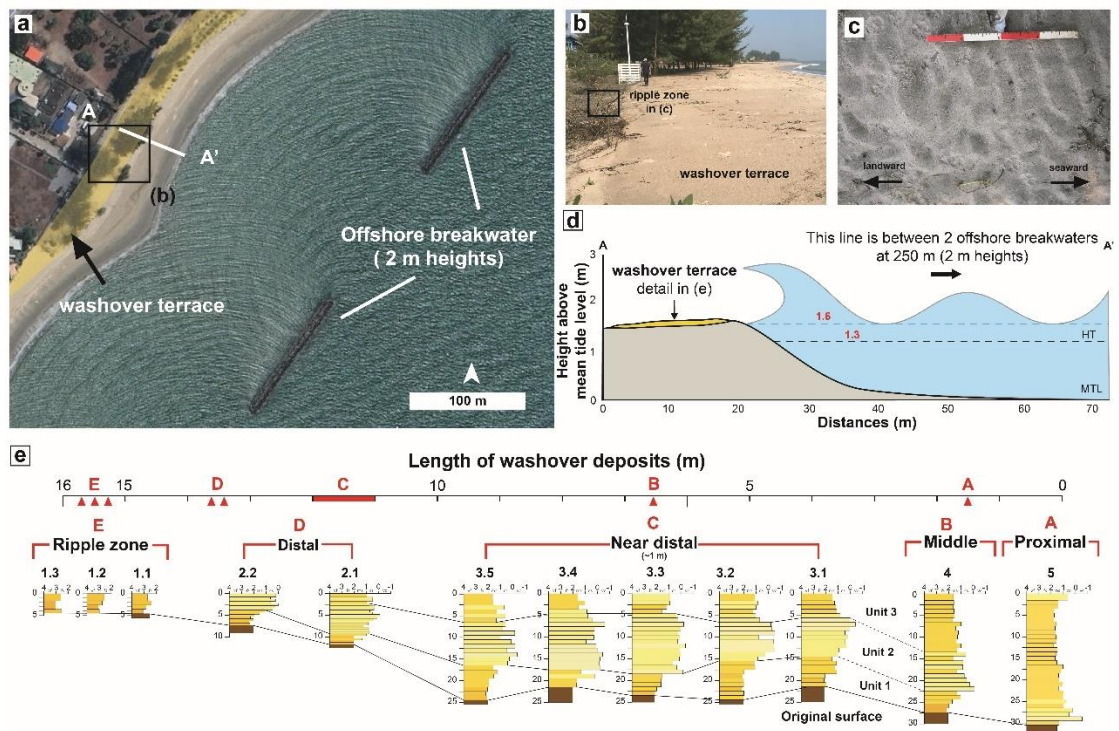


Figure 4.1 Chao Samran Beach (CSR) at Phetchaburi province, western coast of the Gulf of Thailand (a) Satellite images showing washover terrace along the coast with 2 offshore breakwater and studied transect line (A-A') (b) Washover terrace with ripple zone at the distal landward part (c) Current ripple found at distal part of storm deposits (d) Topography of transect line with mean tide level (MTL), high tide level (HT), storm surge level and storm tide above mean tide level in meters (e) positions of pit number 1 to 5 (from landward to seaward) and 12 stratigraphic logs of storm deposits from proximal part (CSR-5), middle part (CSR-4), near distal part (CSR-3.1 to 3.5), distal part (CSR-2.1 to 2.2) and ripple zone (CSR-1.1 to 1.3) though the length of 16 m inland extent. The vertical scale is depth in cm, while horizontal scale is grain size in phi (ϕ) scale.

Although the trend of Pabuk and pre-Pabuk sediments are clearly different, the storm deposits can also be classified into 5 spatial zoning (Figure 5.1e) including proximal part (pit CSR-5), middle part (pit CSR-4), near distal part (pit CSR-3.1 to 3.5), distal part (pit CSR-2.1 to 2.2) and ripple zone (pit CSR-1.1 to 1.3) using the variation of internal sedimentary units. The maximum numbers of horizontal unit within Pabuk deposits are found at the middle and near distal zone that contained 3 clearly distinct units consisting of the underlying unit 1 overtopped by unit 2 and unit 3 at

the surface. Whereas the other part contains only 1 or 2 horizontal units. These units show the differences in both sedimentary structures and grain geometries.

1) Proximal zone (A)

This zone is nearest to the sea. The Pabuk sediments of CSR-5 has 30 cm thickness. The deposits relied on the pre-Pabuk sediments with sharp contact boundary. At CSR-5, larger grain sizes of medium (1.38 ϕ) to very coarse sand (-0.47 ϕ) are accumulated at the lower base of the sequence for 6 cm. The upper units are thicker and contain predominantly medium sand (1.04 – 1.83 ϕ). At the base of this unit, however, contains significantly higher mud contents (1.43%). This might be an effect of strong currents that eroded some muds from the original surface to be mixed in the current and deposited as a thin layer inside the sandy storm sequence. The coarse sand (0.69 ϕ) then was deposited at the surface due to the high shell fragments. This layer is also higher in mud contents (0.89%) due to the late state of inundation that allow settling of muds (Figure 4.3a).

2) Middle zone (B)

CSR-4 is located at 2 m landward far from CSR-5. However, this pit is a representative of the most Pabuk deposits throughout the lengths. the Pabuk sediments seem to be organized into 3 distinct units considering from grain size and sorting. The lower unit 1 contains fine (2.16 ϕ) to medium (1.14 ϕ) grain size with reverse grading of 5 cm thickness with the moderately well to moderately sorted (0.54 – 0.82 ϕ). The middle unit 2 are ~11 cm thick containing mainly coarse to very coarse sand and some thin layers of medium sand (0.10 ϕ to 1.65 ϕ). The sorting is fluctuated ranging from well (0.49 ϕ) to poor (1.31 ϕ) sorted. The topmost unit 3 of 11 cm thickness is quite homogeneous in grain size and sorting with the medium sand (1.06 – 1.72 ϕ) and well to moderately well sorted (0.49 – 0.65 ϕ). Like CSR-5, the top 2 samples show higher mud contents of 1.00 – 1.25 % (Figure 4.3b).

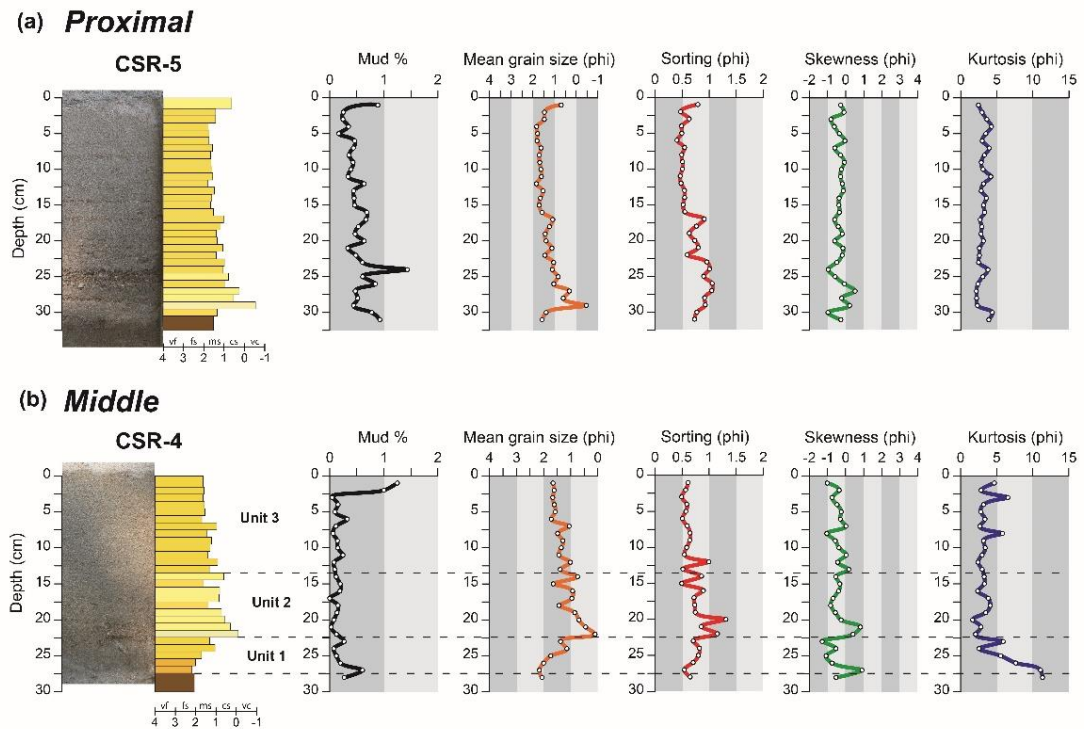


Figure 4.2 Sedimentological characteristics of TS-Pabuk deposits (yellow part) and pre-Pabuk (brown part) at CSR in proximal part (CSR-5) and middle part (CSR-4) showing mud content (%), mean grain size, sorting, skewness and kurtosis. CSR-5 shows fining upward trend with a thin layer of coarse sand capping at the surface. CSR-4 was organized as 3 distinct layers of unit 1 (coarsening upward), unit 2 (largest grain size and poorest sorted) and unit 3 (fining upward). The vertical scale is depth in cm, while horizontal scale is grain size in phi (ϕ) scale.

3) Near distal zone (C)

The 'Near distal zone' is a narrow zone of about 1 m length located between 11th to 12th m of the transect line or 2 m seaward far from distal zone (Figure 4.1e). The sediment samples are collected for 5 vertical sequences within 1 m length including CSR-3.1, 3.2, 3.3, 3.4 and 3.5 from the seaward to landward side, respectively (Figure 4.4a). Although the Pabuk sequence can be classified into 3 units as same as CSR-4 of the middle zone, the sedimentary characteristics are different, especially in unit 2 as following details;

Unit 1 is the most underlying unit of horizontal laminated white to light gray sand that contacts to the pre-Pabuk sediment with sharp and erosional boundary.

The thickness varied from 5 – 9 cm. Although grain size distribution of this unit has a wide range from fine sand (2.15 ϕ) to coarse sand (0.18 ϕ), medium sand is most abundant (average mean grain size of 1.88 ϕ). Furthermore, some thin laminations of coarse sand (CSR-3.4) are also usually presented with large shell fragments. This unit also presents the reverse grading in all sequences. Most sorting ranged from moderately well sorted (0.51 ϕ) at bottom to poor sorted (1.09 ϕ) at top of the unit. Poor sorting seems to be related to large grain size layer. Skewness is quite varied and fluctuated from very coarse skewed (-1.68 ϕ) to fine skewed (1.14 ϕ). Kurtosis in all sequences tends to start from higher value at bottom to lower value at top of the units. The maximum value is 11.23 ϕ (very leptokurtic) at base of CSR-3.3, while the minimum value is 2.28 ϕ (platykurtic) found at CSR-3.1. Moreover, this trend is in reverse to mean grain size as shown in the graph (Figure 4.4b)

Unit 2 is the middle unit of cross laminations of coarse to very coarse sands with the thickness of about 10 - 15 cm. This lamination shows landward direction but different angles. Hence, they are classified into two types; 9° beds and 20° laminations (Figure 4.4a). The 9° beds are two sets of 2.5 - 3 cm thick beds. They contain very coarse sand (-0.28 to -0.61 ϕ) with moderately well sorted (0.53 to 0.70 ϕ). This section was found from CSR-3.1, clearly seen at CSR-3.2 and end up at the foot of CSR-3.3. The two beds were interrupted by coarse sand (0.75 ϕ) with poor sorted (1.26 ϕ). From CSR-3.3 to 3.5, the angle and thickness of sediments are steeper and thinner as called 20° foreset laminations. The grain size ranges from coarse (0.97 ϕ) to very coarse (-0.68 ϕ) sand. Overall trend of skewness ranges from fine skewed (0.85 ϕ) to coarse skewed (-0.69 ϕ). Kurtosis ranges from platykurtic (1.85 ϕ) to mesokurtic (2.55 ϕ).

Unit 3 deposited at the top of all sequences with ~5 cm thickness. This unit shows the same horizontal laminations as found in unit 1. Most pits tend to show normal grading except at CSR-3.3 showing reverse grading. The medium sand (1.18 - 1.61 ϕ) is the main proportion of this unit. However, coarse sand (0.56 – 0.99 ϕ) can

be found in some thin layers. Mud contents at the topmost layer or near surface are a bit higher. The sorting ranges from well sorted (0.46ϕ) to moderately sorted (0.91ϕ). Skewness ranges from very coarse skewed (-0.76ϕ) to symmetrical skewed (0.22ϕ), whereas kurtosis ranges from platykurtic (2.35ϕ) to leptokurtic (4.42ϕ).

Pre-Pabuk sediments were collected for one sample for each sequence. The significant characteristic of the layer is a high organic matter which can be clearly seen from the darker color. The sediments were mixed with some root fragments. However, the results from wet sieve did not indicate the significant high mud contents except at CSR-3.3 which contain the maximum volume up to 4.08 %. Mud contents can also be found higher at near the boundary between unit 1 and unit 2 as shown in the CSR-3.4. Nevertheless, grain size in this unit is distinctly smaller than Pabuk sediments. The main proportion is fine sand (2.20 to 1.15ϕ). Even though the CSR-3.5 pre-Pabuk sand is classified as medium, the grain size parameter is up to 1.91ϕ which is almost as fine as other pits. The sorting ranges from moderately well (0.55ϕ) to moderately sorted (0.72ϕ). Skewness ranges from coarse skewed (-0.55ϕ) to Fine skewed (1.14ϕ). Kurtosis is quite high compared to other units of Pabuk sediments. All samples of pre-Pabuk shows very leptokurtic ranging from 7.33ϕ to 11.23ϕ .

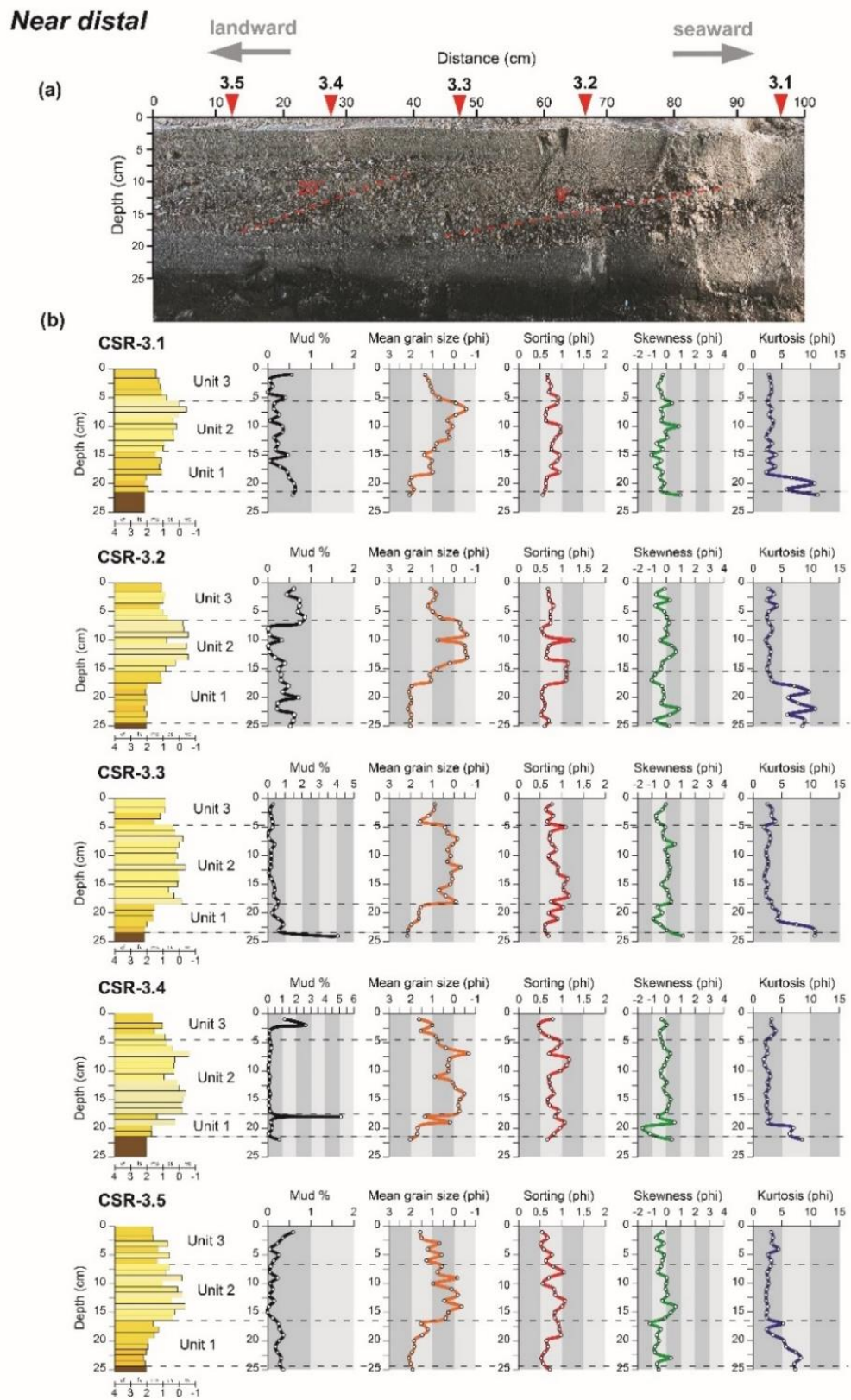


Figure 4.3 Sedimentological characteristics of TS-Pabuk deposits (yellow part) and pre-Pabuk (brown part) at CSR in near distal part (CSR-3.1 to 3.5) located far from the landward avalanched

face for about 4 m. (a) photo of near distal part of 100 cm lengths with the sampling position (red triangle on the horizontal scale). The cross laminated angles (broken red line) are steeper landward from 9° to 20°. (b) sedimentological characteristics of 5 sampling points including mud content (%), mean grain size, sorting, skewness and kurtosis. This part presented the 3 units pattern of storm deposits including the lower unit 1, the middle unit 2 with cross-lamination and the upper unit 3. Coarsening upward at base and fining upward at top are clearly presented. The vertical scale is depth in cm, while horizontal scale is grain size in phi (ϕ) scale.

4) Distal zone (D)

This zone is located at ~13th to 14th m of the transect line. Two vertical sequences were collected; CSR-2.1 and CSR-2.2 (Figure 4.1e). Pabuk sediments at the seaward CSR-2.1 are thicker of 11.5 cm and composed of 3 units, while the landward CSR-2.2 are only 7 cm thick and preserved only unit 1 and 2.

At CSR-2.1 (Figure 4.5a), unit 1 dominantly composed of fine sand (2.05 to 2.08 ϕ) and small amount of medium sand (1.12 ϕ). This layer can be differentiated from the pre-Pabuk sediments by sharp contact which is the difference of organic matters reflecting in distinct color. The upper unit 2 seem to be massive, without inclined or even horizontal lamination. Grain size is also clearly larger composing of mainly coarse sand (0.09 to 0.97 ϕ). The upper most unit 3 tends to be a bit smaller in grain size with the mixing of coarse sand (0.64 ϕ) and medium sand (1.09 ϕ). Mud contents in all 3 units are also vary but less than 1% and cannot be an indicator for each unit. Sorting of unit 1 is fluctuated from well (0.49 ϕ) to poor (1.10 ϕ) sorted, while unit 2 shows homogeneously moderately sorted (0.57 to 0.84 ϕ). Unit 3 is also moderately sorted (0.71 to 0.94 ϕ). However, it is noticeable that the poorer sorted the finer grain size and finer skewness. That means sorting and skewness in this sequence seem to be in reverse order in this unit. Kurtosis start from higher in unit 1 which is up to 7.61 ϕ (very leptokurtic) and tends to be lower to mainly mesokurtic (2.55 to 3.41 ϕ) in unit 2 and 3.

At CSR-2.2 (Figure 4.5b), the reverse grading trend is clearly seen. The lower unit 1 composed of only fine to medium sand (1.30 to 2.23 ϕ) before grading to

coarse sand (0.63 to 0.97 ϕ) of the upper unit 2. Overall mud contents are less than 2% but it seems to be high in the middle of each layer. Sorting is in the range of moderately well to moderately sorted (0.5 to 1.05 ϕ). Skewness is very fluctuated. However, it tends to be coarser from bottom to the top of the sequence. Kurtosis of the two units is clearly distinct. Unit 1 shows the higher values of leptokurtic to very leptokurtic (4.00 to 13.35 ϕ). Whereas, the upper unit 2 shows homogeneously mesokurtic (2.27 to 3.23 ϕ).

Pre-Pabuk sediments in all 2 pits contain low mud contents (0.10 – 0.55 %). However, the darker color which is one indicator for differentiating storm and original sediments reflect the higher organic materials. Grain size is fine sand (2.02 to 2.08 ϕ), moderately well sorted (0.58 to 0.61 ϕ), symmetrical skewed (0.00 to 0.20 ϕ) and very leptokurtic (8.25 to 8.42 ϕ)

5) *Ripple zone (E)*

The edge of washover deposits at about 15th to 16th meter preserved current ripples showing straight and long ridge (Figure 4.1e). The shape of these ripple is asymmetry morphology with the lee side at landward part and stross side at seaward part showing the landward flow direction. The thickness from crest to trough of these 3 ripples are about 2 cm thick with the wavelength from crest to crest of about 10 cm. Grain geometry ranges from fine (2.31 ϕ) to medium (1.79 ϕ) sand, moderately well to moderately (0.51 to 0.81 ϕ) sorted, very coarse to fine skewed (-1.47 to 1.01 ϕ) and leptokurtic to very leptokurtic (5.06 to 12.91 ϕ). Mud contents are a bit higher in the upper part of all ridge. In contrast to pre-Pabuk sediments, collected only one sample from CSR-1.1, the mud percentages are lowest (less than 1%). However, grain size seems to be similar with medium sand almost fine sand (1.92 ϕ). Sorting, skewness and kurtosis are moderately well sorted (0.61 ϕ), coarse skewed (-0.11 ϕ) and leptokurtic (6.86 ϕ), respectively (Figure 4.5c and d).

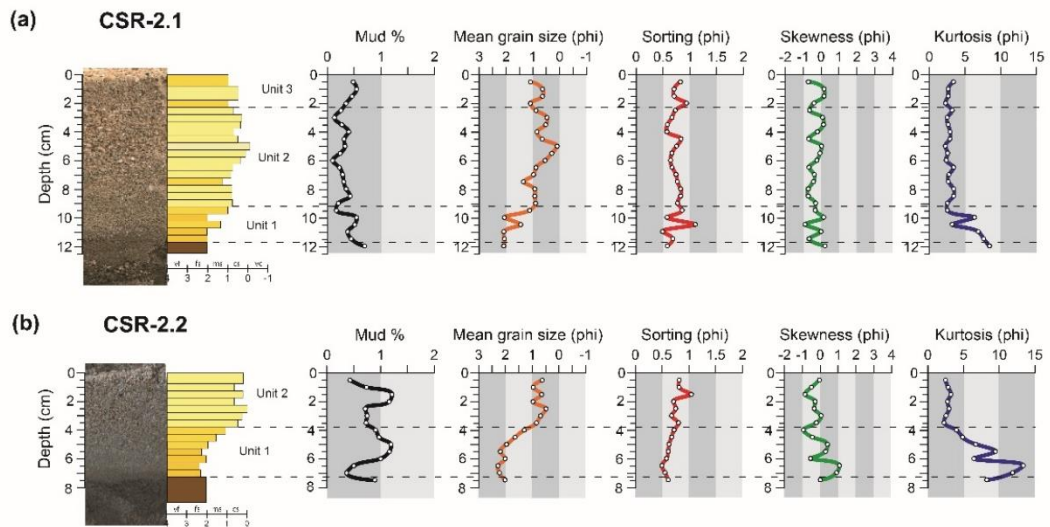
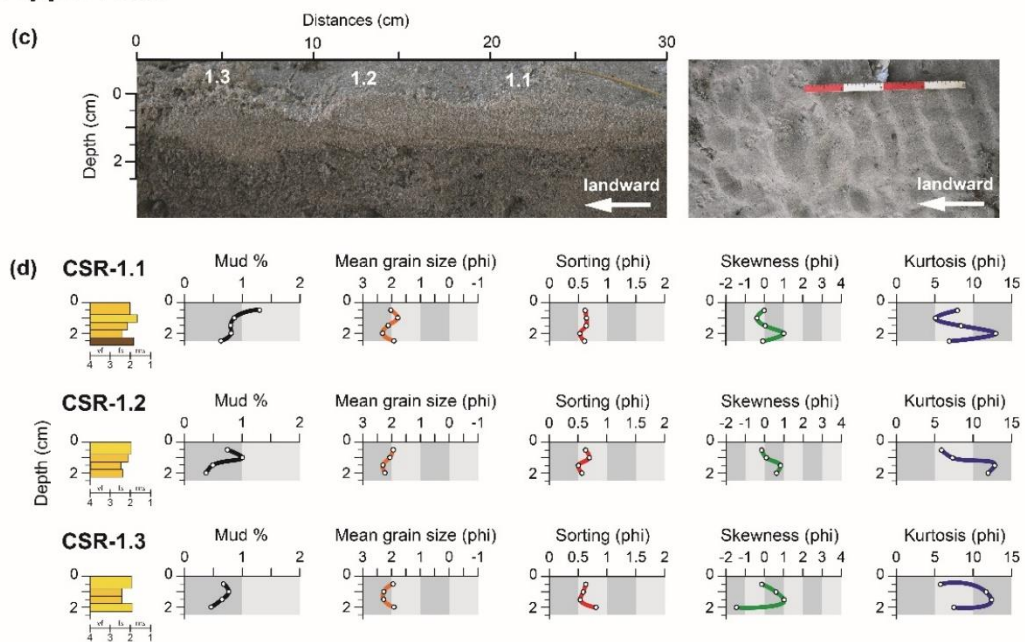
Distal**Ripple zone**

Figure 4.4 Sedimentological characteristics of TS-Pabuk deposits (yellow part) and pre-Pabuk (brown part) at CSR in distal part (CSR-2.1 to 2.2) and ripple zone (CSR-1.1 to 1.3) showing mud content (%), mean grain size, sorting, skewness and kurtosis. The vertical scale is depth in cm, while horizontal scale is grain size in phi (ϕ) scale.

4.1.2 Ban Thung Noi (BTN)

At Ban Thung Noi (BTN) in Prachuap Khiri Khan province, the sandy beach of about 1 km length lies between two rocky headlands of Permian limestone. The beach faces to the open sea without any obstruction. The satellite image from Google Earth on February 24, 2019 showed clearly inundation limit line and washover sediments along the shore. The inundation limit can be clearly notice from the sharp contact between landward green grass zone and seaward brown dry grass zone. This limit range between 50 m in the northern part up to about 100 m in the southern part of the beach (Figure 4.5). Whereas, washover sediments are imaged as several lobe fans in the coastal zone. 3 main transect lines were set up for sedimentological study (BTN-1, BTN-2 and BTN-3).

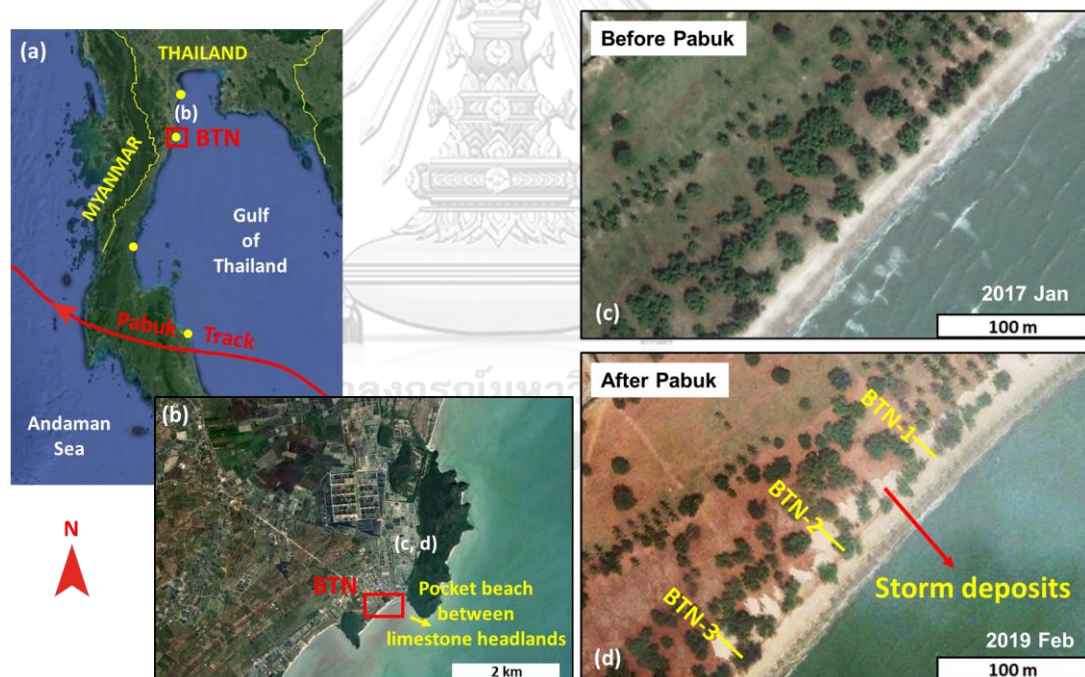


Figure 4.5 Ban Thung Noi (BTN). (a) Location of BTN in Prachuap Khiri Khan province, Western coast of the Gulf of Thailand. (b) BTN located at between the 2 Permian limestone headlands. (c) Satellite images of BTN on 2017 January, 24th before an arrival of TS-Pabuk. (d) Satellite images of BTN on 2019 February, 24th after TS-Pabuk made landfall at Nakhon Si Thammarat on 2019 January, 4th.

According to 17 shallow open pits from 3 transect lines (Figure 4.7, 4.8 and 4.9), Pabuk sediments have maximum thickness of about 25 cm and extend to 23 m length inland. The deposits are thin at the seaside which deposited on sand dune, thickest at the middle part and thinner at the distal landward. Although the main proportion and average grain size of Pabuk sediments is medium sand, the deposits were classified into 2 units using internal structures.

Unit 1 is horizontal laminated sand deposited at the base of Pabuk sediments and on top of the pre-Pabuk original surface with sharp contact. The grain size in this layer has wide range from very fine (3.45 ϕ) to coarse (0.61 ϕ) sand. The very fine and fine sand are always accumulated at base and organized as dark color laminations (BTN-1.3, 1.4). Whereas, coarse and medium sand are assembled with huge amount of shell fragments. It is worth noting that the unit 1 at pit BTN-1.2, 80 cm length open pit, can be classified into 2 subunits; U1A and U1B which were overtopped by unit 2 (Figure 4.6). U1A in this pit contains massive medium sand (1.38 ϕ), moderately well sorted (0.68 ϕ), coarse skewed (-0.72 ϕ) and mesokurtic (3.62 ϕ). This unit lied as sub-horizontal layer above erosional basal contact and may be correlated to unit 1 of CSR. U1B, the middle layer of the sequence between U1A and unit 2, contains coarse sand (0.89 to 0.96 ϕ) at base and normal graded to fine (2.07 to 2.13 ϕ) sand interbedded medium sand (1.25 to 1.64 ϕ) at top. This unit was organized as non-parallel cross laminated and overtopped by horizontal laminations. The cross laminations lie from 10 cm depth at 80 cm distance with low-angle slope (4° and 9°) down to 20 cm depth at landward side. The interval between these two cross laminae is narrower and almost touch at the bottomset. Unit 1 tends to be deposited at the bottommost of middle part of Pabuk sediments, then they are thinner and finally disappeared at the far seaward pits (BTN-2.6) and landward pits (BTN-2.1, 2.2, 2.3, 3.1, 3.2 and 3.3)

Unit 2 is the uppermost semi-massive bed sets of medium sand (average mean grain size of 1.53 ϕ). Collecting samples from this unit is quite difficult because

the sand is very loose and easy to be collapsed. So, the sediment collection is only for a few samples to be a representative of the layer to avoid mixing or contaminating of sediments which can cause misrepresent samples. This unit contains 2 - 3 sets of medium sand with 5-7 cm thickness at the middle pits and thinner at more seaward and landward part. The sets of medium sand are interrupted by very thin layers of shell fragments. However, coarse sand was presented in some pits which always noticeably deposited with shell fragments on the surface.

Pre-Pabuk sediments contains higher mud contents and also organic matters that reflect to the darker color and storm deposits. Grain size tends to be smaller ranging from medium (1.22ϕ) to very fine (3.03ϕ) sand, average sorting is poor sorted (1.21ϕ). Whereas skewness and kurtosis are varied and have no trend.

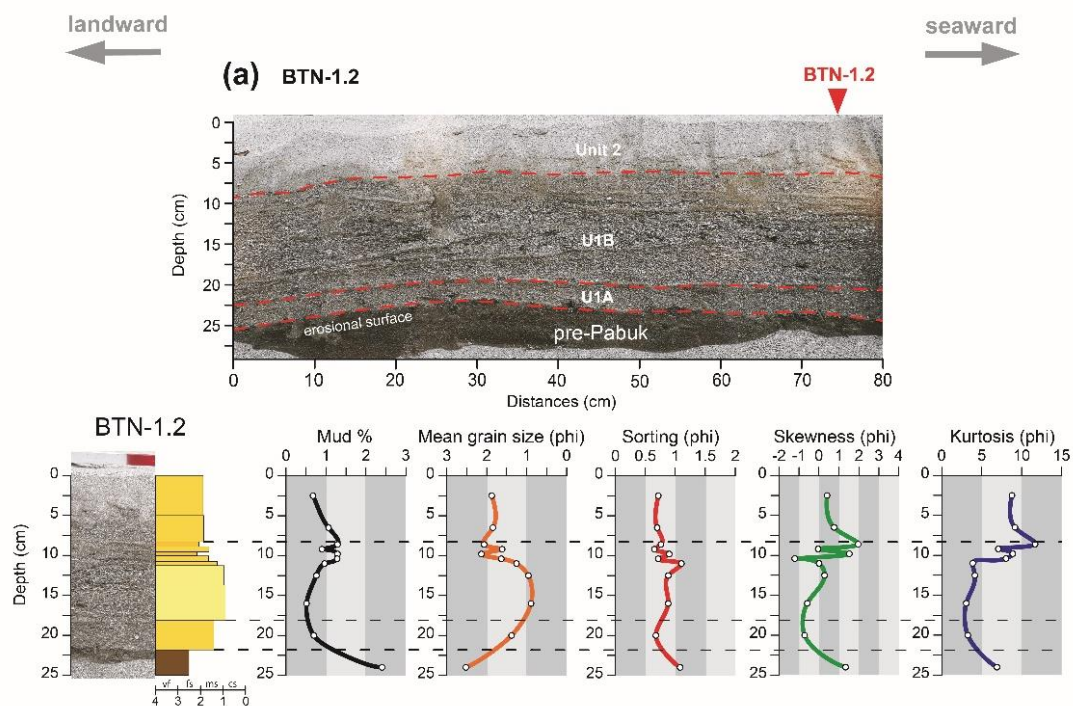


Figure 4.6 Pit BTN-1.2. (a) a photo of open pit with 80 cm width. The Pabuk sediments was classified into 2 subunits; U1A, U1B and Unit 2 lying above pre-Pabuk sediments with sharp erosional surface. (b) sedimentary characteristics of BTN-1.2 including mud contents (%), mean grain size, sorting, skewness and kurtosis. The vertical scale is depth in cm, while horizontal scale is grain size in phi (ϕ) scale.

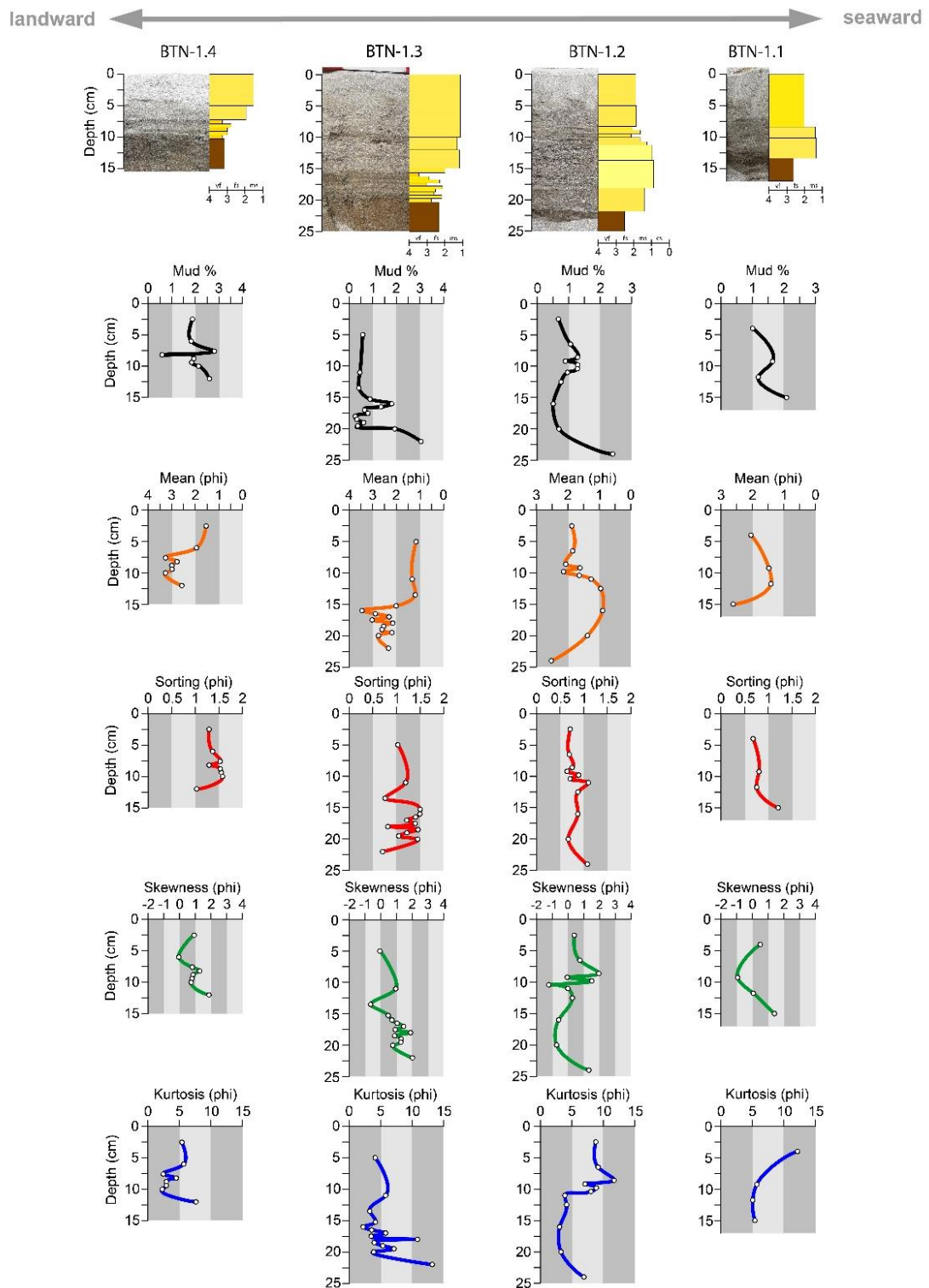


Figure 4.7 Sedimentological characteristics of TS-Pabuk deposits (yellow part) and pre-Pabuk (brown part) at BTN line 1 with 4 pits (BTN-1.1 to 1.4) showing mud content (%), mean grain size, sorting, skewness and kurtosis. The vertical scale is depth in cm, while horizontal scale is grain size in phi (ϕ) scale.

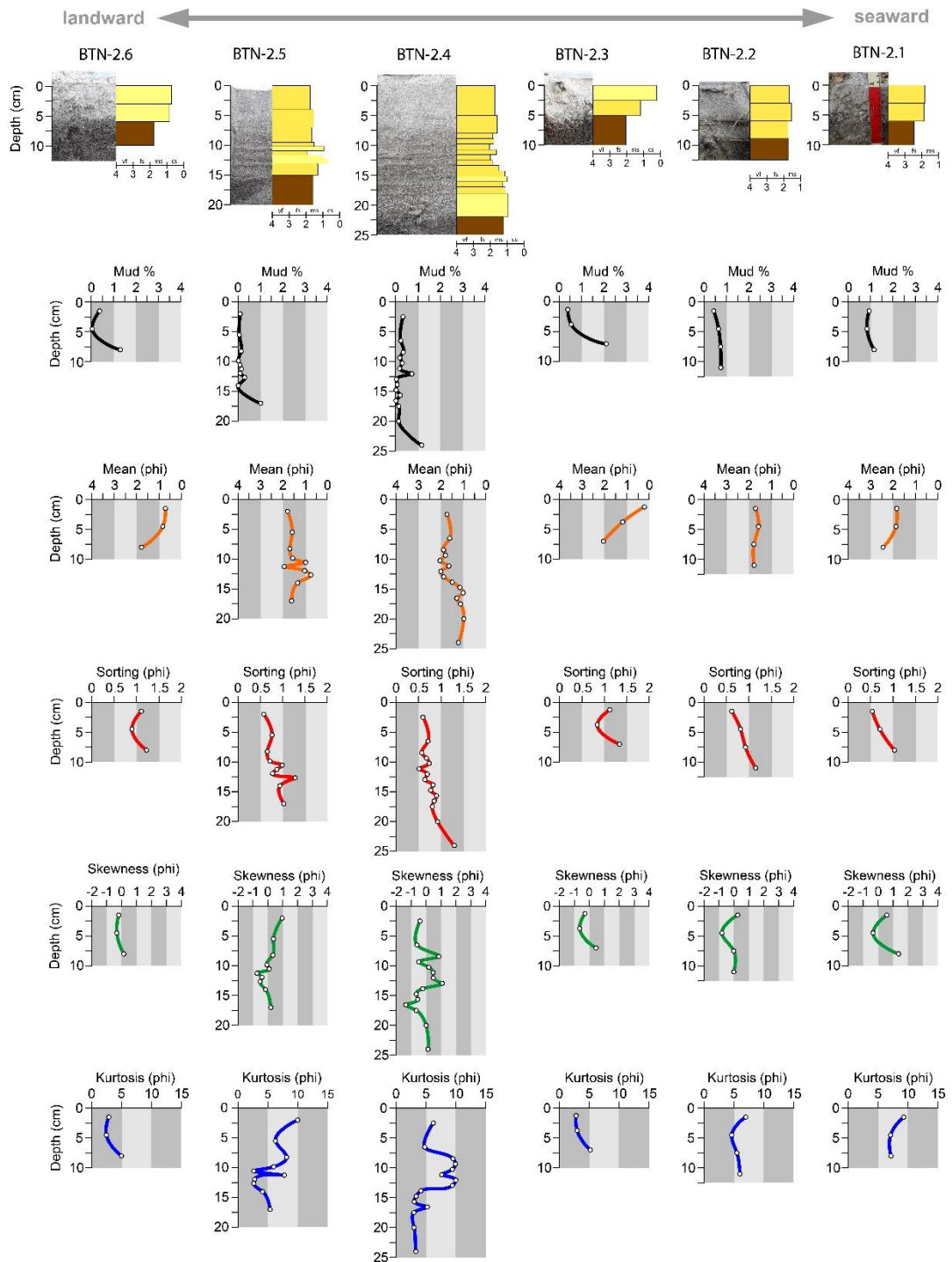


Figure 4.8 Sedimentological characteristics of TS-Pabuk deposits (yellow part) and pre-Pabuk (brown part) at BTN line 2 with 6 pits (BTN-2.1 to 2.6) showing mud content (%), mean grain size, sorting, skewness and kurtosis. The vertical scale is depth in cm, while horizontal scale is grain size in phi (ϕ) scale.

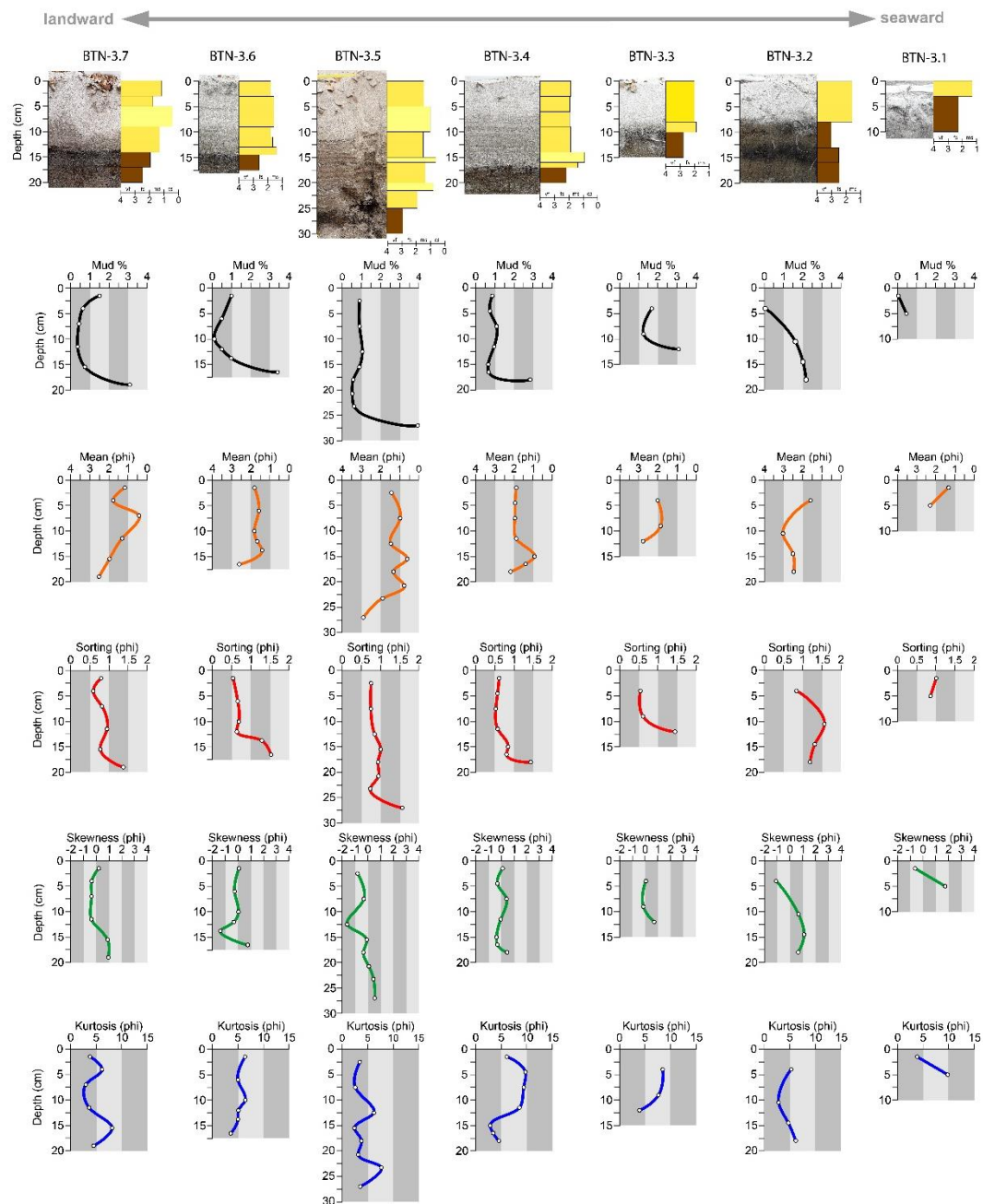


Figure 4.9 Sedimentological characteristics of TS-Pabuk deposits (yellow part) and pre-Pabuk (brown part) at BTN line 3 with 7 pits (BTN-3.1 to 3.7) showing mud content (%), mean grain size, sorting, skewness and kurtosis. The vertical scale is depth in cm, while horizontal scale is grain size in phi (ϕ) scale.

4.1.3 Thung Tako (TTK)

At mudflat TTK coast, The Pabuk sediments were deposited ovetop sand dune into back-dune dry swale which is between dune and road. The storm deposits have ~30 cm maximum thickness, extending ~23 m length, thinning landward and thickest at the proximal to middle part, lying on the sharp contact over the pre-Pabuk sediments. According to all 3 lines of TTK (only TTK-1 is shown in Figure 4.11), the storm deposits were not arranged as clearly distinct units as found in CSR and BTN. The deposits in most pits seem to be massive and contains much large shell fragments and valves. However, the results of grain geometry analysis especially grain size shows a diagnostic trend of reverse grading at base and normal grading on top. In other words, the larger grains were accumulated at the middle layer. This trend is most clearly seen at TTK-1 (Figure 4.11).

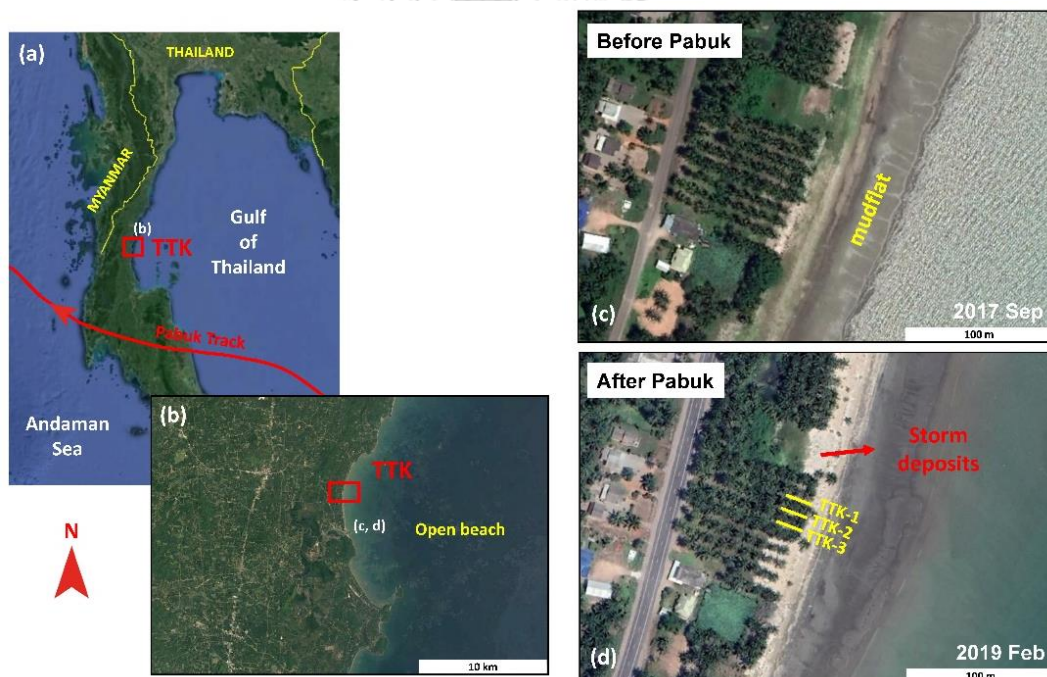


Figure 4.10 Thung Tako (TTK). (a) Location of TTK in Chumphon province, Western coast of the Gulf of Thailand. (b) TTK located semi-bay beach open to the sea. (c) Satellite images of TTK on 2017 September, 9th before an arrival of TS-Pabuk showing mudflat, narrow beach and swale between the beach and main road. (d) Satellite images of TTK on 2019 February after TS-Pabuk

made landfall at Nakhon Si Thammarat on 2019 January, 4th showing an intrusion of storm deposits into the back-beach environments (large swale).

The results from grain size analysis from 3 transect lines show that overall grain size of Pabuk sediments ranges from fine (2.51 ϕ) to very coarse (0.03 ϕ) sand. Medium sand is main proportion of storm deposits. Although the deposits in line 2 and 3 cannot be differentiated into units, TTK-1 transect line shows clearly distinct 3 units of storm deposits as following.

Unit 1 was deposited over the original surface with clearly sharp and erosional contact, yielding from the base from seaward to landward. This unit is also presented as the only unit at TTK-1.6 which is the most landward pit. This unit contains fine (2.51 ϕ) to medium (1.00 ϕ) sand which is smaller than the upper unit 2, moderately (0.97 ϕ) to poorly (1.42 ϕ), symmetrical (-0.28 ϕ) to fine (1.30 ϕ) skewed, mesokurtic (2.95 ϕ) to very leptokurtic (8.17 ϕ). This unit seem to be massive and did not show any sedimentary internal structures.

Unit 2 yields from TTK-1.1 as a middle layer to TTK-1.5 as a topmost layer with vary thickness of about 7 – 12 cm. This unit is massive and contains much and large shell valves and fragments especially at TTK-1.2. Corresponding to the shell, grain size of this unit is quite large ranging from medium (1.81 ϕ) to coarse (0.25 ϕ) sand. However, this coarse grain layer was accumulated at the seaward pits and then thinning and fining landward (see TTK-1.1, 1.2, 1.3 and 1.4). Mud contents are less than 2% and has no significant differences from other units. This storm unit is also poor sorted (1.09 to 1.42 ϕ), fine (0.54 ϕ) to coarse (-0.65 ϕ) skewed, platykurtic (2.38 ϕ) to leptokurtic (4.54 ϕ).

Unit 3 is the topmost unit yielding from TTK-1.1 to TTK-1.4 with about 3 – 7 cm thickness. Unlike the lower two units, this unit shows horizontal structures of 2 – 3 cm medium sand interrupted by very thin shell fragments layers like the unit 2 of BTN which is also the topmost semi-massive unit. Unit 3 contains only medium sand (1.23 to 1.99 ϕ) and was also organized as fining upward with poorly sorted (1.06 to

1.42 ϕ), symmetrical skewed (-0.27 to 0.03 ϕ) and mesokurtic (3.20 ϕ) to leptokurtic (5.45 ϕ). Mud contents are less than 1%.

Pre-Pabuk sediments can be classified into 2 layers. The top black layer of original surface is a few cm of the high mud contents (<1% up to almost 30 %) and high organic matters. The sediments contain fine (2.87 ϕ) to coarse (0.20 ϕ) sand, poor sorted (1.09 to 1.98 ϕ), coarse (-0.84 ϕ) to very fine skewed (1.37 ϕ), mesokurtic (2.66 ϕ) to very leptokurtic (7.89 ϕ)

TTK line 2 (Figure 4.12), additionally, was deposited as massive single layer with 15 – 30 cm thickness. Grain size also ranges from fine to very coarse sand without any significant trend. Although TTK line 3 (Figure 4.13) which is located at the southernmost was seem to be massive and cannot be clearly subdivided, the results from grain size analysis are correspond to TTK line 1 and CSR that is reverse grading at base, large grain at the middle and normal grading at top.

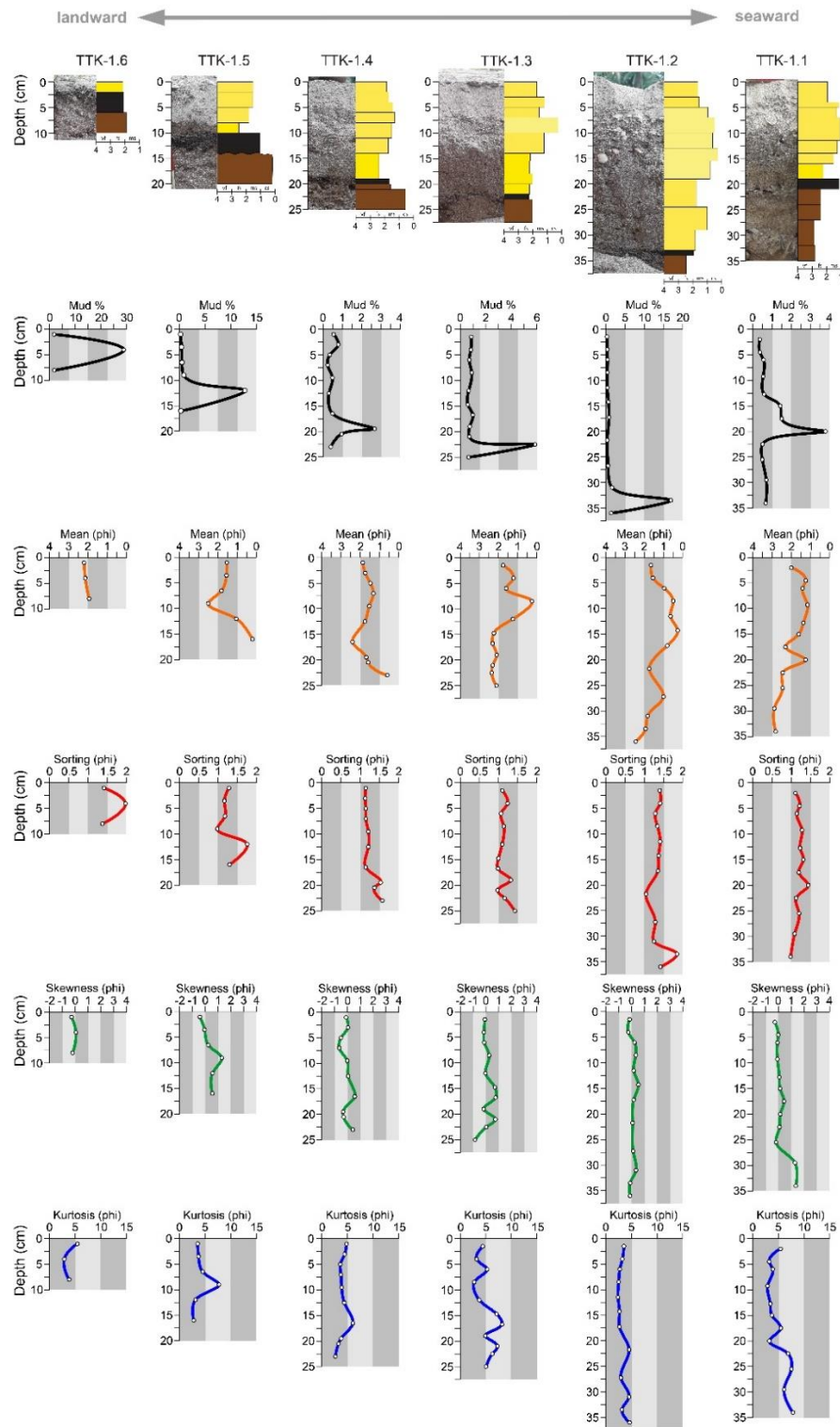


Figure 4.11 Sedimentological characteristics of TS-Pabuk deposits (yellow part) and pre-Pabuk (brown part) at TTK line 1 with 6 pits (TTK-1.1 to 1.6) showing mud content (%), mean grain size, sorting, skewness and kurtosis. The vertical scale is depth in cm, while horizontal scale is grain size in phi (ϕ) scale.

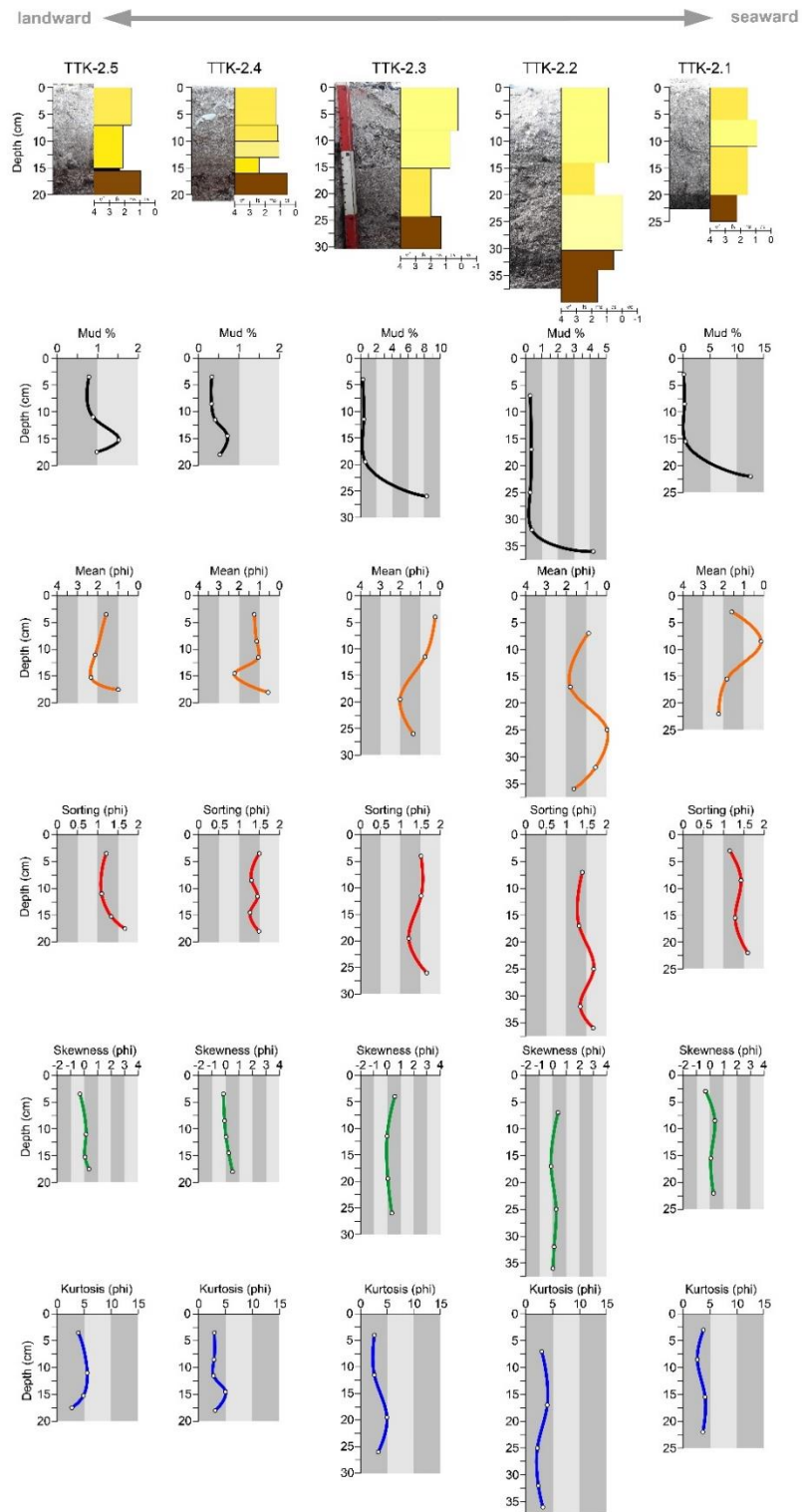


Figure 4.12 Sedimentological characteristics of TS-Pabuk deposits (yellow part) and pre-Pabuk (brown part) at TTK line 2 with 5 pits (TTK-2.1 to 2.5) showing mud content (%), mean grain size, sorting, skewness and kurtosis. The vertical scale is depth in cm, while horizontal scale is grain size in phi (ϕ) scale.

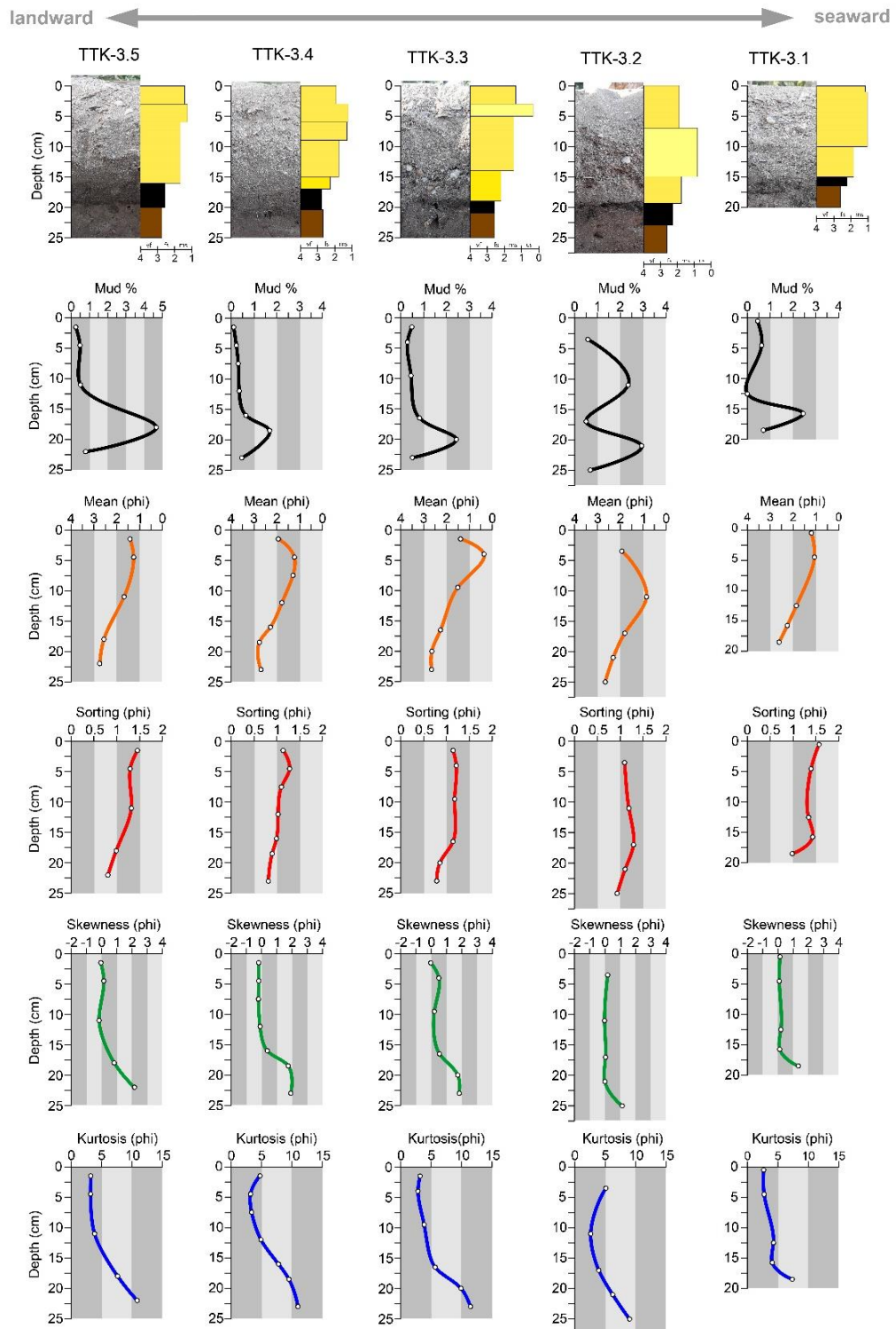


Figure 4.13 Sedimentological characteristics of TS-Pabuk deposits (yellow part) and pre-Pabuk (brown part) at TTK line 3 with 6 pits (TTK-3.1 to 3.5) showing mud content (%), mean grain size, sorting, skewness and kurtosis. The vertical scale is depth in cm, while horizontal scale is grain size in phi (ϕ) scale.

4.1.4 Talumphuk (TLP)

Unlike other locations, TLP coast has an artificial seawall that are located close to the beach for preventing coastal erosion from monsoon and storm surge. In addition, there are shrimp ponds lying along the coast between dune and road. These structures could be important factors controlling the current during storm event. According to the field investigation and satellite image review, there are at least 2 overwash events leaving thick and wide range of washover deposits into the pond from seaward side before Pabuk storm event (Figure 4.15). The first event occurred during 2000 – 2009 and the second event occurred during 2009 – 2012 before an arrival of the 2019 TS-Pabuk. However, Pabuk deposits can be clearly seen in the field as washover fans with current ripples on the surface behind seawalls. The sandy Pabuk sediments lied on top of the old sandy deposits from previous overwash events.

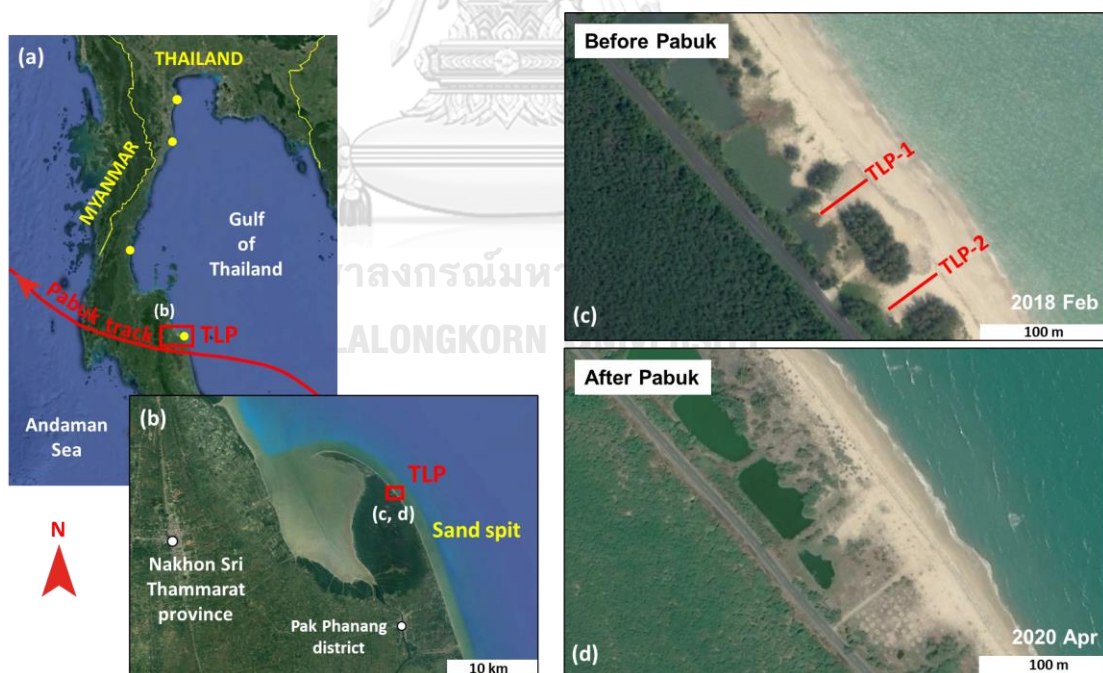


Figure 4.14 Talumphuk (TLP). (a) Location of TLP in Nakhon Si Thammarat province, Western coast of the Gulf of Thailand where is a bit north of the TS-Pabuk landfall location. (b) TLP located near the tip part of Laem Talumphuk cape sand spit. (c) Satellite image of TLP on 2018 September, 18th before an arrival of TS-Pabuk showing narrow sand beach and previous washover

deposits invading into shrimp ponds between beach and main road. (d) Satellite image of TLP on 2020 April, 11st after TS-Pabuk made landfall on 2019 January, 4th. The presence of Pabuk sediments in this image is unclear because the land surface was disturbed more than in fieldwork which were finished within 2019.

Sedimentary characteristics of storm deposits in TLP are mainly derived from TLP-1. Although many pits were excavated in TLP-2, it is difficult to identify the boundary between Pabuk deposits and original sand deposits due to their sand over sand characteristics. Pabuk sediments are thickest at seaward side of ~40 cm and extend up to 67 m length behind seawalls. The thinning landward trend can be seen in this location. In overall, Pabuk sediments range from fine (2.37 ϕ) to coarse (0.28) sand. Sorting is mainly moderately well (0.47 ϕ) to moderately (0.99 ϕ) sorted. However, some samples show well (0.47 ϕ) sorted and poor (1.29 ϕ) sorted. Same as other locations, medium sand is dominant grain size with the average of 1.62 ϕ . Skewness tends to be symmetrical (0.42 ϕ) to coarse (-1.27 ϕ) even very coarse and very fine are presented in some samples. Kurtosis is mainly leptokurtic (3.91 ϕ) to very leptokurtic (18.71 ϕ) even some sample show platykurtic (2.14 ϕ).

Although most pits in TLP-1 cannot be separated into units, pit TLP-1.2 which located seaward shows clearly distinct structures so that storm deposits can be differentiate into 4 subunits (Figure 4.18). The lowermost unit 1A is 15 – 20 cm thick containing compacted large shell fragments. The grain size is coarse (0.28 – 0.63 ϕ) sand, poor sorted (0.25 ϕ), symmetrical (0.29 ϕ) to fine (0.54 ϕ) skewed and platykurtic (2.21 to 2.38 ϕ). This unit contacts to the pre-Pabuk sediments with scouring erosional contact. The shell tends to be organized as horizontal laminations. Unit 1B is about 8 cm thick with very less shell fragments horizontal layers. This unit contact to the basal unit 1 with sharp horizontal contact. The main proportion of sediments is medium sand (1.12 to 1.86 ϕ) with a thin layer of fine sand (2.06 ϕ), moderately sorted (0.71 to 0.89 ϕ) with some poor sorted (1.13 ϕ), symmetrical (-0.06 ϕ) to coarse (-0.74 ϕ) skewed, platykurtic (2.37 ϕ) to leptokurtic (6.83 ϕ). The

upper unit 1C is horizontal lamination of coarse sand (0.40 to 0.77 ϕ) with shell fragments which is quite similar to unit 1. However, the fragments are clearly smaller than fragments in unit 1. This unit is quite homogeneous in sedimentological parameters. In addition to coarse sand, this unit is poor sorted (1.23 to 1.29 ϕ), symmetrical skewed (-0.18 to 0.26 ϕ) and platykurtic (2.14 to 2.37 ϕ). Unit 2 was deposited latest as cross laminations of 6° to 7° angle truncated through unit 3 and also the top part of unit 2 during the first 20 cm of TLP-1.2 (Figure 4.18). This unit has almost no mud contents. Medium sand (1.36 to 1.67 ϕ) is most abundant with a thin layer of fine sand (2.07 ϕ), moderately well (0.62 ϕ) to moderately (0.97 ϕ) sorted, symmetrical (0.06 ϕ) to coarse (-0.82 ϕ) skewed, mesokurtic (3.56 ϕ) to very leptokurtic (8.28 ϕ). Although structure is different from unit 2, all sedimentary parameters of unit 2 seem to be conform to unit 1B.

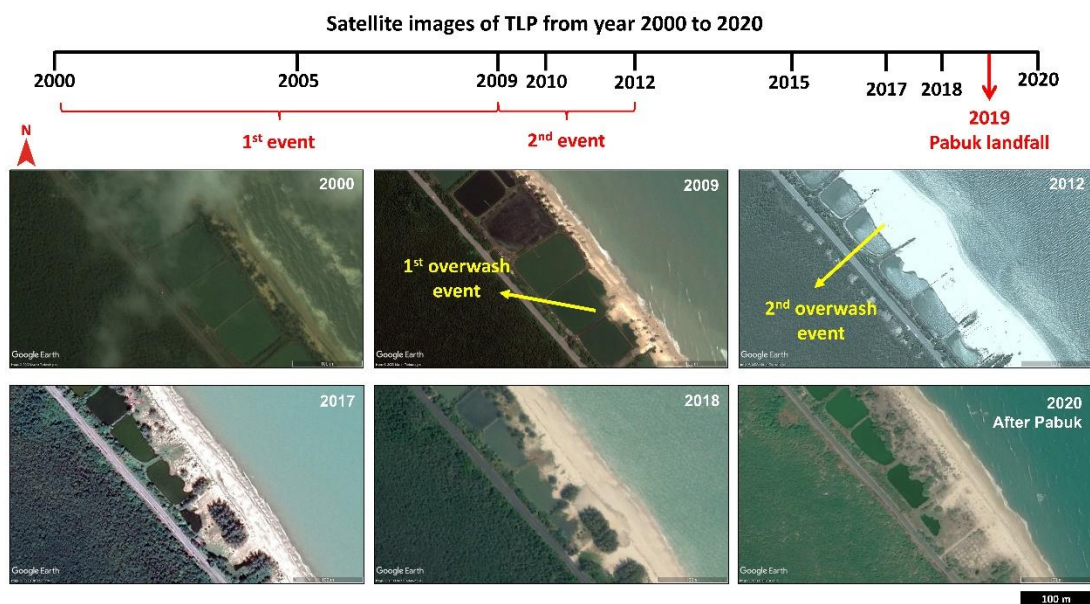


Figure 4.15 Satellite images of TLP from 2000 to 2020 showing at least 2 overwash events during 2000 to 2009 and 2009 to 2012 before the 2019 TS-Pabuk event. The 1st event during 2000 to 2009 caused small amount of sediment invaded the shrimp ponds along the coast. The 2nd event during 2009 to 2012 caused a huge amount of sand overflowing into the ponds. The last event was the 2019 TS-Pabuk that allowed sediments to deposit on top of the previous washover deposits.

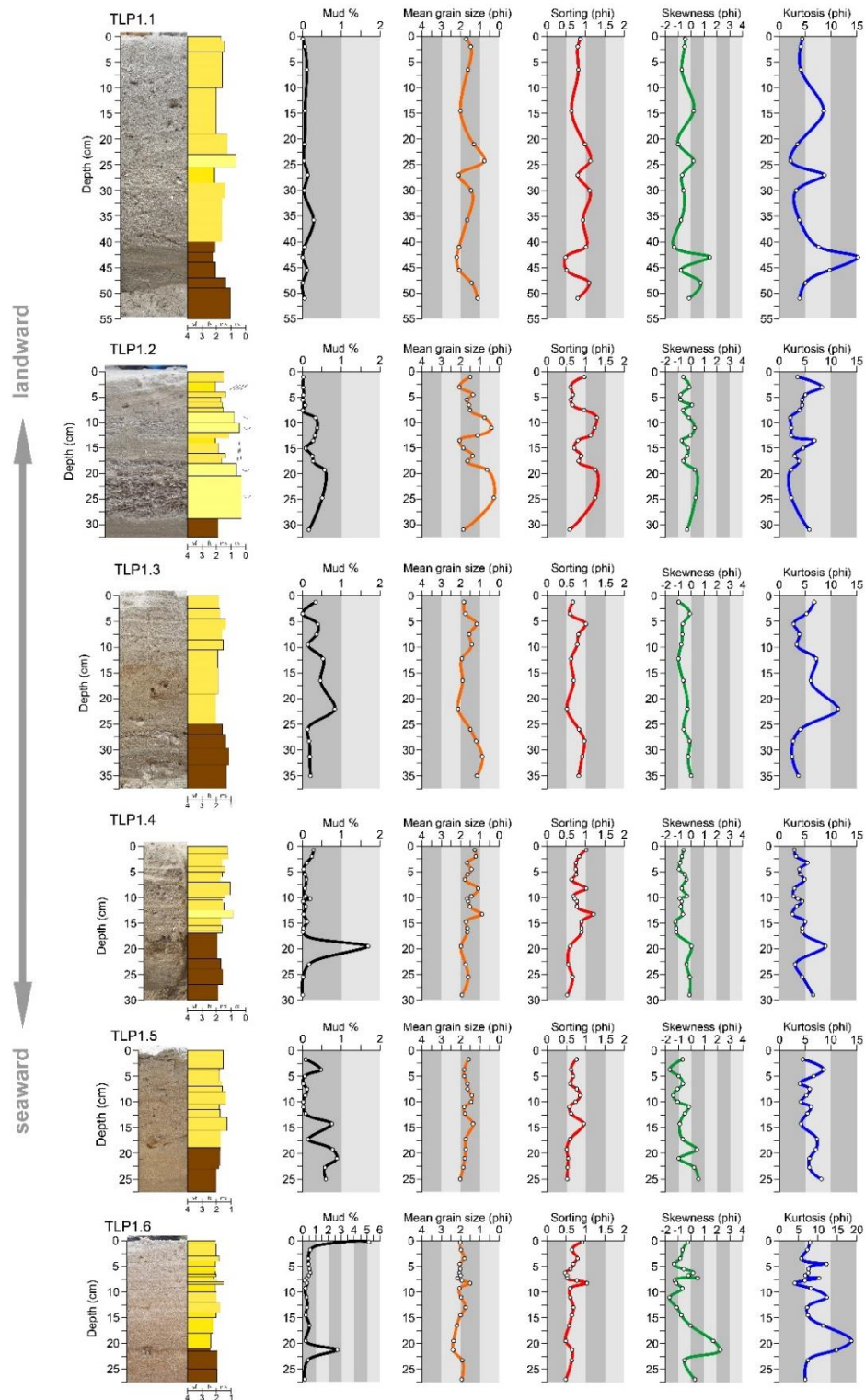


Figure 4.16 Sedimentological characteristics of TS-Pabuk deposits (yellow part) and pre-Pabuk (brown part) at TLP line 1 with 6 pits (TLP-1.1 to 1.6) showing mud content (%), mean grain size, sorting, skewness and kurtosis. The vertical scale is depth in cm, while horizontal scale is grain size in phi (ϕ) scale.

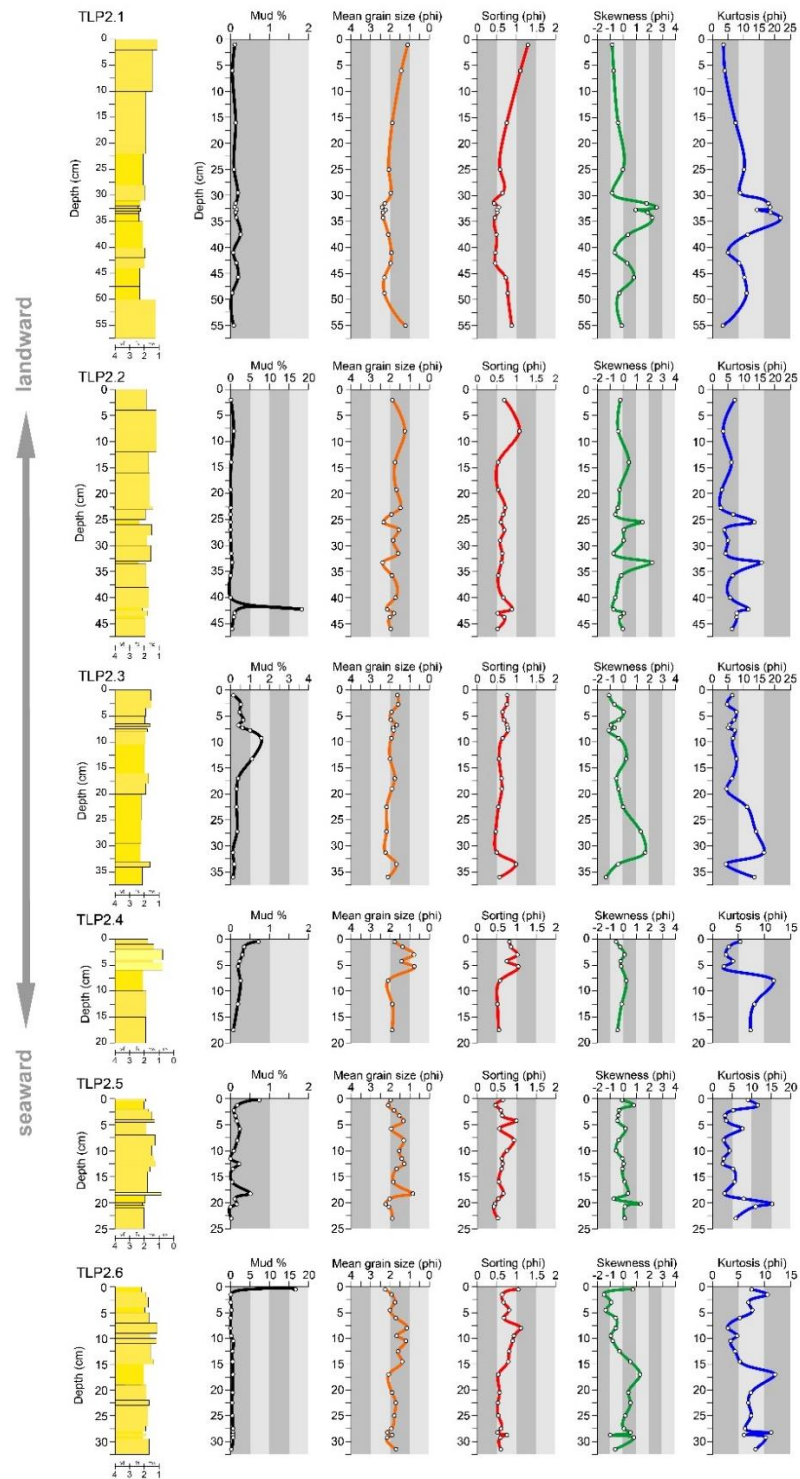


Figure 4.17 Sedimentological characteristics of TS-Pabuk deposits at TLP line 2 with 6 pits (TKK-2.1 to 2.6) showing mud content (%), mean grain size, sorting, skewness and kurtosis. However, the deposits in this line cannot be differentiated from the original sediments both in naked eye from pit walls and in sedimentological parameters. The vertical scale is depth in cm, while horizontal scale is grain size in phi (ϕ) scale.

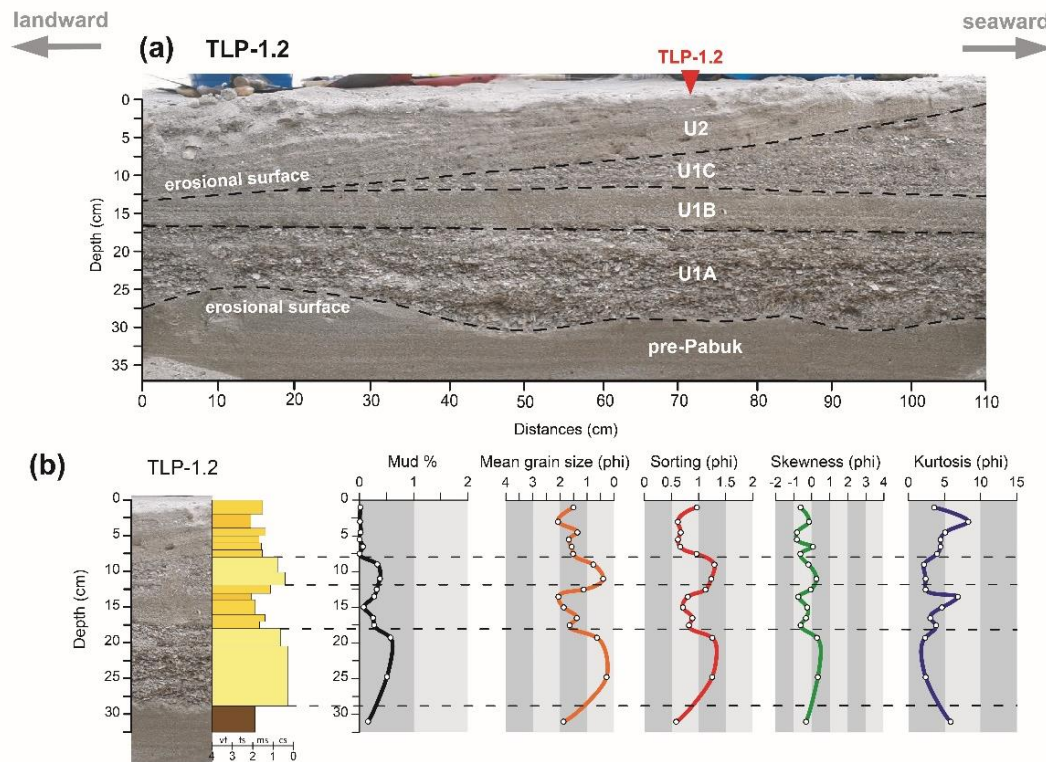


Figure 4.18 Pit TLP-1.2. (a) a photo of open pit with 110 cm width. The Pabuk sediments was classified into 4 subunits; U1A, U1B, U1C and U2 lying above pre-Pabuk sediments with sharp erosional surface. U1A, U1B and U1C are horizontally organized with different grain size and sorting, whereas the U2 is 6° to 7° landward inclined laminations. (b) sedimentary characteristics of TLP-1.2 including mud contents (%), mean grain size, sorting, skewness and kurtosis. The vertical scale is depth in cm, while horizontal scale is grain size in phi (ϕ) scale.

4.2 Microfossils in storm deposits

Microfossils are one proxy that was recorded in storm deposits such as foraminifera, ostracods (Kongsen, 2016; Phantu Wongraj, 2012; Pilarczyk et al., 2014; Pilarczyk et al., 2016; Soria et al., 2017) and diatoms (Haque et al., 2021; Nott et al., 2013). Some of these organisms are useful for identifying the possible minimum depth of storm wave base which could be helpful for inferring the intensity of storm. Although the studies of storm deposits in Thailand by Phantu Wongraj (2012) and (Kongsen, 2016) recorded many species of foraminifera and ostracods, diatoms have no record. To fulfill this knowledge gap and propose the new record of diatoms in storm deposits in Thailand, surface sediment samples were collected from three

locations; BTN, TTK and TLP, for diatom analysis. The diatom species found in each location was summarized in Table 4.1.

Sediment bulk samples for diatom analysis were collected from the ground surface at distal part of storm deposits, proximal part of storm deposits and normal beach sand. Although diatoms in storm deposits are not abundant comparing with those found in normal beach, their diversity is quite high. At least 22 species of diatoms from various origins were identified in the TS-Pabuk sediments (Figure 4.18 and 4.19) as following;

9 Marine species: *Coscinodiscus radiatus*, *Lyrella hennedyi*, *Lyrella spectabilis*, *Odontella aurita*, *Odontella sp.*, *Paralia fenestrata*, *Paralia sp.*, *Thalassionema nitzschioides* and *Trachyneis sp.*

5 Brackish to marine species: *Cyclotella litoralis*, *Diploneis weissflogii*, *Fallacia forcopata*, *Grammatophora oceanica* and *Tryblionella granulata*

2 Freshwater to brackish species: *Luticola mutica* and *Luticola sp.*

1 Freshwater species; *Hantzschia amphioxys*

2 Freshwater to marine species: *Navicula sp.* and *Nitzschia sp.*

3 Unknown habitat species; *Coscinodiscus or Thalassiosira sp.*, *Naviculaceae sp.* and *Pinnuavis (?) sp.*

According to this information, the species that reflect the storm wave base is still unable to be indicated. However, the diversity of diatoms reflected that storm deposits were influenced by various environments from marine to freshwater. The marine origin species indicated that storm sediments come from the sea. Whereas the freshwater species indicated that freshwater from mainland flooded the area after the deposition of storm sediments. This freshwater may come from heavy rain flooded the area during the storm event or from back-barrier channels or shrimp ponds depending on the areas, especially at TTK and TLP area where have freshwater source in the areas.

Table 4.1 Summary of diatom species found in BTN, TTK and TLP areas.

	Diatom species	BTN	TTK	TLP	Habitat
1	<i>Coscinodiscus radiatus</i>	-	✓	-	Marine
2	<i>Lyrella hennedyi</i>	-	✓	-	Marine
3	<i>Lyrella spectabilis</i>	-	✓	-	Marine
4	<i>Odontella aurita</i>	-	✓	-	Marine
5	<i>Odontella sp.</i>	-	✓	-	Marine
6	<i>Paralia fenestrata</i>	-	✓	✓	Marine
7	<i>Paralia sp.</i>	✓	-	-	Marine
8	<i>Thalassionema nitzschioides</i>	✓	-	-	Marine
9	<i>Trachyneis sp.</i>	-	✓	-	Marine
10	<i>Cyclotella litoralis</i>	✓	✓	✓	Brackish-Marine
11	<i>Diploneis weissflogii</i>	-	✓	-	Brackish-Marine
12	<i>Fallacia forcopata</i>	-	✓	-	Brackish-Marine
13	<i>Grammatophora oceanica</i>	✓	-	-	Brackish-Marine
14	<i>Tryblionella granulata</i>	✓	✓	-	Brackish-Marine
15	<i>Luticola mutica</i>	-	✓	-	Freshwater-Brackish
16	<i>Luticola sp.</i>	-	✓	-	Freshwater-Brackish
17	<i>Hantzschia amphioxys</i>	-	✓	✓	Freshwater
18	<i>Navicula sp.</i>	-	✓	-	Freshwater-Marine
19	<i>Nitzschia sp.</i>	-	✓	-	Freshwater-Marine
20	<i>Coscinodiscus or Thalassiosira sp.</i>	-	✓	✓	unkhown
21	<i>Naviculaceae sp.</i>	-	✓	✓	unkhown
22	<i>Pinnuavis (?) sp.</i>	-	-	✓	unkhown

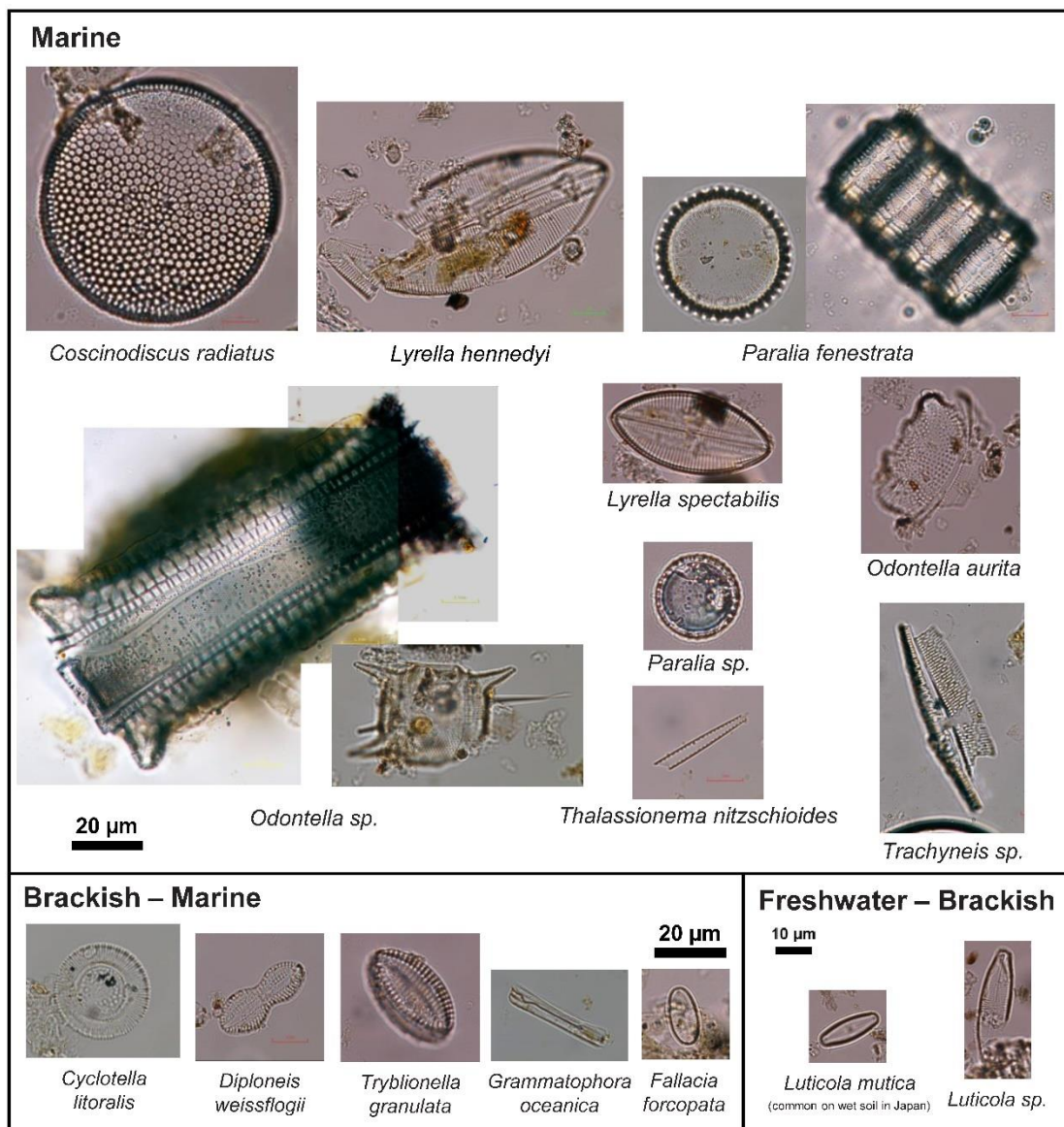


Figure 4.19 Diatoms found in storm (TS-Pabuk) deposits in BTN, TTK and TLP including 9 Marine species: *Coscinodiscus radiatus*, *Lyrella hennedyi*, *Lyrella spectabilis*, *Odontella aurita*, *Odontella sp.*, *Paralia fenestrata*, *Paralia sp.*, *Thalassionema nitzschioides* and *Trachyneis sp.*, 5 Brackish to marine species: *Cyclotella litoralis*, *Diploneis weissflogii*, *Fallacia forcopata*, *Grammatophora oceanica* and *Tryblionella granulata* and 2 Freshwater to brackish species: *Luticola mutica* and *Luticola sp.*

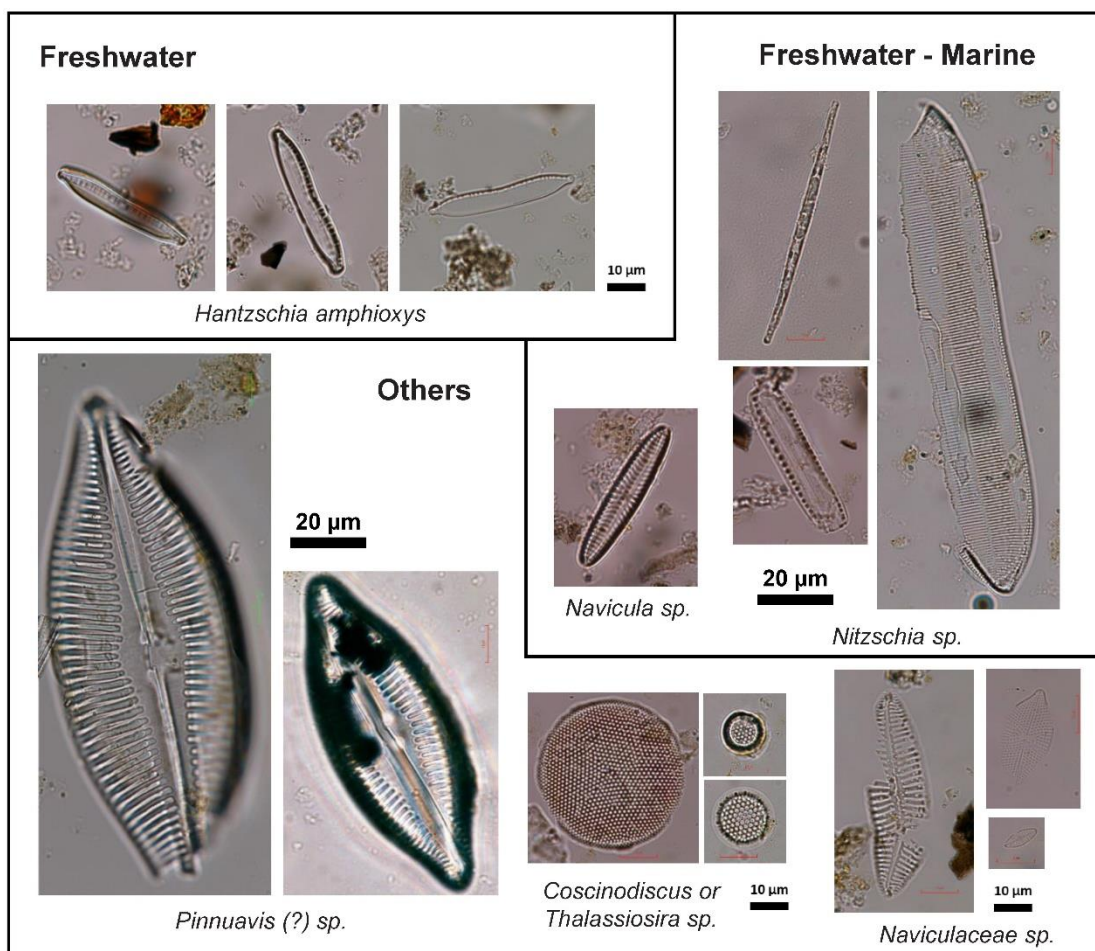


Figure 4.20 Diatoms found in storm (TS-Pabuk) deposits in BTN, TTK and TLP including 1 Freshwater specie; *Hantzschia amphioxys*, 2 Freshwater to marine species: *Navicula sp.* and *Nitzschia sp.* and 3 Unknown habitat species; *Coscinodiscus or Thalassiosira sp.*, *Naviculaceae sp.* and *Pinnuavis (?) sp.*

CHAPTER 5

GROUND PENETRATING RADAR

Ground Penetrating Radar (GPR) with 3 frequencies of shield antennas; 200 MHz, 400 MHz and 900 MHz, was applied on the storm deposits in the parallel line perpendicular to the shore as the open-pit transect line for sediments. However, GPR was set up only for BTN, TTK and TLP, not include CSR due to the limitation of fieldwork period that the deposits at CSR maybe disturbed and not in a proper condition for collecting GPR data. The GPR transect line were set up parallel to the sediment pit lines as close as possible. The offset between them is less than 1 m. The measurements were accomplished with sample rate of 512 samples/scan and dielectric constant of 8. This constant provides velocity which can reflect the relationship between times and depths. The relationship between dielectric constant (ϵ_r) and velocity (v) can be calculated by equation 5.1 (Arjwech & Titimakorn, 2023).

$$v = \frac{c}{\sqrt{\mu_r \epsilon_r}} \quad \text{equation 5.1}$$

When v = velocity of electromagnetic wave (m/s)

C = velocity of light in vacuum (2.998×10^8 m/s)

μ_r = magnetic permeability (in normal medium, μ_r is closed to 1)

ϵ_r = dielectric constant

Relationship between velocity of electromagnetic wave (v) and wavelength (λ) can be calculated by equation 5.2

$$\lambda = vT = \frac{v}{f} \quad \text{equation 5.2}$$

When λ = wavelength (m)

V = velocity of electromagnetic wave (m/s)

T = period (s)

f = frequency (Hz)

Applying dielectric constant of 8 for equation 5.1 would provide the velocity of electromagnetic wave (v) of about 105,995,306.5 m/s or 0.105×10^9 m/s. The

frequency of electromagnetic waves used in this research is 200, 400 and 900 MHz. Consequently, after applying frequency and velocity of electromagnetic waves in equation 5.2, the wavelength of 200, 400 and 900 MHz is 0.53, 0.26 and 0.18 m respectively. The vertical resolution of each frequency; 200, 400 and 900 MHz is a quarter of wavelength which is 13.25, 6.63 and 2.95 cm respectively.

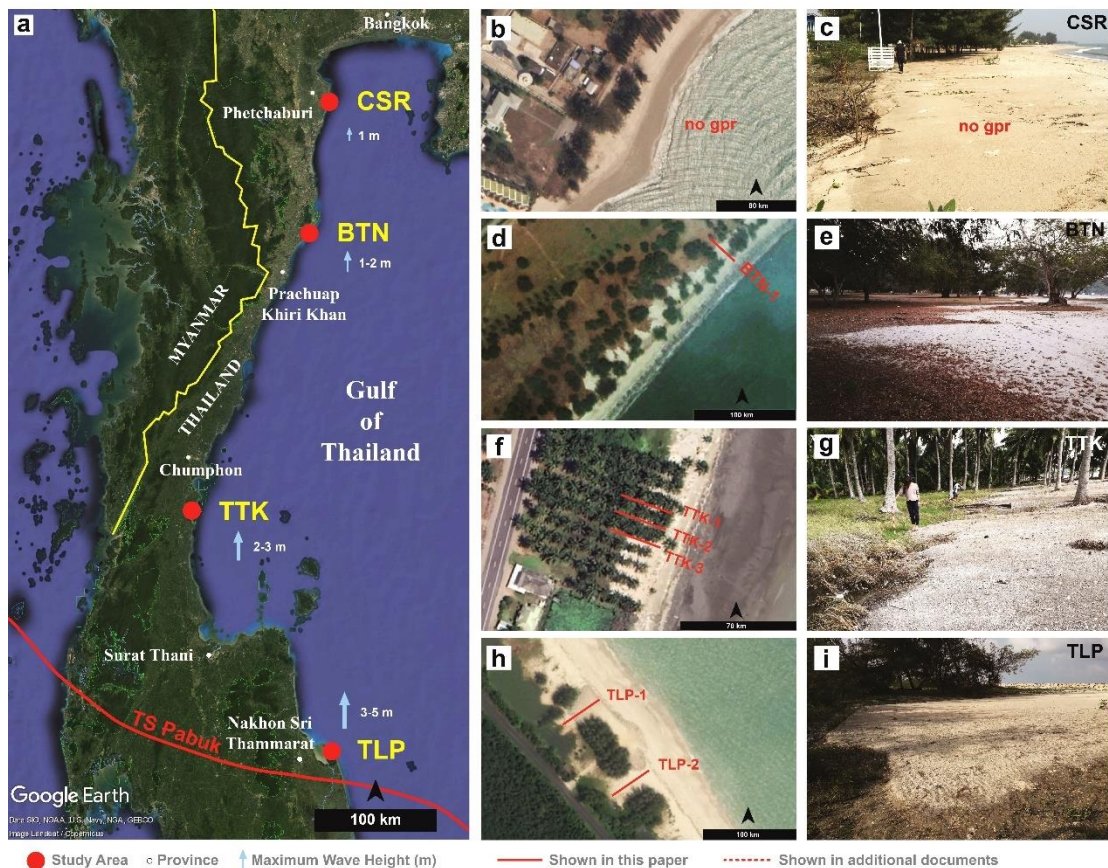


Figure 5.1 (A) The western coast of the Gulf of Thailand showing study sites including BTN in Prachuap Khiri Khan, TTK in Chumphon and TLP in Nakhon Sri Thammarat (red dot). (B) GPR line transect perpendicular to the shore with 1 line ant BTN, 3 lines at TTK and 2 lines at TLP. (C) Washover deposits found at back dune environments on the coastal area in BTN, TTK and TLP.

5.1 Radar Surfaces and Radar Facies

According to the 6 GPR profile lines in 3 study locations including BTN, TTK and TLP, the antenna with different frequencies provided clearly distinct resolutions, depths and internal details.

However, the best resolution was found at 900 MHz profile. Pabuk deposits can be clearly illustrated by this frequency. Hence, 3 types of radar surface; downlap

(RS1), toplap (RS2) and truncation (RS3), were classified based on terminology defining the relationship between distinct reflections which represent depositional break or contact. Additionally, 7 radar facies consisting subhorizontal (RF1), landward inclined (RF2), seaward inclined (RS3), concave (RS4), convex (RF5), chaotic (RF6) and transparent (RF7) were also classified based on shape of reflections, dip angle, continuity and relationship between reflections which represent internal structures (Figure 5.2).



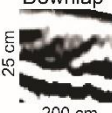
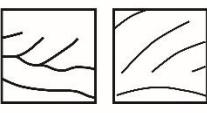




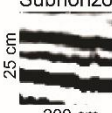
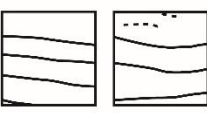

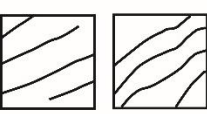










	900 MHz		Tracing	Description	Interpretation
Radar Surfaces					
RS1	Downlap  25 cm 200 cm			medium to high amplitude, moderately continuous, downlap with dip 35° landward concave and convex	washover progradation on top of horizontal layers
	RS2	Toplap  25 cm 500 cm			medium to high amplitude, moderately continuous, toplap with dipping landward, dip 40-65°
RS3		Truncation 			medium to high amplitude, moderately continuous, dipping landward with 10-30°, overtopped by seaward continuous surface with dip 18°
Radar Facies					
RF1	Subhorizontal  25 cm 200 cm			high amplitude, highly continuous, subhorizontal, planar	deposition of sand size sediments
RF2	Landward inclined 			medium to high amplitude, moderately continuous, slightly planar, dipping landward, dip: 20 - 40°	washover deposits
RF3	Seaward inclined 			medium to high amplitude, moderately continuous, planar to slightly planar, dipping seaward, dip: 20-55°	beach progradation
RF4	Concave 			high amplitude, moderately to highly continuous	deposition in a swale
RF5	Convex 			medium to high amplitude, moderately continuous	sand dune
RF6	Chaotic 			low to high amplitude, highly discontinuous	deposition of mud or high concentration of small grain size sediments
RF7	Transparent 			medium to high amplitude, diffraction hyperbola	concentration of vegetal remains (roots or branches), gravel, rock fragment from human activities (TLP)

Figure 5.2 Radar Surface (RS) and Radar facies (RF). Radar image from 900 MHz antenna, reflection tracing, description and interpretation.

5.2 Ban Thung Noi (BTN)

At Ban Thung Noi (BTN) in Prachuap Khiri Khan province, the sandy beach of about 1 km length lies between two rocky headlands of Permian limestone. The beach faces to the open sea without any obstruction. The satellite image from Google Earth on February 24, 2019 showed clearly inundation limit line and washover sediments along the shore. The inundation limit can be clearly notice from the sharp contact between landward green grass zone and seaward brown dry grass zone. This limit range between 50 m in the northern part up to about 100 m in the southern part of the beach. Whereas, washover sediments are imaged as several lobe fans in the coastal zone. Three main transect lines were set up for sedimentological study (BTN-1, BTN-2 and BTN-3). However, GPR with 3 frequencies (200, 400 and 900 MHz) were applied only on BTN-1 (Figure 5.3).

The 200 MHz antenna can penetrate into ~6 m depth, even the wave starts attenuation at ~3 m depth. TS-Pabuk deposits are too thin (~25 cm maximum thickness) to be detected visibly by this frequency. However, large-scale structures are clearly seen such as beach progradation whose bedding dip seaward and previous washover deposits which are sub-horizontal to landward dipping layers (Figure 5.3). The 400 MHz wave can penetrate into almost 3 m depth and give the better resolution than the 200 MHz. Pabuk deposits are more visible as thinning landward layer at topmost of the sequence and lie on sets of the beach progradation. An erosional contact between Pabuk and original surface is quite clear. The 900 MHz profile shows the best resolution but the worst depth of only 1 m. Pabuk layers in GPR signal seem to be fit to four sedimentary logs. Boundaries of TS-Pabuk sediments can be captures as thick reflectors at top and bottom. However, the proximal part of washover deposits located at top of seaward dune cannot be differentiated from the normal shore sand. The white layer reflector lies continuously cross the dune to foredune beach. Therefore, sedimentary logs for ground truth are essential to help in interpretation with GPR.

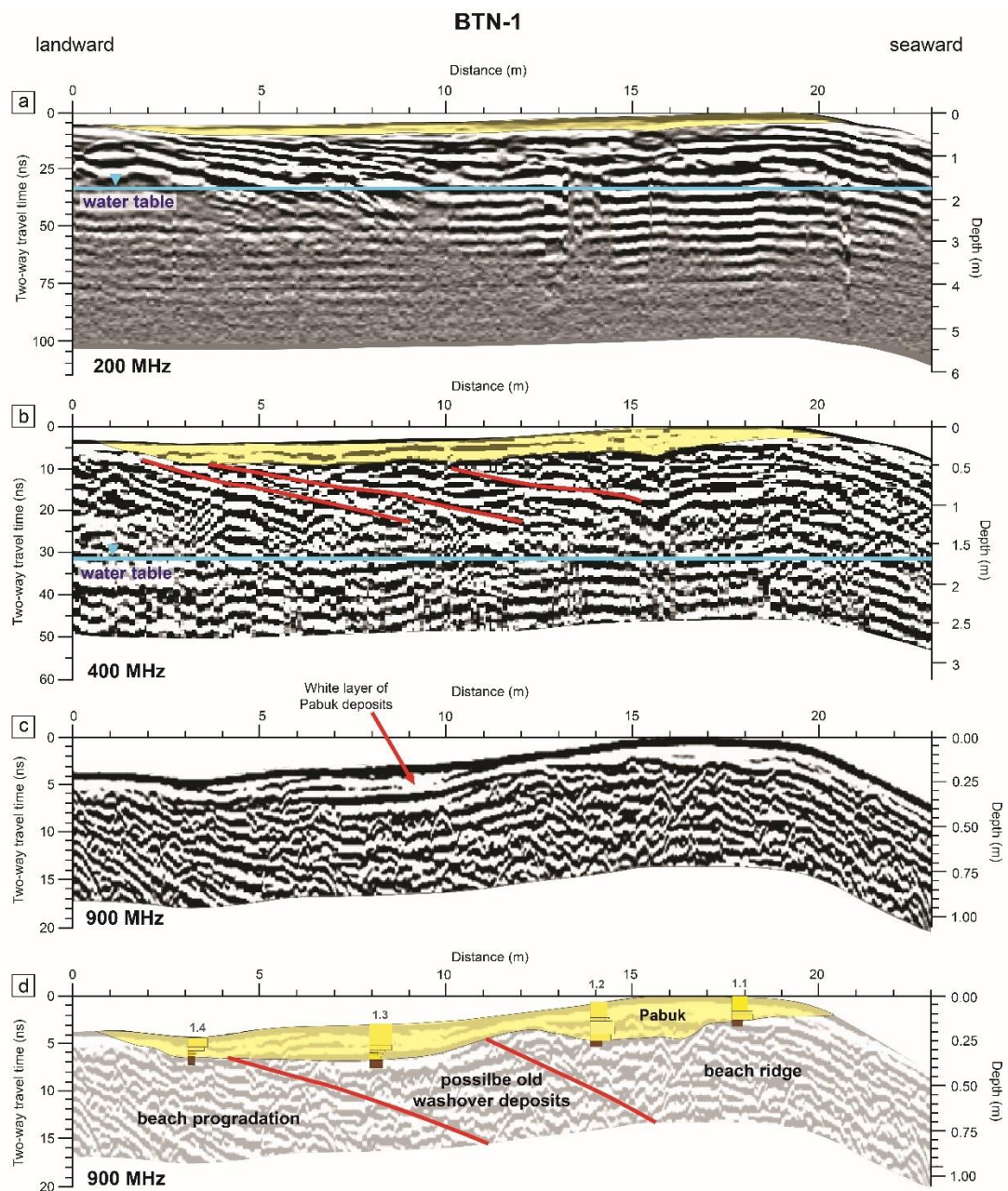


Figure 5.3 GPR profile of BTN-1 from 3 frequencies; 200, 400 and 900 MHz (a) 200 MHz profile with about 5 m depth (b) 400 MHz profile with about 2.5 m depth (c) 900 MHz with almost 75 cm depth and (d) 900 MHz with interpretation of TS-Pabuk deposits (yellow area) and sedimentary logs from 4 shallow pits (BTN-1.1 to 1.4).

5.3 Thung Tako (TTK)

At mudflat TTK coast, The Pabuk sediments were deposited overtop sand dune into back-dune dry swale. GPR was applied in 3 lines including TTK-1, TTK-2

and TTK-3 (Figure 5.4, 5.5 and 5.6). The distance between each line is only 10 m. Hence, the profile signals of GPR are quite not much different. In overall trend, although 200 MHz antenna cannot capture internal details inside washover deposits, it can penetrate into almost 5.5 m depth. Most structures are large-scale horizontal to sub-horizontal layers. Like 200 MHz, 400 MHz antenna was presented as a thick white reflection on top of the section without any internal detail inside. However, the original ground structures are more visible. Half-lens feature of thick reflection was found in swale on landward side at 0.5 to 1.5 m depth which is clearly seen TTK-1 and TTK-2 (Figure 5.4 and 5.5). This feature can be illustrated very well in 900 MHz profile. The half lens reflections are more continuous and thicker than the overtop unit which are more chaotic and discontinuous. These characteristics are quite similar to the signals of Pabuk sand deposits. As a result, this lens has a potential to be a representative of previous washover deposits in the swale. Pabuk deposits are very well imaged by the 900 MHz frequency. Sub-horizontal lamination inside the layers can be clearly seen. Moreover, small landward inclinations are found at the proximal part of Pabuk. This structure cannot be captured by 200 and 400 MHz frequency because their wavelengths are too large to detect the thinner structure. Also, this inclination cannot be observed in the open pit because the pit width is too short to present the large inclined structure. The 900 MHz, consequently, is very helpful for studying the process of storm surge together with sedimentary logging.

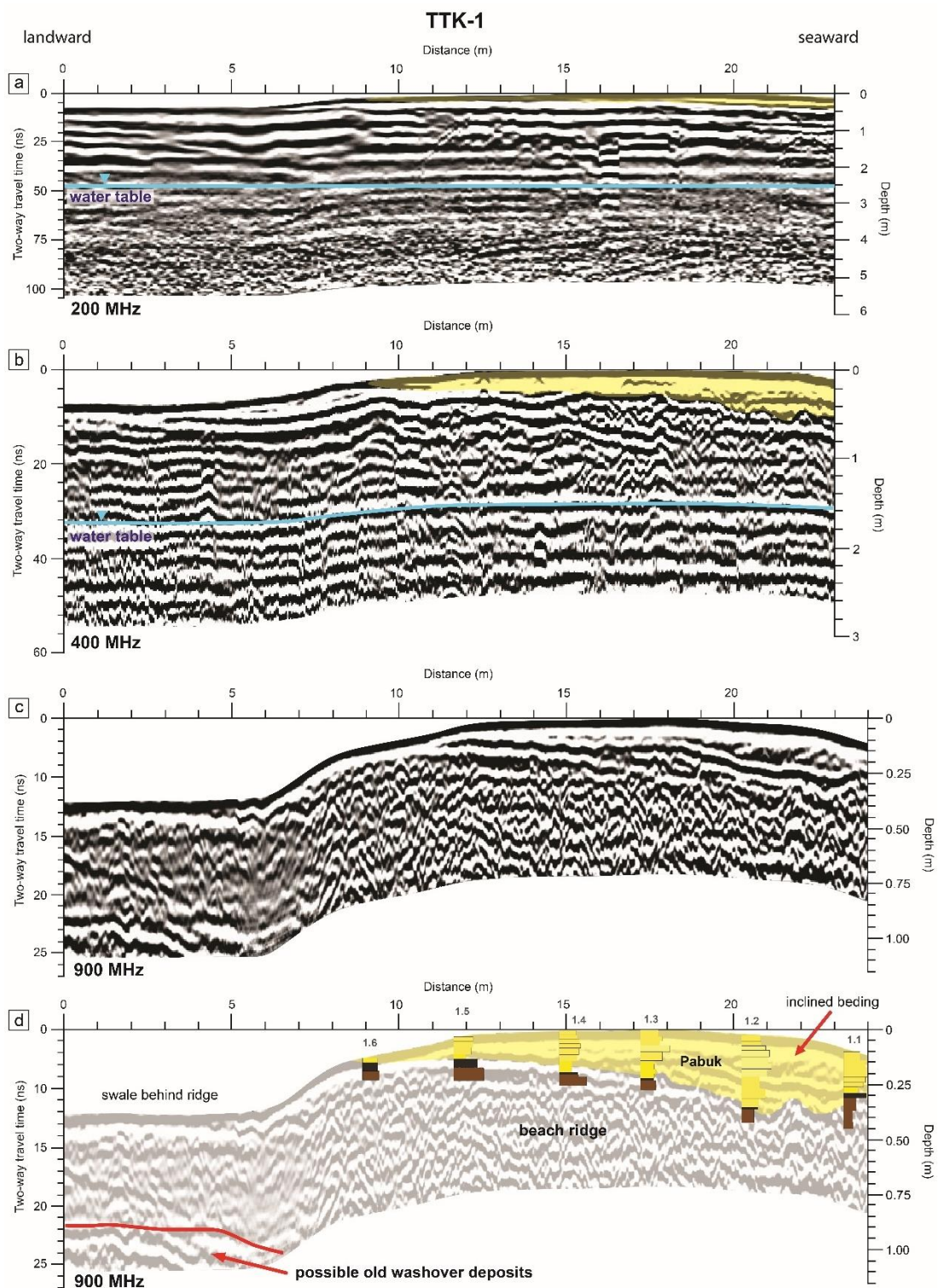


Figure 5.4 GPR profile of TTK-1 from 3 frequencies; 200, 400 and 900 MHz (a) 200 MHz profile with about 5 m depth (b) 400 MHz profile with about 2.5 m depth (c) 900 MHz with almost 75 cm depth and (d) 900 MHz with interpretation of TS-Pabuk deposits (yellow area) and sedimentary logs from 6 shallow pits (TTK-1.1 to 1.6).

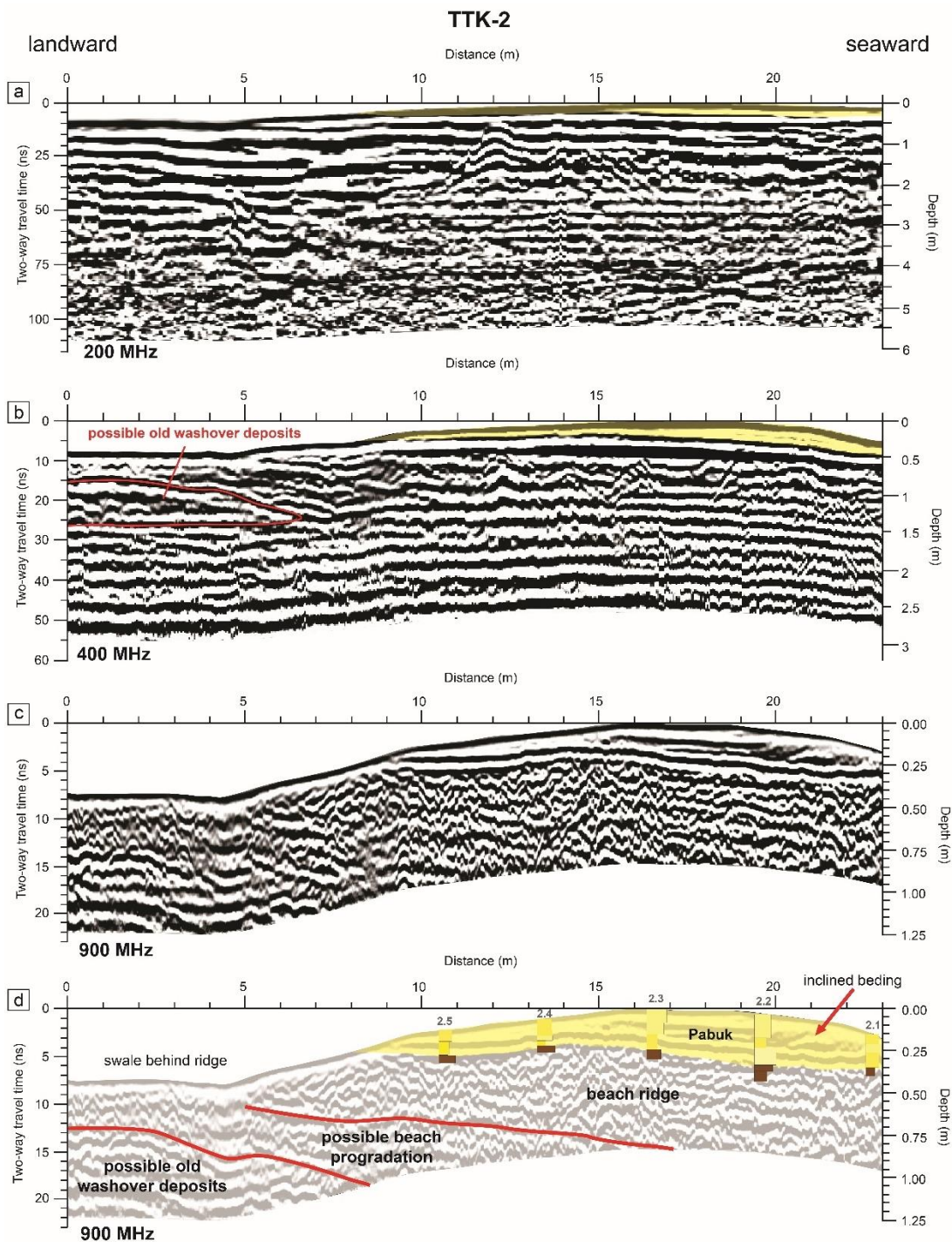


Figure 5.5 GPR profile of TTK-2 from 3 frequencies; 200, 400 and 900 MHz (a) 200 MHz profile with about 5 m depth (b) 400 MHz profile with about 2.5 m depth (c) 900 MHz with almost 75 cm depth and (d) 900 MHz with interpretation of TS-Pabuk deposits (yellow area) and sedimentary logs from 5 shallow pits (TTK-2.1 to 2.5).

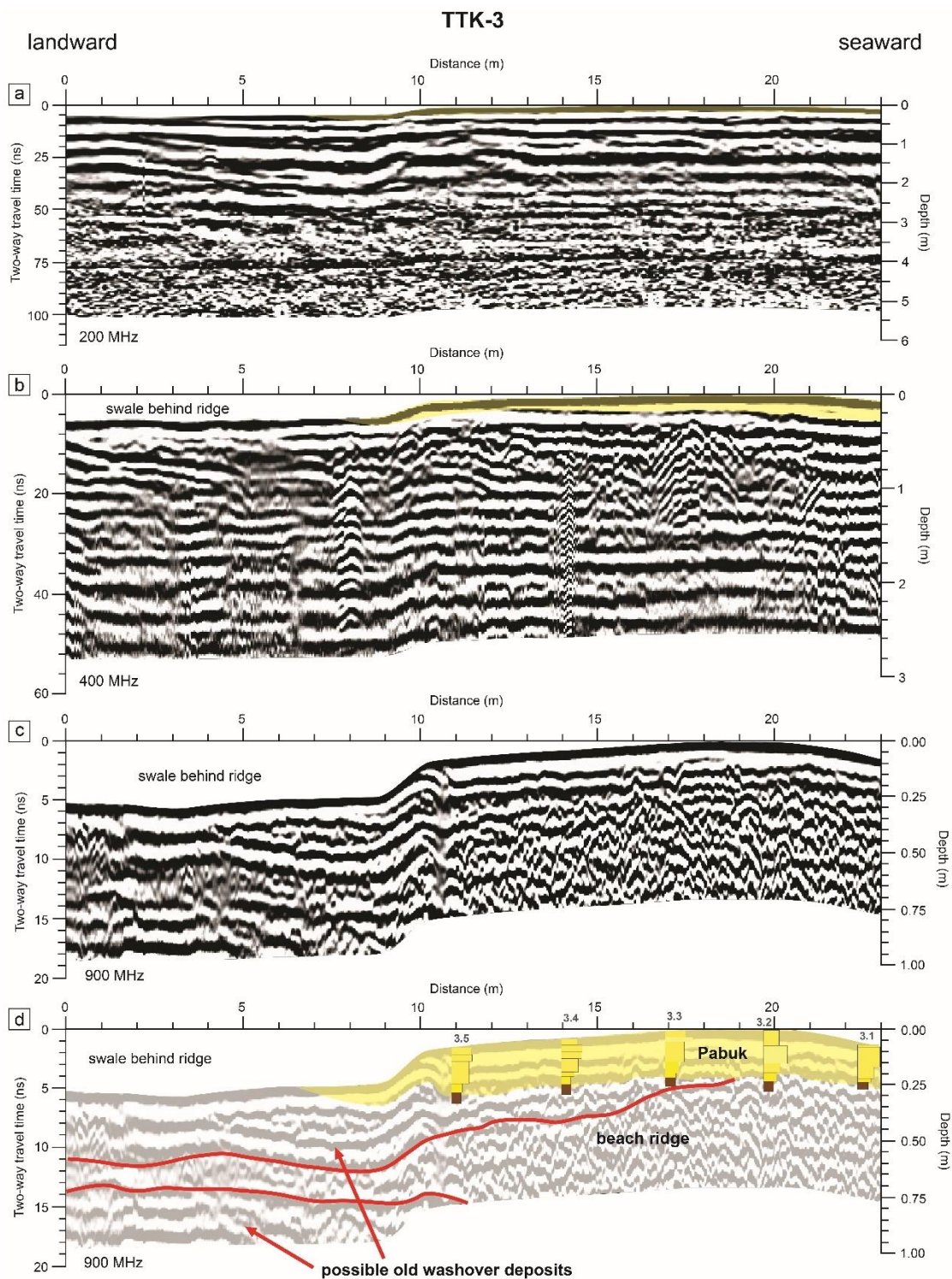


Figure 5.6 GPR profile of TTK-3 from 3 frequencies; 200, 400 and 900 MHz (a) 200 MHz profile with about 5 m depth (b) 400 MHz profile with about 2.5 m depth (c) 900 MHz with almost 75 cm depth and (d) 900 MHz with interpretation of TS-Pabuk deposits (yellow area) and sedimentary logs from 5 shallow pits (TTK-3.1 to 3.5).

5.4 Talumphuk (TLP)

Unlike other locations, TLP coast has an artificial structure – seawall – for preventing coastal erosion from monsoon and storm surge. In addition, there are shrimp ponds lying along the coast between back-dune swale and road. These structures could be important factors controlling the current. According to the field investigation and satellite image review, there are at least one inundation event leaving thick washover deposits into the pond at seaward side before Pabuk storm event. However, Pabuk deposits can be clearly seen as washover fans with current ripples on the surface behind seawalls. The sandy Pabuk sediments lied on the old sandy deposits from previous overwash events.

GPR was applied for 2 lines; TLP-1 and TLP-2 in this area. They are located 100 m far from each other. It is noticeable that the boundary of storm deposits from TLP-2 cannot be identified in the sediment pits. Even using GPR, differentiating them from original environments is still a problem. In this study, thus, the results mainly derived from TLP-1 which sedimentary logs and GPR signals can be compared. However, GPR signals of TLP-2 still give us some interesting structures which will be mentioned later. Considering TLP-1, the 200 MHz antenna provided up to ~5 m depth. However, Pabuk deposits are too thin to present any detail. Moreover, the landward pond outside GPR profile contains much water which can seep into surrounded area. This leads to low amplitude reflections in landward side of 200 MHz profile at ~1 to 3 m depth (Figure 5.7). The low amplitude also disturbs subsurface internal structures. Pabuk deposits are identified as a thin layer at topmost of the section. The 400 MHz antenna shows better resolutions. Internal structures such as horizontal layers are found within Pabuk unit. Especially at the proximal side, Pabuk shows seaward inclined bedding. Although this is unusual for washover deposits, it is proved by sedimentary open pit. The seawalls in front of sand dune might influence this deposition which will be discussed later. By this frequency, large-scale subsurface structures seem to be more visible. Sets of

landward foreset bedding (RS2) are imaged at below 0.5 to 1.5 m depth. Truncation of reflections (RS3) showing seaward erosion was found at proximal part of the profile at around 47-67 m distances. However, the signals started fading away at below 1.5 m due to humidity and end at ~2.5 m depth. The best internal detail of depositions appears in 900 MHz profile. Although this section yielded only less than 1 m depth, it shows different structures and signal patterns. An erosional boundary of Pabuk deposits was insisted using GPR profile and sedimentary pits. The deposition is thickest at the proximal part and thinner at the distal part. Other subsurface structures are clearly visible such as sets of foreset bedding, beach progradation and previous washover deposits.



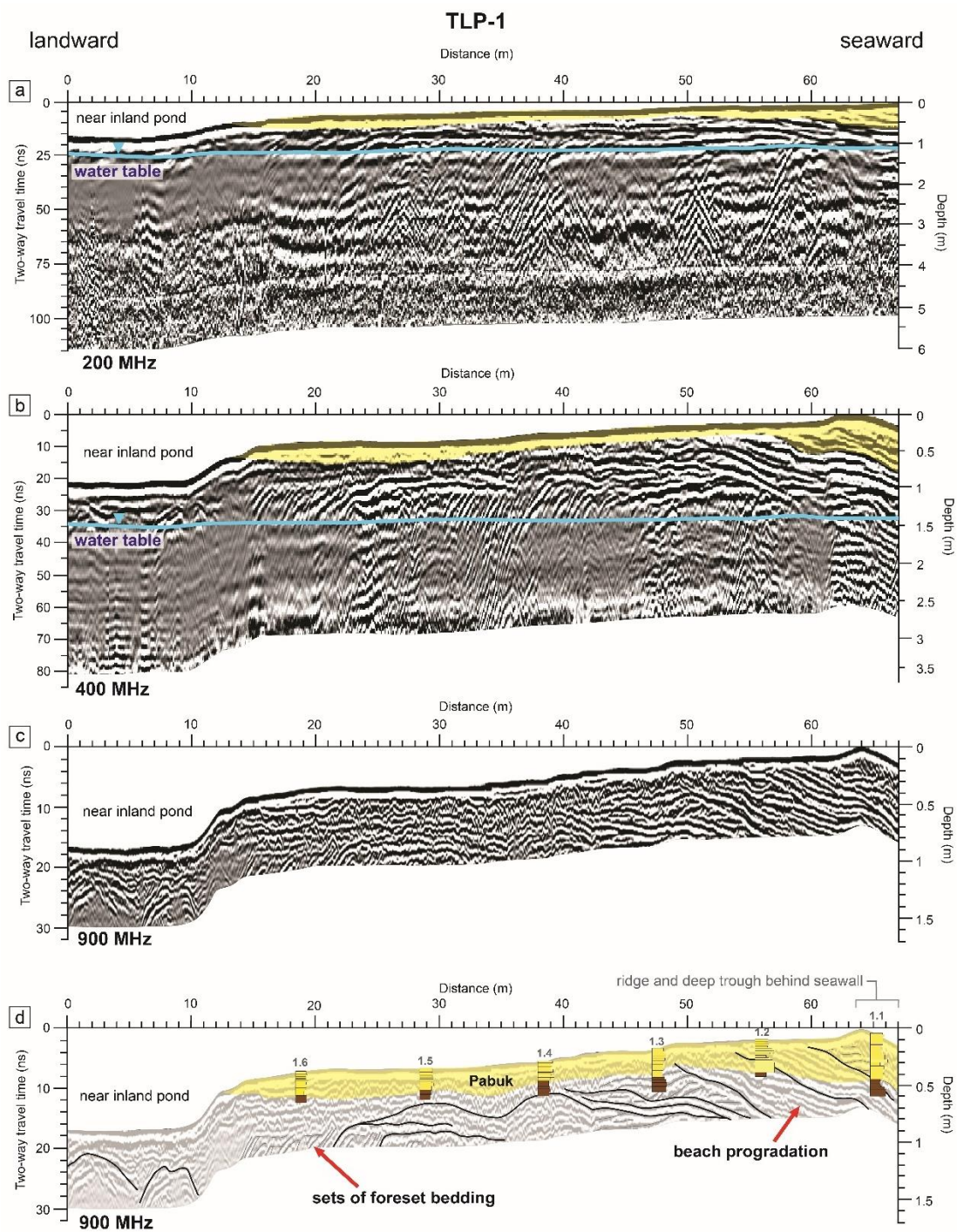
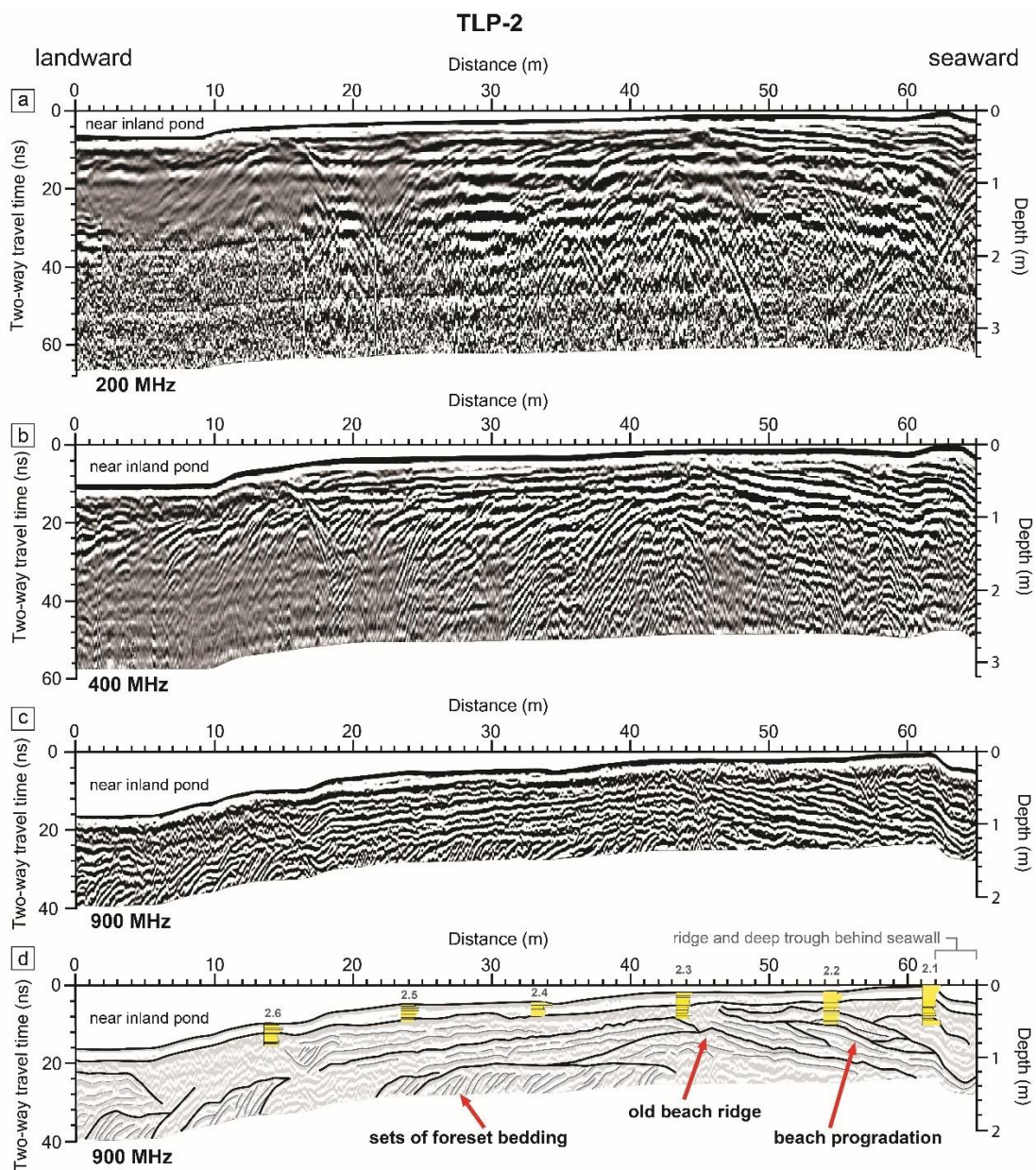


Figure 5.7 GPR profile of TLP-1 from 3 frequencies; 200, 400 and 900 MHz (a) 200 MHz profile with about 5 m depth (b) 400 MHz profile with about 2.5 m depth (c) 900 MHz with almost 75 cm depth and (d) 900 MHz with interpretation of TS-Pabuk deposits (yellow area) and sedimentary logs from 6 shallow pits (TLP-1.1 to 1.6).



*The lower base of washover deposits is not clear. However, the surface geometry can be clearly seen.

Figure 5.8 GPR profiles of TLP-2 from 3 frequencies; 200, 400 and 900 MHz (a) 200 MHz profile with about 5 m depth (b) 400 MHz profile with about 2.5 m depth (c) 900 MHz with almost 75 cm depth and (d) 900 MHz with interpretation of underlying structures and sedimentary logs from 6 shallow pits (TLP-2.1 to 2.6). However, the TS-Pabuk deposits cannot be identified in this location both in the field shallow pit walls and in the sedimentological analysis logs.

Table 5.1 Summary table of GPR frequencies used in this research, depth (m), horizontal resolution (cm) and internal structures found in each frequency.

GPR frequency	Depth (m)	Vertical resolution (cm)	Internal Structures
200 MHz	~5.5	13.25	- Seaward dipping of beach progradation - Water level
400 MHz	2.5	6.63	- Seaward dipping of beach progradation - Water level
900 MHz	0.75	2.95	- Landward inclined bedding inside TS-Pabuk deposits (TTK) - Landward foreset bedding of old washover deposits (TLP) - Parallel slightly landward inclined bedding of old washover deposits (BTN, TLP) - Seaward dipping of beach progradation (BTN, TLP) - Sharp contact (BTN, TTK)



CHAPTER 6

DISCUSSIONS

6.1 Hydrodynamic conditions in ascending order to distances from landfall site

6.1.1 Storm intensity and inland extent of washover deposits

The tropical storm Pabuk 2019 induced wave height and tidal range significantly higher than normal especially along the W-GOT. Many tide gauge stations showed that storm surge heights were higher than 0.5 m above maximum tide at that time. The high storm surge accompanied with high tide level can induce the height of storm tide up to 1.4 - 1.7 m above mean sea level. These conditions brought sediments to deposit in the coastal low-lying areas and also caused an erosion of modern beaches along the Gulf of Thailand coast. Considering hydrodynamic conditions, the conclusion is that the intensity of storm surge depends on local high tide which vary to the areas, storm surge height and wave height which directly related to distances from landfall site, the farther from landfall site the less effects (Figure 6.1).

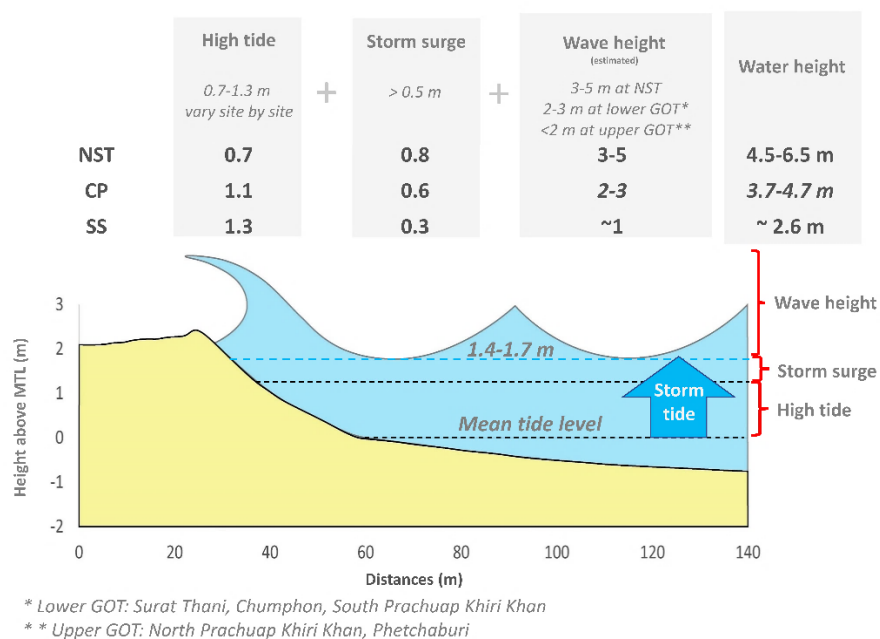


Figure 6.1 The intensity of storm events (water height) is the combination between high tide, storm surge height and wave height

The most severe site is Nakhon Sri Thammarat (NST) where is reasonably related to the landfall site. This site experienced the most intense wind speeds of almost 100 km/h, wave height of about 5 m and tidal range of 0.8 m above mean sea level. Consequently, inundation reaching the maximum of 330 m from coastline induced washover deposits to extend the farthest length of 150 m from coastline. Other sites received less suffer both in term of hydrodynamic conditions and sediment deposition. However, the main factor that control the inland extent of washover deposits is beach topography relative to water level. Here the example model of Phetchaburi is presented (Figure 6.2). This location is located farthest from the landfall location and received less intense of hydrodynamic conditions, but the washover deposits can extend far 90 m inland which is the second most length after at Nakhon Sri Thammarat. This may be an effect of other local controlling factors, as mentioned by Morton (2002) and Morton and Sallenger (2003), such as topography, vegetation cover, human activity or artificial structures and sediment supply.

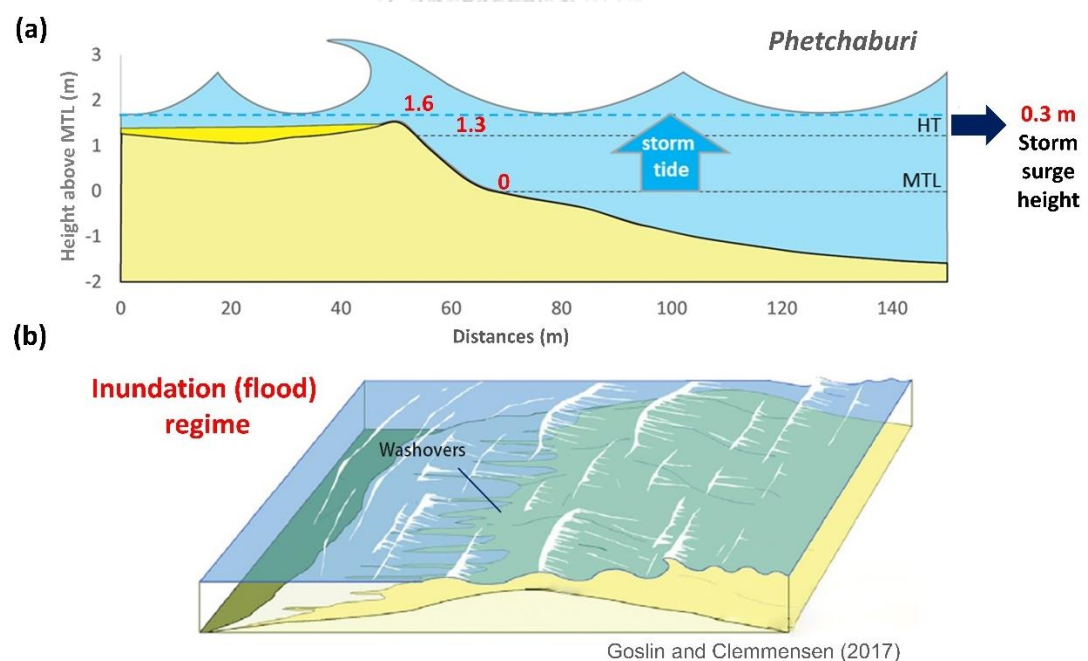


Figure 6.2 Schematic model of washover terrace generated during inundation regime (a) Storm tide level and wave runup at Phetchaburi compared with beach topography generated washover terrace behind the ridge (b) inundation regime that the water level is higher than beach ridge and fully cover back-barrier environment causing washover terrace (Goslin & Clemmensen, 2017)

6.1.2 Thickness of storm deposits

The common thickness of the deposits in this study is range from a few cm to about 30 cm. Washover thickness seem to be more relied on local morphology than distances from the landfall site. For example, sites 3, 4 and 5 (Table 3.1) in NST the nearest site to landfall location of storm's eye underwent extreme wind speeds, wave height and tidal range during storm surge event. Nevertheless, the deposit thicknesses preserved at gentle and flat sand beaches are ranged from a few cm to 30 cm. While the thicker deposits of 20-60 cm and 40 cm can be preserved at site 15 in ST and site 19 in CP, respectively. These sites are relatively low areas of channel inlet (Figure 6.4) connected to swale between beach ridges. Consequently, we suggested that although the landfall site experienced most intense conditions, thickness does not reflect that the nearer to landfall location the thicker of deposits. The thickest deposits were commonly found at channel inlet where is relatively low-lying area. However, the channel inlet is an active channel so that the deposits can be easily destroyed. This feature, so, has less preservation potential for storm deposits. Other features including washover types, erosional features, sedimentary structures and inundation, vary in each location which may also be an effect of local factors.

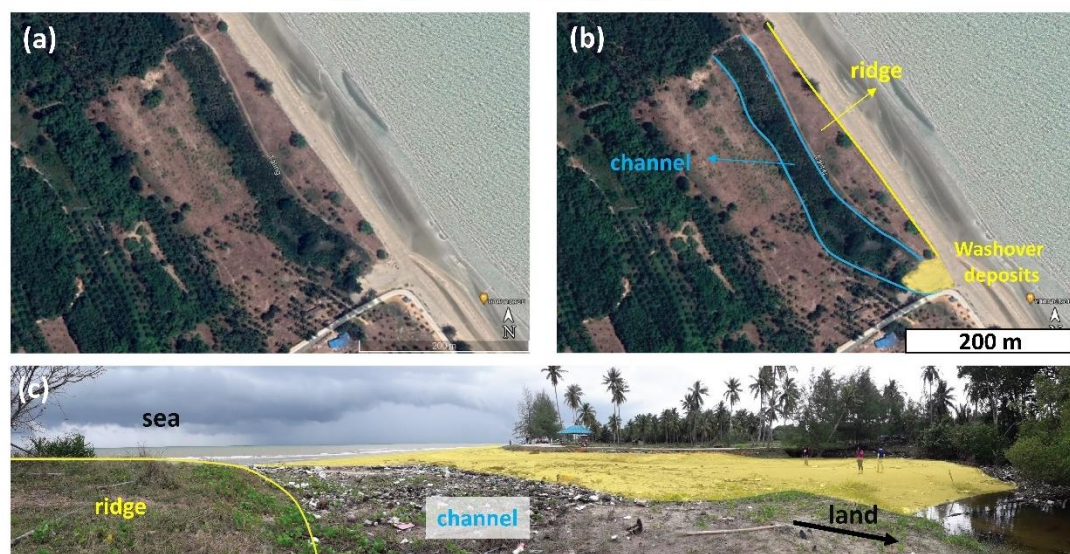


Figure 6.3 Pak Khlong Taling channel inlet (site 19) at Tha Chana district, Suratthani (a) satellite image of the channel and surrounded environments (b) the channel lying parallel to the shore

and beach ridge with the inlet that were covered by washover deposits after the TS-Pabuk event (c) photo of washover perched fan penetrated into the channel for 45 m distances with average 30 cm depth.

Sedimentary characteristics including surface morphology and structures which are resulting from the tropical storm Pabuk have a tendency to be vary on each location. The local morphology may play important roles on the preservation potential of sediments both in term of length and thickness. While the intensity of hydrologic conditions such as wind speeds, wave height and tidal range, are indistinctly related to the sediment deposition. However, effects of intense storm may be imprinted on the other characteristics such as grain size, grain geometry, grading and sorting. To be better understand the relation of storm and sediment characteristics, consequently, the studies in sedimentary detail are needed to collect the maximum possible amount of modern storm characteristics. This information would be an important key for analyzing paleostorm deposits and for better understanding the chronology of coastal hazards in this region.

6.2 Characteristics of Tropical storm deposits and flow conditions

Overall sedimentological characteristics that favor the TS-Pabuk deposits in the 4 study areas are thin (mostly < 30 cm) sand beds, wide ranges of grain size (fine to very coarse sand), larger grain accumulation in the middle layer of sequence, moderately well to poorly sorted, low mud contents, numerous sub-horizontal to horizontal planar laminations at the base, landward incline laminations at the top of the middle layers of the deposits, common landward thinning, maximum thickness is near the shore or in the middle part of lenticular antecedent surface depending on local topography, sharp and erosional basal contact of sand or shelly sand, shell fragments organized in thick bed or several laminations. Considering all sedimentary parameters and characteristics in detail, it can be conclude that there are 3 vertically organized patterns (Unit A, B, and C) of TS-Pabuk deposits. Each pattern is located at a specific section along the length of storm deposits (Figure 6.4). These variations can reveal flow behaviors of storm surges impacting the area and possible local factors that can control the flow.

6.2.1 Three dominant stratigraphies of event deposits in trench scale

In the vertical trench scale, this pattern was preserved at the middle to near distal part of CSR, proximal to the middle part of TTK. The 3 units were classified base on grain size and sedimentary structure. Whereas sorting, skewness and kurtosis did not show a significant trend in each unit but they are useful for distinguishing Pabuk sediments from the underlying pre-Pabuk.

Unit A is the horizontal planar laminations deposited at the base of Pabuk deposits and consists of finer grain size (fine to medium sand) at all pits in all transects of all 4 locations. This unit lies on the pre-Pabuk sediments with sharp and erosional contact. The sediments are also graded from smaller at the base to larger at the top of the sequence (reverse grading) which is clearly seen in CSR (Figure 4.1, 4.2, 4.3 and 4.4). Even though this trend may not be clear at TTK, the overall sequence still shows that unit A graded from smaller to larger grains in the upper unit B. This kind of vertical grading has been reported in both storm and tsunami deposits such as 2015 Tropical Cyclone Pam (Hong et al., 2018), 2013 Typhoon Haiyan (Brill et al., 2016; Soria et al., 2017), 2005 Hurricane Rita (Williams, 2009), 2004 Hurricane Frances and Jeanne (Wang & Horwitz, 2007) and 2004 Indian Ocean tsunami (Choowong, Murakoshi, Hisada, Charoentirat, et al., 2008). Furthermore, the study of Phantuwongraj et al. (2013) on washover deposits induced by strong monsoon and low-pressure systems at Surat Thani and Prachuap Khiri Khan province located at the W-GOT also reported the existence of multiple reverse grading. We proposed that the reverse grading at the lowest unit of storm deposits is a result of high grain concentration and collision within traction load transport or grain flow condition during the early state of storm surge which has a low flow depth (Choowong, Murakoshi, Hisada, Charoentirat, et al., 2008; Hand, 1997; Phantuwongraj et al., 2013; Tucker, 2003). One possibility is that continuously increasing flow intensity from the early state to the peak state induced larger grain to deposit on the upper part (Tucker, 2003). In some areas, unit A may contain a few amounts of mud because strong currents can erode the underlying mud to mix in the current and deposit with sand. Additionally, shell fragments can also be found as thin lamination to thick beds in some places. However, the main criteria for distinguishing this unit

from the others are parallel sub-horizontal to horizontal lamina sets at the base. This structure is directly related to multiple small and short periods of continuously individual storm wave pulse at the initial state of the storm event (Brill et al., 2016; Kitamura et al., 2020; Xiong et al., 2018).

Unit B, the larger grain size (medium to coarse or very coarse sand) accumulated as the middle layer with significantly high and large shell fragments and valves. In contrast to Unit A, this unit does not extend along all lengths as far as Unit 1 but is limited in specific sections and varied in study areas. Apart from massive and horizontal laminations, cross laminations are also observed only in these units. In CSR, sedimentary structures of unit 2 started from horizontal at the seaward and middle part for almost 10 m to low-angle cross laminations (9°) and to high-angle laminations (20°) at the near distal edge of storm deposits. This inclined structure was preserved for only 1 m and terminated at the near avalanche face. This pattern is similar to storm deposits of 2003 Hurricane Isabel at the Hatteras Island of North Carolina, USA where the landward dipping of 3° - 6° and 9° at the avalanching face were preserved (Morton et al., 2007). Although this structural trend is not visible at TTK, the larger grain trend was also clearly presented as an almost massive layer. Moreover, the fining landward was also presented in this location at TTK-1 (Figure 4.11). The cross laminations are also found in TLP-1.2. Although the overall trend of TLP cannot be differentiated and most of them are just horizontally laminated to massive, TLP-1.2 shows clearly distinct units. The cross laminations were preserved as a topmost unit with a parallel 6° - 7° angle and cut across the two lower units reflecting the higher energy of currents. The landward dipping cross laminations or inclined laminations in storm deposits were also reported in many works (Brill et al., 2016; Phantuwongraj et al., 2013; Sedgwick & Davis, 2003; Williams, 2009). This unit was deposited during the peak intensity of storm events which generated the maximum water level resulting from the combination between wave runup height and storm surge height (Donnelly et al., 2006). The inclined structure is also an indicator of bed load transportation (Morton et al., 2007). Furthermore, it is worth noting that non-parallel cross lamination was also found at BTN-1.2 (Figure 4.6). The two laminae show low angle landward dip direction, 4° at the upper part and 9° at

the lower part, with a narrower interval that is specifically presented within the small scale of about 1 m length. This characteristic is quite distinct from normal parallel cross-lamination found in other locations. This structure is possible to be the convex-upward laminae with trough-shape base (ud) of antidune (Alexander et al., 2001; Araya & Masuda, 2001; Choowong, Murakoshi, Hisada, Charoentitirat, et al., 2008), even though an upstream dip filling in the trough were not be seen. Consequently, the flow condition causing this unit should be high, in the upper flow regime or possibly up to supercritical flow conditions.

The uppermost unit C contains semi-massive to horizontal medium sand. At CSR, the characteristics of unit C and the lower unit B are clearly distinct and can be seen by the naked eye at the near terminal part of storm deposits (CSR-3.1 to 3.5), while the middle part (CSR-4) is not much clear due to the same horizontal lamination structure. However, the results of grain size analysis show the difference in mean grain size and sorting. The upper unit C contains mainly medium sand and is better sorted. At TTK, unit C lies on top of the condensed shell and larger grain layer of unit B, clearly seen at the proximal and middle part before thinning and disappearing at the distal part as same as at CSR. Normal grading is an important feature that is dominant in this unit which is also clearly seen at CSR and the 2 transect lines of TTK (TTK-1 and 2). Although the major grain proportion is medium sand, they are slightly graded from larger grains at the base to smaller grains on top. However, this grading trend is not presented at BTN, only a semi-massive trend was deposited as the topmost unit in the area (Unit 2). This characteristic reflects the late state of storm surge which has lower energy after the peak of storm surge has passed. This state is under the inundation flow regime and stagnant water that allows the suspended sediments to settle down as normal grading (Brill et al., 2016; Donnelly et al., 2006). Moreover, thinning landward trend was also found in this unit at CSR and TTK. Whereas the trend at BTN and TLP was varied and unclear. This may be an effect of the local topography.

6.2.2 Horizontal variation of storm deposits in transect scale

Even the vertical depositional pattern was classified into 3 units as mentioned above, they are located in different and specific positions on the horizontal transect scale of storm deposits. Some features, structures, or units did not extend along the transect lines which were set up perpendicular to the current or the shore. The proximal part of storm deposits tends to preserve the thick layer of single unit A (CSR-5 and TLP-1.1) or double layers of unit A overtopped by unit C (BTN-1.1), except TTK-1.1 showing triple layers. This part shows only a parallel horizontal or semi-massive structure. Whereas, the near proximal or middle, or near distal part has the potential to preserve the triple layers of units A, B, and C. The larger grain with inclined structures is deposited only in this range of deposits. This trend was presented in all locations but with a bit of lateral shift of section. The distal part preserved the double layer of units A and B at CSR and TTK, and units A and C at BTN. Although there are differences in details, they show the same vertical grading trend.

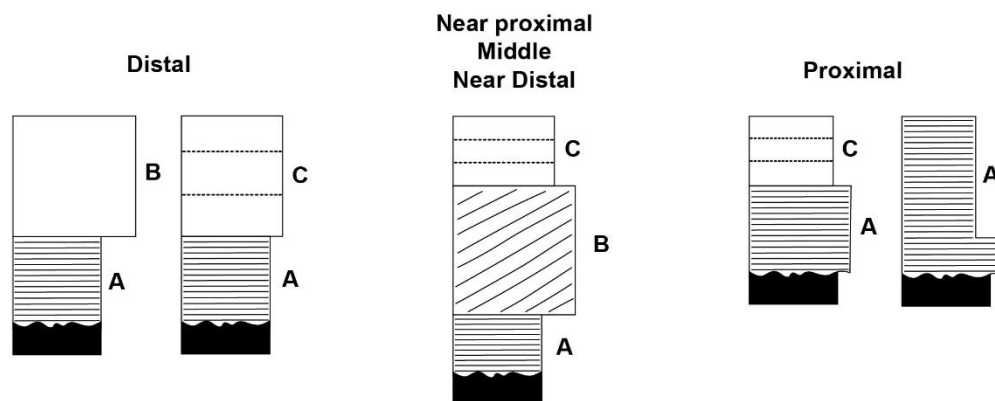


Figure 6.4 Schematic model showing patterns of sediment stratification at distal part, near distal to middle to near proximal and proximal part of the TS-Pabuk deposits. Unit A is horizontal lamination of fine grains which always found at base of the storm deposits and over the sharp erosional surface. Unit B is massive coarse grain layer with or without landward inclined stratification. Unit C is semi-massive layer of fine grains.

6.3 Local geomorphological controlling factors, storminess regime and storm deposits

According to the vertical stratigraphy pattern and horizontal variation, it is clearly seen that the pattern of storm deposits at CSR and TTK are very similar. The deposits were classified as washover terraces that extend many hundred meters along the shore. The thickness tends to be thinning landward, even some line at TTK shows lenticular thickness. Their overall trend also starts from laminated finer grain at the base (unit A) and slightly reverse graded to coarse or very coarse grain at the middle layer (unit B) and finally overtopped by a normal graded layer of medium sand (unit C). Local topographic information coupled with hydrodynamic conditions during storm events reveals that storm deposits in these two locations experienced maximum storminess regime classified by Sallenger (2000), inundation.

In the case of CSR (Figure 4.1), this location is located farthest from the landfall site of TS-Pabuk and experienced the least hydrodynamic intensities. However, the local high tide combined storm surge height was up to 1.6 m, and wave runup height can be up to 1 m at the peak intensity while the beach elevation is only 1.7 m. These hydrological parameters are high enough to exceed the beach and cause seawater flooding into coastal areas. Offshore breakwaters which are 2 m higher than msl cannot completely protect effects from inundation. Additionally, the bay between 2 breakwaters may behave like a channel that allows seawater to intrude directly into the beach. The sampling transect line is located at this location.

For TTK (Figure 6.5), the mudflat area is located closer to the landfall site than CSR. So, TTK could experience stronger hydrodynamic conditions. Although the storm tide was only 1.7 m, seems to be low when compared with the dune crest of 3.3 m. The possible wave height in this location can be up to 2-3 m. That means the water level in the site could be up to 3.7 to 4.7 m corresponding to the confirmation of eyewitnesses that confirm the flooding of seawater. Moreover, the storm also migrated the sand dune 5 to 6 m to the landside and deposited it as a washover terrace.

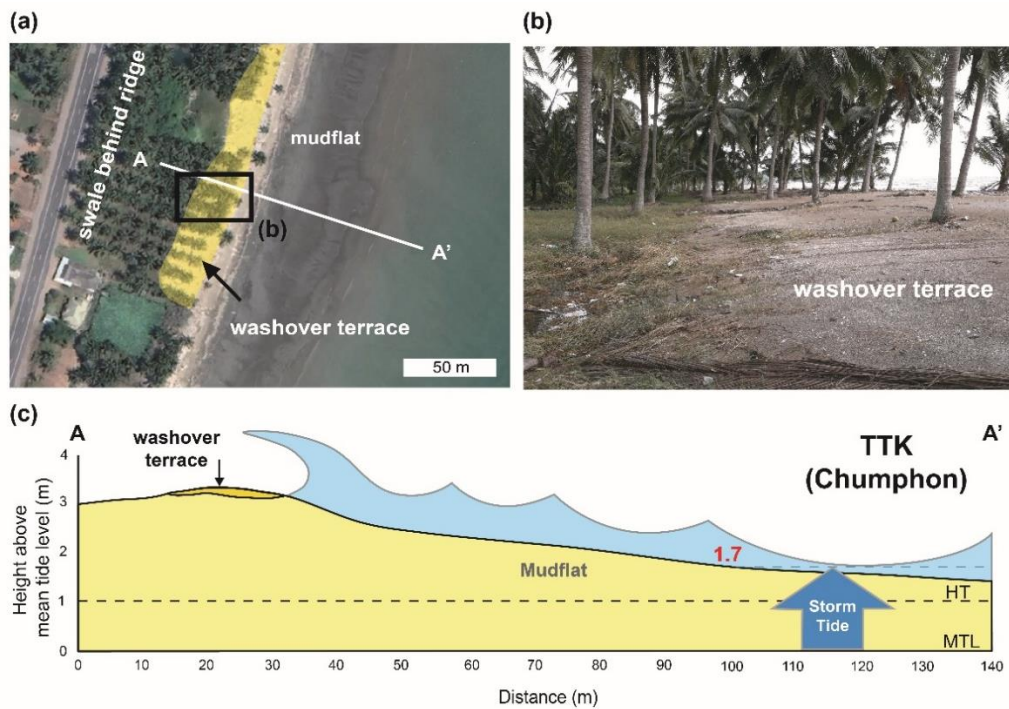


Figure 6.5 Details of transect TTK-1 (a) a satellite image showing storm deposits along the coastal area of TTK where are mudflat environments with swale behind beach ridge along the shore (b) washover terrace invading coastal area (c) beach topography cross-section (A-A') with mean tide level (MTL), high tide level (HT) and storm tide level at 1.7 m above mtl.

Storm deposits at BTN and TLP were classified as perched fans. However, the storminess regime of these areas is different. BTN experienced an inundation regime, whereas TLP experienced only an overwash regime. At BTN (Figure 6.6), the dune crest is about 2.4 m. The storm tide level is only 1.6 m. However, the wave runup height can be 1-2 m. So, the possible water level during the storm event could be up to 2.6 to 3.6 m which was enough to exceed the dune crest and allow flooding in this area. Another evidence of flooding is the limit line between lively green grass at the landside and brown dead grass at the seaside which can be visible from satellite images (Figure 6.5a and b). Although this area experienced the maximum storminess regime, the sand supply in this area is limited due to the geomorphology. This beach is a pocket beach between two limestone headlands. There is a canal that feeds fine particles to the shallow sea. Satellite images during low tide illustrated the mudflat at the intertidal zone. Consequently, it is possible that during overwash regime, strong wave runup but not exceeding the dune, waves can break the dune to

deposit as single perched fans at the back-barrier environment. Each fan was affected by varied intensities of currents. So, the cross lamination or antidune was not preserved at every lobe fan. When the wave runup was higher until covered the dune crest and reached the inundation regime, seawater flooded into the coastal area as far as 100 m from the coastline with very less amount of sand due to the limited sand supply in this area.

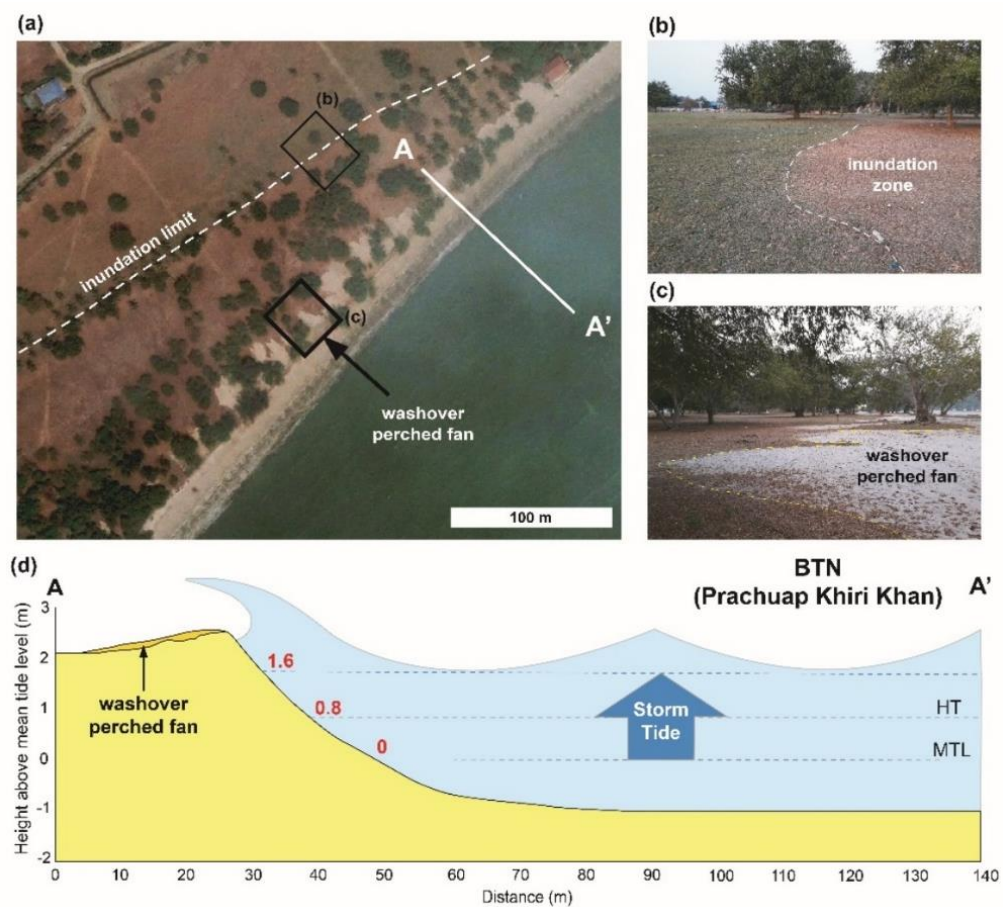


Figure 6.6 Details of transect BTN-1 (a) a satellite image showing storm deposits along the coastal area of BTN with the inundation limit line (b) inundation zone (brown grass) separated from non-inundation zone (green grass) (c) washover perched fan penetrating into the coastal area within inundation zone (d) beach topography cross-section (A-A') showing steep slope of the beach with mean tide level (MTL), high tide level (HT) and storm tide level of 1.6 m above mtl.

In the case of TLP (Figure 6.7), this area is the nearest to the landfall site of the storm eye which experienced the strongest hydrodynamic and meteorologic intensities among the 4 study areas. This area was protected by artificial seawalls

along the shore for at least 1 km which is about 3.2-3.3 m higher than msl. The storm tide during Pabuk landfall is about 1.5 m but the wave runup height was about 3-5 m. So, the water level could be up to 4.5 to 6.5 m which can cause the inundation. However, evidences of inundation is absent in this area such as debris line, watermark on the tree, or even the eyewitness. In the field survey, it was clearly seen that the fresh sandy sediments with current ripples of TS-Pabuk were deposited on top of the underlying sand of possibly old washover deposits. Satellite images insist that this area is a full water pond that was filled up by washover sediments from at least 2 events during 2000-2009 and 2009-2012 before Pabuk's arrival. The event during 2009-2012 seems to be the strongest because it brought the sediments to deposit as a washover terrace for more than 1 km along the shore. Whereas Pabuk deposits are only a few perched fan lobes that reflect lower energy of currents. It can be assumed that the event during 2009-2013 should be the November 2010 depression that covers the southern part of Thailand. Even though the intensity of the depression is less than tropical storm Pabuk, this study area in 2010 did not have a seawall to protect the coastal area. Therefore, depression intensity is enough to cause severe effects on the coastal area. On the other hand, this area in 2019 has a high seawall to relieve the effects of the strong wave from TS-Pabuk. This area may not experience inundation but regime only overwash. This artificial structure also plays an important role in the storm deposits behind them. The deposits have no diagnostic sedimentological trend as same as other areas. Moreover, the backside (landward) seawall is the deep trough that allows the currents to be turbulent. So, pit TTK-1.1 shows a single massive thick layer of ~40 cm which is the thickest among all pits in this research due to the original topography affected by an artificial structure.

According to the 4 study areas lying from the farthest to the nearest to the landfall site of the storm eye including CSR, BTN, TTK, and TLP, respectively, the storm deposits are visibly distinct place by place, vary in sedimentary structures, thickness grain size, stratigraphy pattern, and other characteristics. The conclusion is that distances from landfall location have no more influent on the characteristics of storm deposits than local controlling factors. The deposits are directly related to the

flow or current in the area of which behaviors were controlled by these factors; 1) local high tide level which is a specific character of the area 2) storm surge height which corresponds to the distances from landfall location, the farther the lower storm surge height 3) wave runup height which also depends on the distances from landfall site 4) elevations of dune crest 5) artificial structure like offshore breakwater or seawall and 6) amount and type of sediments supply.

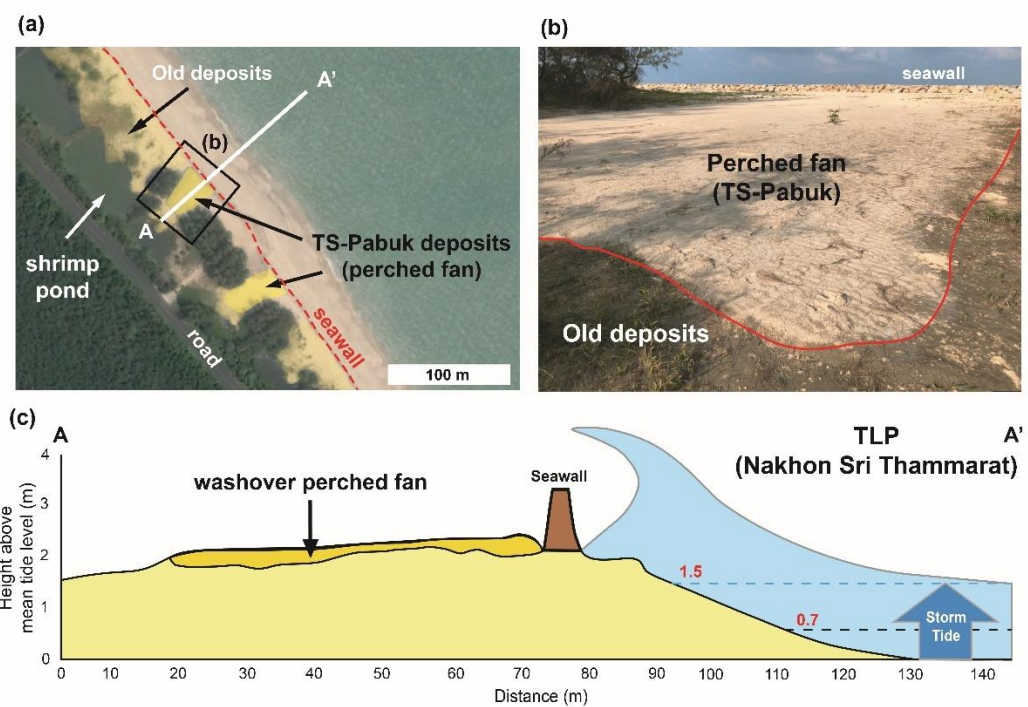


Figure 6.7 Details of transect TLP-1 (a) a satellite image showing the TS-Pabuk deposits over old deposits along the coastal area of TLP where (b) washover perched fan behind artificial seawall (c) beach topography cross-section (A-A') with mean tide level (MTL), high tide level (HT) and storm tide level at 1.5 m above mtl.

6.4 Comparison of Pabuk and other modern storm deposits

The 2019 tropical storm Pabuk made landfall at the W-GOT providing well-preserved evidence including washover deposits, internal details, morphological change, and hydrological data from tide gauge stations which are very useful for understanding the relationship between the flow event during the storm surge and the deposits. Most studies of modern storms in the past focused on hurricanes or typhoons or cyclones (Boughton et al., 2011; Brill et al., 2016; Doran et al., 2009;

Haque et al., 2021; Hawkes & Horton, 2012; Morton & Barras, 2011; Morton et al., 2007; Nott et al., 2013; Pilarczyk et al., 2016; Soria et al., 2017; Soria et al., 2021; Takagi et al., 2014; Williams, 2009; Williams, 2010) which has the maximum intensity (119 kph to >252 kph) according to the classification of Saffir-Simpson scale (Table 6.1). Although the tropical storm Pabuk is in the lower category with the weakest intensity among them, the inherited sedimentary evidence shows that there are other local factors that have more influence on the deposits than the hydrodynamic intensity of the storm.

The most intense storm in Table 6.1 made landfall with strong intensities and caused severe inundation or overwash impact along the coastal area that can extend the deposits to several hundred meters or even more than 1 km and 2 km such as the Cat-5 Typhoon Haiyan at Leyte Gulf, Philippines (Soria et al., 2017) and Cat-2 Hurricane Ike at Texas (Williams, 2010), respectively. Whereas the TS-Pabuk deposits yield less than 100 m of the maximum inland extent. Agreeable with Morton (2002) that high-velocity wind-driven currents can influence the maximum distance of inland penetration. The thickness of storm deposits is less than 1 m and also variable locally. The same trend found in most modern storm deposits is the landward thinning, rare to low mud contents, sharp erosional and depositional contact. The grain size of storm deposits can range from very fine sand to very coarse sand or even gravel as found in Typhoon Durian 2006 (Soria et al., 2021). Sedimentary structures include massive, planar horizontal lamination, landward cross lamination, foreset bedding, and possible antidune. Some of them display as a single layer, while they were organized as distinct 2 to 3 layers in other locations. For example, TS-Pabuk displays 2 units of the lower horizontal planar laminations and the upper semi-massive with landward dipping lamination, possible antidune. These characteristics are similar to those found in deposits of Hurricane Rita in 2005 at Louisiana, USA (Williams, 2009). Moreover, the lateral change of structures was also found in some storm deposits. The deposits started with planar horizontal lamination and migrate into foreset laminae at the landward terminus in Typhoon Durian 2006 (Soria et al., 2021) as same as those found in TS-Pabuk. The Pabuk deposits of the middle unit 2 at CSR also start with planar horizontal lamination before migrating to

cross lamination of 9° and to 20° at the near terminus of the washover edge. Sorting in overall trend is variable from well to poorly sorted. Vertical grading includes both fining upward and coarsening upward trends. Most studies in the past contain a maximum of 2 units of storm deposits with distinct grading trends but only Pabuk deposits display the 3 distinct units which present the new pattern of vertical grading. At CSR and TTK, Pabuk deposits start from finer grain at the base and gradually grade up to coarser grain at the middle unit and finally graded to finer grain at the top unit. This full pattern has never been reported before. Fining landward of lateral grading is also one important feature reported in many storm deposits. Pabuk deposits also show this trend in some locations but are still varied and can be representative of all Pabuk deposits. In some locations and some units, Pabuk graded from finer at seaward to coarser at the middle and finer again at the middle. Whereas, some locations cannot be defined as any lateral grading trend due to the turbulent currents. Furthermore, among the modern storm studies in Table 6.1 and 6.2, there are some locations that reported the presence of artificial structures along the shore. For example, the embankment at Kuakata, Bangladesh (Haque et al., 2021) is similar to the seawall at TLP, Thailand, and the offshore breakwaters at Constance Beach, Louisiana USA (Williams, 2009) are similar to CSR, Thailand. Although, these studies have not directly reported the effect of these hard structures. Seawall adjacent to the beach plays an important role in the deposits behind them. The currents behind seawalls could be turbulent so that the storm sediments could not display similar characteristics as those found in another natural beach due to unnatural currents. However, a record of the beach topography of this area before the landfall of Pabuk is absent. So, it is difficult to estimate the erosion effect of the beach in front of the seawall. For offshore breakwaters located far in the sea, this structure cannot directly affect the depositions but can relieve the intensities of currents such as the wave height and velocity. However, the height of these structures could be considered with the height of the water level during storm surges for each locality to predict the currents of each area.

Table 6.1 Meteorology, hydrology and sedimentary characteristics of TS-Pabuk deposits and Typhoon Haiyan, Cyclone Yasi and Hurricane Ike.

Name of Storm		Tropical storm Pabuk		Typhoon Haiyan		Cyclone Yasi		Hurricane Ike		
Meteorology	Landfall date	2019 January	2013 November	2013 November	2011 February	2009 September				
	Landfall location	Western coast of the Gulf of Thailand	Philippines	Philippines	Australia	USA				
	Peak intensity	Tropical storm (994 hPa; 85 kph)	Category 5 (995 hPa; 314 kph)	Category 5 (995 hPa; 314 kph)	Category 5 (929 hPa; 205 kph)	Category 4 (231 kph)				
	Landfall intensity moving speed	996 hPa; 80 kph	Category 5 (296 kph)	Category 5 (296 kph)	Category 5	Category 2 (175 kph)				
	reference	25 kph	41 kph	41 kph		20 kph				
	Site location	Phetchaburi (CSR-1)	Prachuap Khiri Khan (BFN-1,2,3)	Chumphon (TTK-1,2,3)	Nakhon Si Thammarat (TLP-1)	South of Cairns, northeast Queensland,	Galveston and San Luis Islands, Texas			
	Distances from landfall location	500 km	400 km	200 km	15 km	30 km	25 to 80 km			
	Coastal morphology	Beach between canals and several offshore breakwaters	Pocket beach between two headlands	Narrow beach in middle with swale parallel to the shore	Beach on sand spit with seawall	Sandy beach	Barrier islands (ridge and swale topography)			
	Ground surface elevation above msd	-1.7 m of ridge crest, 2 m of offshore breakwater top	-2.4 m of ridge crest	3.2-3.4 m of dike crest	3.2-3.3 m of seawall top and 2.4 of dike crest behind seawall	1.5 to 2 m	0.75 to 2.2 m			
	Storm tide above msd	-1.6 m	-1.6 m	-1.7 m	-1.2 m	5-6 m	3-6 m			
	Wave height above msd	-1 m	1.2 m	2.3 m	3.5 m	-1 hr	3-4 m			
	Inundation duration	N/A	N/A	N/A	N/A	-1 hr	12 hrs (peak inundation lasting for 2 hrs)			
	Inundation distances	N/A	50-100 m	75 cm	N/A	2 km	Not reported			
	Reference		This study	This study	Placzek et al. (2016), Sorin et al. (2017)	Brill et al. (2016)	Williams, 2010; Dean et al., 2009			
	Hydrodynamic conditions and settings	Washover cross-shore geometry	Washover terrace, thinning landward pits	Perched fans, thickest at the middle	Washover terrace, thinning landward	Perched fans, thinning landward	Overall but not systematic landward thinning depressions but generally thick in	Overall landward thinning trend	Landward thinning; thicker deposits on the swales	Fining and thinning landward
Inland extent		20 m	23 m	23 m	67 m	1600 m	Overall landward fining	110 to 320 m	2700 m	
Lateral grading		Unit 1: no systematic trend in distal and distal part, coarser at the middle	No systematic trend	Unit 1: no systematic trend in distal part, coarser at the middle	Overall landward fining	Unit 1: no systematic trend in distal part, coarser at the middle	Unit 1: no systematic trend	Unit 1: no systematic trend in one site, no systematic trend in another site	Not reported	
Thickness of deposits		4-30 cm from distal to proximal	3-25 cm	2-33 cm	Up to 40 cm at proximal pits (behind seawall)	2 m (distal) 10-20 cm (proximal)	2-20 cm	5 cm (87 m from shore); 20-50 cm (50 m from the shore)	51-64 cm (within 200 m); 3-10 cm (>200 m)	
Vertical change in Grain size		Overall: reverse grading at base, normal grading at top (coarse at middle)	Unit 1: very fine - coarse	Unit 1: moderately - poorly sorted	Overall: fine - coarse sand with no systematic trend	Unit 1: coarsening upward	Unit 1: normal graded, massive to laminated fine to medium sand	Fining upward with fine-skewed trends	Coarsening upward; alternate coarsening and fining upwards	
Sorting		Unit 1: med. well - poorly sorted	Unit 1: med. well - poorly sorted	Unit 1: moderately - poorly sorted	Unit 1: moderately - poorly sorted	Unit 1: moderately - poorly sorted	Unit 1: moderately - poorly sorted	Unit 1: moderately - poorly sorted	Unit 1: moderately - poorly sorted	
Sedimentary structures		Unit 1: horizontal planar lamination with current ripples at distal part	Unit 1: horizontal planar lamination	Unit 1: horizontal planar lamination	Overall: horizontal planar lamination, massive	Unit 1: massive to horizontal planar lamination	Unit 1: massive to horizontal planar lamination	Unit 1: massive to horizontal planar lamination	Unit 1: massive to horizontal planar lamination	
Shell fragments		Common in unit 2	Common in unit 1	Common in unit 2	Common in unit 1 and 3	Common in unit 1 and 3	Common in unit 1 and 3	Common in unit 1 and 3	Common in unit 1 and 3	
Internal mud		Low mud contents	Low mud contents	Low mud contents	Low mud contents	Low mud contents	Low mud contents	Low mud contents	Low mud contents	
Basal contact		Sharp, erosional	Sharp, erosional	Sharp, erosional	Sharp, erosional (scouring)	Sharp, erosional	Sharp, erosional	Sharp, erosional	Sharp, erosional	
References			This study	This study	Placzek et al. (2016), Sorin et al. (2017)	Brill et al. (2016)	Brill et al. (2016)	Not et al. (2013)	Hawkes and Horton, 2012	Williams, 2010
Sedimentological characteristics		Reference		This study	This study	Placzek et al. (2016), Sorin et al. (2017)	Brill et al. (2016)	Not et al. (2013)	Hawkes and Horton, 2012	Williams, 2010
		Washover cross-shore geometry	Washover terrace, thinning landward pits	Perched fans, thickest at the middle	Washover terrace, thinning landward	Perched fans, thinning landward	Overall but not systematic landward thinning depressions but generally thick in	Overall landward thinning trend	Landward thinning; thicker deposits on the swales	Fining and thinning landward
		Inland extent	20 m	23 m	23 m	67 m	1600 m	Overall landward fining	110 to 320 m	2700 m
		Lateral grading	Unit 1: no systematic trend in distal and distal part, coarser at the middle	No systematic trend	Unit 1: no systematic trend in distal part, coarser at the middle	Overall landward fining	Unit 1: no systematic trend in distal part, coarser at the middle	Unit 1: no systematic trend	Unit 1: no systematic trend in one site, no systematic trend in another site	Not reported
	Thickness of deposits	4-30 cm from distal to proximal	3-25 cm	2-33 cm	Up to 40 cm at proximal pits (behind seawall)	2 m (distal) 10-20 cm (proximal)	2-20 cm	5 cm (87 m from shore); 20-50 cm (50 m from the shore)	51-64 cm (within 200 m); 3-10 cm (>200 m)	
	Vertical change in Grain size	Overall: reverse grading at base, normal grading at top (coarse at middle)	Unit 1: very fine - coarse	Unit 1: moderately - poorly sorted	Overall: fine - coarse sand with no systematic trend	Unit 1: coarsening upward	Unit 1: normal graded, massive to laminated fine to medium sand	Fining upward with fine-skewed trends	Coarsening upward; alternate coarsening and fining upwards	
	Sorting	Unit 1: med. well - poorly sorted	Unit 1: med. well - poorly sorted	Unit 1: moderately - poorly sorted	Unit 1: moderately - poorly sorted	Unit 1: moderately - poorly sorted	Unit 1: moderately - poorly sorted	Unit 1: moderately - poorly sorted	Unit 1: moderately - poorly sorted	
	Sedimentary structures	Unit 1: horizontal planar lamination with current ripples at distal part	Unit 1: horizontal planar lamination	Unit 1: horizontal planar lamination	Overall: horizontal planar lamination, massive	Unit 1: massive to horizontal planar lamination	Unit 1: massive to horizontal planar lamination	Unit 1: massive to horizontal planar lamination	Unit 1: massive to horizontal planar lamination	
	Shell fragments	Common in unit 2	Common in unit 1	Common in unit 2	Common in unit 1 and 3	Common in unit 1 and 3	Common in unit 1 and 3	Common in unit 1 and 3	Common in unit 1 and 3	
	Internal mud	Low mud contents	Low mud contents	Low mud contents	Low mud contents	Low mud contents	Low mud contents	Low mud contents	Low mud contents	
	Basal contact	Sharp, erosional	Sharp, erosional	Sharp, erosional	Sharp, erosional (scouring)	Sharp, erosional	Sharp, erosional	Sharp, erosional	Sharp, erosional	
	References		This study	This study	Placzek et al. (2016), Sorin et al. (2017)	Brill et al. (2016)	Brill et al. (2016)	Not et al. (2013)	Hawkes and Horton, 2012	Williams, 2010

Table 6.2 Meteorology, hydrology and sedimentary characteristics of TS-Pabuk deposits and Cyclone Sidr, Typhoon Durian, Hurricane Rita and Hurricane Isabel.

Name of Storm		Tropical storm Pabuk		Cyclone Sidr		Typhoon Durian		Hurricane Rita		Hurricane Isabel		
Meteorolo	Landfall date	2019 January	Western coast of the Gulf of Thailand	2007 November	Philippines	2006 November	USA	2005 September	USA	2003 September	USA	
	Landfall location	Western coast of the Gulf of Thailand		Bangladesh		USA		USA				
	Peak intensity	Tropical storm (994 hPa; 85 kph)		Cat 4 (918 hPa; 250 kph)		Cat 5 (897 hPa; 288 kph)		Cat 5 (897 hPa; 288 kph)			Cat 5 (~270 kph)	
	Landfall intensity	996 hPa; 80 kph		Cat 4		Cat 5 (190 kph)		Cat 5 (190 kph)			Cat 2	
	moving speeds	25 kph				19 kph		19 kph				
	reference			O'Hara, J. F., 2007		Williams, 2009; Morton and Barnes, 2011		Williams, 2009; Morton and Barnes, 2011			Morton et al., 2007	
	Sub location	Prachup Khiri Khan (BTN-1,2,3)	Chumphon (TLP-1,2,3)	Kuabahn	Lagoon Gulf, Malinao	Constantine Beach, Louisiana		Constantine Beach, Louisiana			Hattness Is, North Carolina	
	Distances from landfall location	400 km	200 km	N/A	Direct hit (within storm eye)	35 km		35 km			55 km	
	Coastal morphology	Pocket beach between two headlands	Narrow beach in middle with scale parallel to the shore	Sandy beach in delta in with artificial embankment	Barrier spit	Beach ridge separated by low ridge, muddy marshes with offshore breakwaters		Beach ridge separated by low ridge, muddy marshes with offshore breakwaters			Barrier island with dunes	
	Ground surface elevation (above msd)	-1.7 m of ridge crest, 2 m of offshore beachward top	3.2-3.4 m of ridge crest	5 m of embankment top	3-4 m	0.5 to 1 m of ridge		0.5 to 1 m of ridge			Dunes at 3 to 4 m	
	Storm tide above msd (m)	-1.6 m	-1.7 m	Not reported	Not reported	4-5 m storm surge height		4-5 m storm surge height			2.7 m (open-coast) >3 m to 4 m	
	Wave height above msd (m)	-1 m	2-3 m	Not reported	Not reported	Not reported		Not reported			8.1 m offshore	
	Inundation duration	1-2 m	3-5 m	Not reported	Not reported	6 hours		6 hours			9 hrs (with peak inundation lasting for 5 hrs)	
	Inundation distances	N/A	7.8 cm	Not reported	≥150 m	Not reported		Not reported			18 to 30 km	
	Reference	504100 m	This study	Not reported	Williams, 2009; McGee et al., 2013	Williams, 2009; McGee et al., 2013		Williams, 2009; McGee et al., 2013			Morton et al., 2007	
	Washover cross-shore geometry	Peched fans, Thinning landward	Washover terrace, Thinning landward	Unit 1: landward thinning trend Unit 2: highly variable thickness	Washover fan, landward thinning	Unit A: Broad thin drupe, landward thinning Unit B: steeply sloped washover terrace with landward thinning		Unit A: Broad thin drupe, landward thinning Unit B: steeply sloped washover terrace with landward thinning			washover terrace terminating in avalanche faces	
	Inland extent	20 m	25 m	305 m	~150 m	Maximum 260 m, average 200 m (terrace)		Unit A: Landward fining Unit B: No trend			Not reported	
	Lateral Grading	Unit 1: no systematic trend Unit 2: finer at proximal distal part, coarser in the middle Unit 3: no systematic trend	Unit 1: no systematic trend Unit 2: finer at proximal distal part, coarser in the middle Unit 3: no systematic trend	Unit 1: landward fining trend Unit 2: no systematic trend found in this unit	Landward fining	Unit A: Landward fining Unit B: No trend		Unit A: Landward fining Unit B: No trend			Not reported	
	Thickness of deposits	4-30 cm from distal to proximal	3-25 cm	5-55 cm	Up to 4 m (proximal), 10 cm (near fan terminus)	2-50 cm		2-50 cm			40-97 cm	
	Vertical change in Grain size	Overall: reverse grading at base, normal grading at top (normal to middle) Unit 1: medium sand Unit 2: very coarse sand Unit 3: medium sand	Overall: reverse grading at base, normal grading at top (normal to middle) Unit 1: fine - medium sand Unit 2: medium - coarse sand Unit 3: coarse sand	Unit 1: white to light gray normal to medium coarse of gravel coarse sand Unit 2: olive gray normal graded sandy silt. It shows bimodal grain size distribution dominated by silt (40-60 μm) and fine sand (75-250 μm).	Fining and coarsening upward sequence of gravel coarse sand	Unit A: Inverse grading of muddy fine sand Unit B: Inverse grading of muddy fine sand Unit C: Inverse grading of muddy fine sand Unit D: Inverse grading of muddy fine sand		Unit A: Inverse grading of muddy fine sand Unit B: Inverse grading of muddy fine sand Unit C: Inverse grading of muddy fine sand Unit D: Inverse grading of muddy fine sand			Two cycles of upward coarse sand, medium sand and silt cycles of upward coarse sand/fining at top of medium sand	
	Sorting	Moderately well - well sorted	Moderately well - well sorted	Moderate to poorly sorted	Moderately sorted	Overall: well sorted		Overall: well sorted			Well sorted	
	Sedimentary structures	Unit 1: horizontal planar lamination with current ripples at distal part Unit 2: landward cross laminations (9°-20°) Unit 3: horizontal planar lamination	Unit 1: horizontal planar lamination, massive Unit 2: horizontal to massive Unit 3: planar horizontal lamination (8° angle) Surface: Current ripples	Unit 1: massive to marked laminae Unit 2: Parallel laminae but change to massive at upper part	Planar laminations, forest stratification	Unit A: Planar laminae with locally reworked ripples Unit B: Common forests, rough cross bedded sand		Unit A: Planar laminae with locally reworked ripples Unit B: Common forests, rough cross bedded sand				Subhorizontal planar stratification, landward dipping at alternating zone, some forests, midline, landward dips from 3°-6° and 9° at avalanche face
	Shell fragments	Common in unit 2 of coarsest sand	Common in unit 1	Common in unit 1 and 3 of coarsest sand		Unit A: News Unit B: Common		Unit A: News Unit B: Common			rare	
	Internal mud Layer	Low mud contents	Low mud contents	Low mud contents		Unit A: Common mud cap Unit B: rare		Unit A: Common mud cap Unit B: rare			No mud layer, no rip-up clay	
	Basal contact	Sharp, erosional	Sharp, erosional	Sharp, erosional (scouring)		Overall: Abrupt and depositional underlying organic rich soil		Overall: Abrupt and depositional underlying organic rich soil			Abrupt sand contact with underlying organic rich soil	
	References	This study	This study	Haque et al. (2021)		Williams, 2009		Williams, 2009			Morton et al., 2007	

6.5 GPR for shallow deposits induced by storm and possible paleostorms captured by 900 MHz frequency GPR

The best frequency of Ground Penetrating Radar (GPR) technique that is suitable for studying shallow storm deposits is 900 MHz which is the highest resolution using in this research. Although the 900 MHz gave the poorest depth with only 75 cm less than those from 400 and 200 MHz, this frequency gave the best resolution. With 900 MHz antenna, the GPR signal can illustrate large-scale sedimentary structures such as landward inclined structure or cross bedding at TTK-1 and TTK-2. This structure is invisible by naked eyes in the field open-pit due to the limitation of the width of pits. This structure is too large to be notice in a small pit but shown in GPR signals.

In case of transect TLP-1 and TLP-2, additionally, GPR with 900 MHz frequency can capture sets of landward foreset bedding at base of the signals with about 75 cm depth from ground surface (Figure 6.8). This structure is similar to those reported by Schwartz (1975) which represented the deposition of sediments into water body. This condition causes the decrease of sediment velocities and allows the deposition of sediments as a steep lamination dipping to the water body as delta foreset stratification. Above this foreset lamination, horizontal stratifications were deposited which indicate the subaerial depositions of storm sediments. The TS-Pauk deposits, then, deposited at the topmost thin layer (thick white band in the GPR signal) as horizontal stratification. It can be concluded that storm surge induced by the TS-Pabuk brought seaward sediments to deposits on top of the previous washover deposits under subaerial surface, not into the water body.

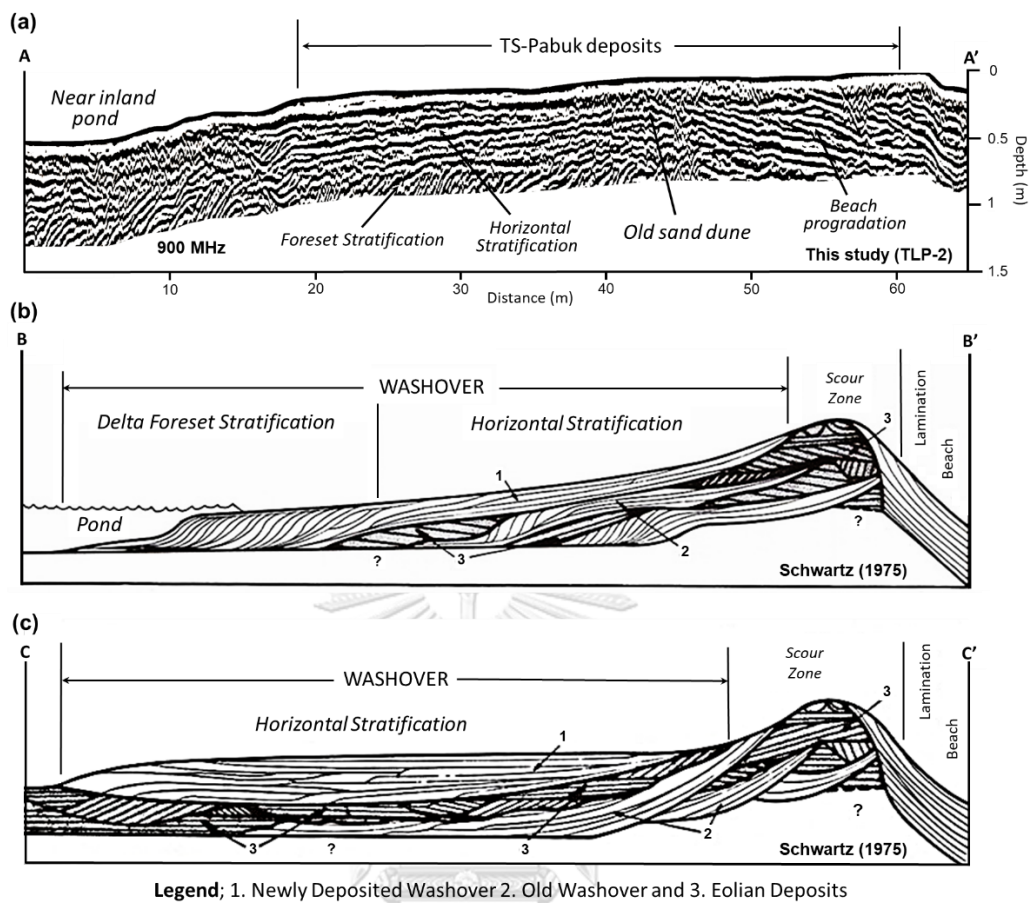


Figure 6.8 Foreset stratification and horizontal lamination in washover deposits (a) GPR signal from 900 MHz antenna at TLP-2 of this study (b) schematic cross-section through washover fans deposited into standing water and cause delta foreset stratification at the landward edge of fans (c) schematic cross-section through washover fans resulting from flow across a subaerial surface showing horizontal stratification. Details of numbers and all marks in (b) and (c) are shown in (Schwartz, 1975)

CHAPTER 7

CONCLUSIONS

The tropical storm Pabuk made landfall at Pak Phanang district, Nakhon Sri Thammarat on January 4th, 2019 and generated hydrological effects along the western coast of the Gulf of Thailand from Nakhon Sri Thammarat to Phetchaburi province. The hydrological storm intensity was considered from high tide level which is locally varied, storm surge level and wave runup height which are related to distances from the landfall location. The farther from landfall site, the lower storm surge and wave runup height. However, the deposition of storm sediments in term of both inland extent and thickness are not rely on only the hydrological intensity but also other local factors. The main factors that play important roles on the deposits is beach topography relative to water level.

According to the surveying study of 44 locations along the W-GOT. The maximum inland extent of storm deposits induced by the TS-Pabuk is 150 m from the coast found at Nakhon Sri Thammarat. However, the second most length is 90 m found at Phetchaburi, the farthest location from landfall site. This strongly insists the influence of local beach topography that quite low relative to hydrological intensity. The maximum depth of storm deposits can be up to 40-45 cm. Most of these thick deposits found at channel inlets where are relatively low-lying area so that they can hold much sediments. Nevertheless, due to their very active area of inflow and outflow, channel inlet is not a good area of preservation potential.

The 4 main locations that storm sediments are well preserved were selected including Chao Samran Beach (CSR) at Phetchaburi, Ban Thung Noi (BTN) at Prachuap Khiri Khan, Thung Tako (TTK) at Chumphon and Laem Talumphuk (TLP) at Nakhon Sri Thammarat located in descending order from the landfall location (Pak Panang). These areas vary in depositional environments and far in descending order distances from the landfall site which are 500, 400, 200, and 15 km, respectively. At CSR and TTK, storm deposits were deposits as washover terrace. Whereas, perched fans were

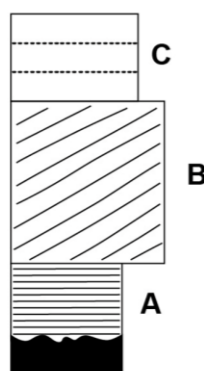
presented at BTN and TLP. The internal sedimentary details are varied by locations as summarized in Table 7.1.

The results from sedimentary analysis at these 4 locations show that storm deposits from the TS-Pabuk can be classified into 3 vertical units (Figure 7.1). Unit A is located at base above an erosional contact. Their compositions are mainly fine grain sediments that were arranged as horizontal planar laminations with reverse grading. This unit was deposited by bedload transportation during an initial stage of storm surge that has lowest energy before gradually intensifying. Unit B is located at the middle layer. Grain compositions are larger sediments with large shell fragments and valves. Sedimentary structures in this units range from massive, horizontal laminations to inclined structures. Moreover, the inclined structures such as foreset bedding or laminations and antidune can be found only in this unit. Unit B were also formed under the bedload transportation of grain flow with the high depth of water during the peak intensity of the storm event. Lastly, Unit C is semi-massive to horizontal laminations of fine grain sediments with mainly normal grading. This unit were deposits under an inundation condition during the final stage of the event. The stagnant water allowed suspended sediments to settle down generating normal grading structure. In some locations, unit C can be overtopped by thin mud layer settling down at the most final stage.

Some large sedimentary structures cannot be considered in small and narrow sedimentary pits. However, GPR can captured these structures and gave us the very useful information. GPR with 200 and 400 MHz antenna can penetrate into 5-6 m and 2.5 m, respectively. They can illustrate large-scale morphology under the recent storm deposits very well. However, the internal details of TS-Pabuk deposits are not well presented by these frequencies. The best frequency suitable for recent storm deposits is 900 MHz which can penetrate into 75 cm depth and gave the best resolution enough to detect some internal structures inside the deposits. With this frequency, sharp erosional contact can be clearly detected at BTN and TTK. In addition, 900 MHz can capture landward inclined structure inside the TS-Pabuk

deposits at TTK which is invisible in sedimentary pits. This frequency can also clearly show the landward foreset bedding of old washover deposits from previous overwash events which are located deeper than the recent TS-Pabuk deposits. This can strengthen an importance of using GPR and sedimentary method together for better understanding the coastal process.

Diatoms found in the TS-Pabuk were collected from surface both at proximal and distal part. At least 22 species were identified. The TS-Pabuk deposits has high diversity of diatoms including 9 Marine, 5 Brackish to marine, 2 Freshwater to brackish, 1 Freshwater, 2 Freshwater to marine and 3 Unknown habitat species. Even the amount and proportion of each specie cannot be summarized for each sample of each location due to time limit, this information can be a record that storm deposits can contain various origins of diatom, even freshwater. The freshwater diatom found in Pabuk deposits insist the heavy precipitation that cause the overbanking flood from inland river or channels. To be better understand about the storm wave base, information from diatom analysis is essential.



Unit	Internal structures	Grain Size and Vertical Grading	Depositional Conditions (Interpretation)
Unit C	semi-massive to horizontal laminations	finer grain sediments with mainly <u>normal grading</u>	Inundation (flooding) during the late stage of storm surge inducing suspended sediments to settle down
Unit B	massive, horizontal laminations to inclined structures such as foreset bedding or laminations and antidune	larger sediments with large shell fragments and valves	Bedload transportation of grain flow during the peak intensity with maximum water depth storm surge
Unit A	horizontal planar laminations	finer grain size (fine to medium sand) with mainly <u>reverse grading</u> *shell fragments can be found at some location (TLP)	Bedload transportation of grain flow during an initial stage of low energy storm surge
Commonly sharp erosional contact (sand over sand is possible at TLP)			
Original surface	Commonly finer than TS-Pabuk sediments, contains higher mud contents and organic materials, darker in color		

Figure 7.1 Summary details of three dominant stratigraphy of the TS-Pabuk deposits in trench scale (vertical) with depositional conditions (interpretation).

Table 7.1 Summary of storm deposits from the tropical storm Pabuk at CSR, BTN, TTK and TLP.

Characteristics	CSR-1	BTN-1-2-3	TTK-1-2-3	TLP-1
Depositional setting	Beach between canals and several offshore breakwaters	Pocket beach between two headlands	Narrow beach in mudflat with swale parallel to the shore	Beach on sand spit with seawall
Washover geometry	Washover terrace	Perched fans	Washover terrace	Perched fans
Grain size range				
<i>Pabuk</i>	Fine - very coarse	Very fine - very coarse	Fine - very coarse	Fine - coarse
<i>Original surface</i>	Fine - medium	Fine - medium	Fine - coarse	Fine - medium
Internal mud Layer	No mud	No mud	No mud	No mud
Sorting				
<i>Pabuk</i>	Mod.well – well	Mod.well - well	Poor	Mod.well - well
<i>Original surface</i>	Mod.well – well	Poor	Poor	Mod.well - well
Grading	Reverse grading, Normal grading	Reverse grading, Normal grading	Reverse grading, Normal grading	Reverse grading, Normal grading
Thickness (cm)	4-30 cm from distal to proximal	3-25 cm	2-33 cm	Up to 40 cm at proximal pits (behind seawall)
Cross-shore geometry	Thinning landward	Thickest at the middle pits	Thinning landward	Thinning landward
Basal contact	Sharp sand contact with underlying higher mud or finer grain sand	Sharp contact with underlying higher mud contents	Sharp and erosional contact with underlying rich-organic soils	Erosional contact (scouring) with underlying sand
Internal sedimentary structures in Pits	Planar laminations, cross laminations	Semi-massive, planar laminations	Semi-massive, planar laminations	Horizontal planar laminations
Length of deposits	20 m	18-23 m	18-23 m	67 m
Limit of inundation	N/A	50-100 m	75 cm (limit at road along the shore)	N/A
Washover Geometry	Washover terrace	Perched fans	Washover terrace	Perched fans
Distances from landfall location	~500 km	~400 km	~200 km	~15 km
GPR applying	no	900 MHz	200, 400, 900 MHz	200, 400, 900 MHz
Structures found in GPR	no	Sharp contact of Pabuk deposits, Beach progradation	Landward inclined bedding in Pabuk deposits, sharp erosional contact, possible old washover deposits	Foreset bedding of old washover deposits, Beach progradation

REFERENCES

- Alexander, J., Bridge, J. S., Cheel, R. J., & Leclair, S. F. (2001). Bedforms and associated sedimentary structures formed under supercritical water flows over aggrading sand beds. *Sedimentology*, *48*(1), 133–152. <https://doi.org/10.1046/J.1365-3091.2001.00357.X>.
- Araya, T., & Masuda, F. (2001). Sedimentary structures of antidunes. *Journal of the Sedimentological Society of Japan*, *53*, 1-15. <https://doi.org/10.4096/jssj1995.53.1>
- Arjwech, R., & Titimakorn, T. (2023). *Engineering Geophysics* (Vol. 1). Khon Kaen University
- Boughton, G. N., Henderson, D. J., Ginger, J. D., Holmes, J. D., Walker, G. R., Leitch, C. J., Somerville, L. R., Frye, U., Jayasinghe, N. C., & Kim, P. Y. (2011). *Tropical Cyclone Yasi : structural damage to buildings*.
- Brandon, C. M., Woodruff, J. D., Donnelly, J. P., & Sullivan, R. M. (2014). How unique was Hurricane Sandy? Sedimentary reconstructions of extreme flooding from New York Harbor. *Sci Rep*, *4*, 7366. <https://doi.org/10.1038/srep07366>
- Brill, D., May, S. M., Engel, M., Reyes, M., Pint, A., Opitz, S., Dierick, M., Gonzalo, L. A., Esser, S., & Brückner, H. (2016). Typhoon Haiyan's sedimentary record in coastal environments of the Philippines and its palaeotempestological implications. *Natural Hazards and Earth System Sciences*, *16*(12), 2799-2822. <https://doi.org/10.5194/nhess-16-2799-2016>
- Choowong, M., Murakoshi, N., Hisada, K.-i., Charoentitirat, T., Charusiri, P., Phantuwongraj, S., Wongkok, P., Choowong, A., Subsayjun, R., Chutakositkanon, V., Jankaew, K., & Kanjanapayont, P. (2008). Flow conditions of the 2004 Indian Ocean tsunami in Thailand, inferred from capping bedforms and sedimentary structures. *Terra Nova*, *20*(2), 141-149. <https://doi.org/10.1111/j.1365->

[3121.2008.00799.x](#)

- Choowong, M., Murakoshi, N., Hisada, K.-i., Charusiri, P., Charoentitirat, T., Chutakositkanon, V., Jankaew, K., Kanjanapayont, P., & Phantuwongraj, S. (2008). 2004 Indian Ocean tsunami inflow and outflow at Phuket, Thailand. *Marine Geology*, 248(3-4), 179-192. <https://doi.org/10.1016/j.margeo.2007.10.011>
- Choowong, M., Murakoshi, N., K., H., Charusiri, P., Daorerk, V., Charoentitirat, T., Chutakositkanon, V., Jankaew, K., & Kanjanapayont, P. (2007). Erosion and Deposition by the 2004 Indian Ocean Tsunami in Phuket and Phang-nga Provinces, Thailand. *Journal of Coastal Research*, 23. <https://doi.org/10.2112/05-0561.1>
- Donnelly, C., Kraus, N., & Larson, M. (2006). State of Knowledge on Measurement and Modeling of Coastal Overwash. *Journal of Coastal Research - J COASTAL RES*, 22, 965-991. <https://doi.org/10.2112/04-0431.1>
- Donnelly, J. P., Butler, J., Roll, S., Wengren, M., & Webb, T. (2004). A backbarrier overwash record of intense storms from Brigantine, New Jersey. *Marine Geology*, 210(1-4), 107-121. <https://doi.org/10.1016/j.margeo.2004.05.005>
- Donnelly, J. P., Roll, S., Wengren, M., Butler, J., Lederer, R., & Webb lii, T. (2001). Sedimentary evidence of intense hurricane strikes from New Jersey. *Geological Society of America Bulletin*, 29, 615-618.
- Donnelly, J. P., & Woodruff, J. D. (2007). Intense hurricane activity over the past 5,000 years controlled by El Nino and the West African monsoon. *Nature*, 447(7143), 465-468. <https://doi.org/10.1038/nature05834>
- Doran, K. S., Plant, N. G., Stockdon, H. F., Sallenger, A. H., & Serafin, K. A. (2009). *Hurricane Ike: Observations and analysis of coastal change* [Report](2009-1061). (Open-File Report, Issue. U. S. G. Survey. <http://pubs.er.usgs.gov/publication/ofr20091061>
- Fujino, S., Naruse, H., Matsumoto, D., Sakakura, N., Suphawajruksakul, A., &

- Jarupongsakul, T. (2010). Detailed measurements of thickness and grain size of a widespread onshore tsunami deposit in Phang-nga Province, southwestern Thailand. *Island Arc*, 19(3), 389-398. <https://doi.org/10.1111/j.1440-1738.2010.00730.x>
- Fujino, S., Naruse, H., Suphawajruksakul, A., Jarupongsakul, T., Murayama, M., & Ichihara, T. (2008). Thickness and Grain-Size Distribution of Indian Ocean Tsunami Deposits at Khao Lak and Phra Thong Island, South-Western Thailand. In *Tsunamiites* (pp. 123-132). <https://doi.org/10.1016/b978-0-444-51552-0.00008-4>
- Goslin, J., & Clemmensen, L. B. (2017). Proxy records of Holocene storm events in coastal barrier systems: Storm-wave induced markers. *Quaternary Science Reviews*, 174, 80-119. <https://doi.org/10.1016/j.quascirev.2017.08.026>
- Gouramanis, C., Switzer, A. D., Pham, D. T., Rubin, C., Lee, Y. S., Bristow, C., & Jankaew, K. (2014). *Thin-bed Ground-penetrating radar analysis of preserved modern and palaeotsunami deposits from Phra Thong Island, Thailand* Proceedings of the 15th International Conference on Ground Penetrating Radar,
- Gouramanis, C., Switzer, A. D., Polivka, P. M., Bristow, C. S., Jankaew, K., Dat, P. T., Pile, J., Rubin, C. M., Yingsin, L., Ildefonso, S. R., & Jol, H. M. (2015). Ground penetrating radar examination of thin tsunami beds — A case study from Phra Thong Island, Thailand. *Sedimentary Geology*, 329, 149-165. <https://doi.org/10.1016/j.sedgeo.2015.09.011>
- Hand, B. M. (1997). Inverse grading resulting from coarse-sediment transport lag. *Journal of Sedimentary Research*, 67(1), 124-129. <https://doi.org/10.1306/D426850E-2B26-11D7-8648000102C1865D>
- Haque, M. M., Yamada, M., Uchiyama, S., & Hoyanagi, K. (2021). Depositional setup and characteristics of the storm deposit by the 2007 Cyclone Sidr on Kuakata Coast, Bangladesh. *Marine Geology*, 442, 106652. <https://doi.org/10.1016/j.margeo.2021.106652>

- Hawkes, A. D., & Horton, B. P. (2012). Sedimentary record of storm deposits from Hurricane Ike, Galveston and San Luis Islands, Texas. *Geomorphology*, 171-172, 180-189. <https://doi.org/10.1016/j.geomorph.2012.05.017>
- Hippensteel, S. P., & Martin, R. E. (1999). Foraminifera as an indicator of overwash deposits, Barrier Island sediment supply, and Barrier Island evolution: Folly Island, South Carolina. *Palaeogeography, Palaeoclimatology, Palaeoecology*, 149(1-4), 115-125. [https://doi.org/10.1016/s0031-0182\(98\)00196-5](https://doi.org/10.1016/s0031-0182(98)00196-5)
- Hong, I., Pilarczyk, J. E., Horton, B. P., Fritz, H. M., Kosciuch, T. J., Wallace, D. J., Dike, C., Rarai, A., Harrison, M. J., & Jockley, F. R. (2018). Sedimentological characteristics of the 2015 Tropical Cyclone Pam overwash sediments from Vanuatu, South Pacific. *Marine Geology*, 396, 205-214. <https://doi.org/10.1016/j.margeo.2017.05.011>
- Jankaew, K., Atwater, B. F., Sawai, Y., Choowong, M., Charoentitirat, T., Martin, M. E., & Prendergast, A. (2008). Medieval forewarning of the 2004 Indian Ocean tsunami in Thailand. *Nature*, 455(7217), 1228-1231. <https://doi.org/10.1038/nature07373>
- Kitamura, A., Yuka, Y., Kenji, H., & Toyofuku, T. (2020). Identifying storm surge deposits in the muddy intertidal zone of Ena Bay, Central Japan. *Marine Geology*, 426. <https://doi.org/10.1016/j.margeo.2020.106228>
- Kongsen, S. (2016). *Analysis of Ancient Storm Deposits in Changwat Prachuap Khiri Khan* [Chulalongkorn University].
- López, G. (2016). Grain Size Analysis. In (pp. 341-348). https://doi.org/10.1007/978-1-4020-4409-0_18
- Masselink, G., & Heteren, S. v. (2014). Response of wave-dominated and mixed-energy barriers to storms. *Marine Geology*, 352, 321-347. <https://doi.org/10.1016/j.margeo.2013.11.004>
- Morton, R., & Barras, J. (2011). Hurricane Impacts on Coastal Wetlands: A Half-Century

- Record of Storm-Generated Features from Southern Louisiana. *Journal of Coastal Research*, 27, 27-43. <https://doi.org/10.2307/41315913>
- Morton, R. A. (2002). Factors Controlling Storm Impacts on Coastal Barriers and Beaches: A Preliminary Basis for near Real-Time Forecasting. *Journal of Coastal Research*, 18, 486-501.
- Morton, R. A., Gelfenbaum, G., & Jaffe, B. E. (2007). Physical criteria for distinguishing sandy tsunami and storm deposits using modern examples. *Sedimentary Geology*, 200(3-4), 184-207. <https://doi.org/10.1016/j.sedgeo.2007.01.003>
- Morton, R. A., & Sallenger, A. H. (2003). Morphological Impacts of Extreme Storms on Sandy Beaches and Barriers. *Journal of Coastal Research*, 19, 560-573.
- Nott, J. (2004). Palaeotempestology: the study of prehistoric tropical cyclones--a review and implications for hazard assessment. *Environ Int*, 30(3), 433-447. <https://doi.org/10.1016/j.envint.2003.09.010>
- Nott, J., Chague-Goff, C., Goff, J., Sloss, C., & Riggs, N. (2013). Anatomy of sand beach ridges: Evidence from severe Tropical Cyclone Yasi and its predecessors, northeast Queensland, Australia. *Journal of Geophysical Research: Earth Surface*, 118(3), 1710-1719. <https://doi.org/10.1002/jgrf.20122>
- Phantuwongraj, S. (2012). Sedimentological Characteristics of Storm-induced Washover Deposits along the Coastal Zone of Changwat Prachuap Khiri Khan to Nakhon Si Thammarat, Thailand. *Department of Geology, Doctor of Philosophy in Geology*, 127.
- Phantuwongraj, S., & Choowong, M. (2012). Tsunamis versus storm deposits from Thailand. *Natural Hazards*, 63(1), 31-50. <https://doi.org/10.1007/s11069-011-9717-8>
- Phantuwongraj, S., Choowong, M., & Chutakositkanon, V. (2008). *Possible Storm Deposits from Surat Thani and Nakhon Si Thammarat Provinces, the Southern Peninsular Thailand*.

- Phantuwongraj, S., Choowong, M., Nanayama, F., Hisada, K., Charusiri, P., Churakositkanon, V., Pailoplee, S., & Chabangbon, A. (2013). Coastal geomorphic conditions and styles of storm surge washover deposits from southern Thailand. *Geomorphology*, 192, 43-58. <https://doi.org/10.1016/j.geomorph.2013.03.016>
- Phantuwongraj, S., M., C., & Silaphanth, P. (2010). Geological evidence of sea-level change: a preliminary investigation at Panang Tak area, Chumphon province, Thailand. *The 117th Annual Meeting of the Geological Society of Japan*. Geological Society of Japan, Toyama, Japan
- 185.
- Phantuwongraj, S., M., C., & V., C. (2008). Possible Storm Deposits from Surat Thani and Nakhon Si Thammarat Provinces, the Southern Peninsular Thailand. *Proceedings of the International Symposia on Geoscience Resources and Environments of Asian Terranes (GREAT 2008)*.
- Pilarczyk, J. E., Dura, T., Horton, B. P., Engelhart, S. E., Kemp, A. C., & Sawai, Y. (2014). Microfossils from coastal environments as indicators of paleo-earthquakes, tsunamis and storms. *Palaeogeography, Palaeoclimatology, Palaeoecology*, 413, 144-157. <https://doi.org/10.1016/j.palaeo.2014.06.033>
- Pilarczyk, J. E., Horton, B. P., Soria, J. L. A., Switzer, A. D., Siringan, F., Fritz, H. M., Khan, N. S., Ildefonso, S., Doctor, A. A., & Garcia, M. L. (2016). Micropaleontology of the 2013 Typhoon Haiyan overwash sediments from the Leyte Gulf, Philippines. *Sedimentary Geology*, 339, 104-114. <https://doi.org/10.1016/j.sedgeo.2016.04.001>
- Pile, J., Switzer, A. D., Soria, J. L. A., Siringan, F., & Daag, A. (2016). An investigation of recent storm histories using Ground Penetrating Radar at Bay-Bay Spit, Bicol, Central Philippines. *16th International Conference on Ground Penetrating Radar (GPR)*.
- Sallenger, A. H. (2000). Storm Impact Scale for Barrier Islands. *Journal of Coastal*

Research, 16, 890-895.

- Schwartz, R. (1975). *Nature and genesis of some storm washover deposits*.
<https://doi.org/10.13140/RG.2.1.2216.9449>
- Sedgwick, P. E., & Davis, R. A. (2003). Stratigraphy of washover deposits in Florida: implications for recognition in the stratigraphic record. *Marine Geology*, 200(1), 31-48. [https://doi.org/10.1016/S0025-3227\(03\)00163-4](https://doi.org/10.1016/S0025-3227(03)00163-4)
- Soria, J. L. A., Switzer, A. D., Pilarczyk, J. E., Siringan, F. P., Khan, N. S., & Fritz, H. M. (2017). Typhoon Haiyan overwash sediments from Leyte Gulf coastlines show local spatial variations with hybrid storm and tsunami signatures. *Sedimentary Geology*, 358, 121-138. <https://doi.org/10.1016/j.sedgeo.2017.06.006>
- Soria, J. L. A., Switzer, A. D., Pile, J., Siringan, F. P., Brill, D., & Daag, A. (2021). Geomorphological and sedimentological records of recent storms on a volcanoclastic coast in Bicol, Philippines. *Geomorphology*, 386. <https://doi.org/10.1016/j.geomorph.2021.107753>
- Switzer, A. D., & Jones, B. G. (2008). Setup, Deposition, and Sedimentary Characteristics of Two Storm Overwash Deposits, Abrahams Bosom Beach, Southeastern Australia. *Journal of Coastal Research*, 1, 189-200. <https://doi.org/10.2112/05-0487.1>
- Switzer, A. D., & Pile, J. (2015). *Grain size analysis*. John Wiley & Sons, Ltd.
- Syvitski, J. P. M. (1991). *Principles, methods, and application of particle size analysis*. Cambridge University Press. <https://doi.org/10.1017/cbo9780511626142>
- Takagi, H., Esteban, M., Shibayama, T., Mikami, T., Matsumaru, R., Leon, M., Thao, N., Oyama, T., & Nakamura, R. (2014). Track Analysis, Simulation and Field Survey of the 2013 Typhoon Haiyan Storm Surge. *Journal of Flood Risk Management*, 10. <https://doi.org/10.1111/jfr3.12136>
- Tucker, M. E. (2003). *Sedimentary Rocks in the Field* (3 ed.). John Wiley & Sons Ltd.

- Wallace, D. J., Woodruff, J. D., Anderson, J. B., & Donnelly, J. P. (2014). Palaeohurricane reconstructions from sedimentary archives along the Gulf of Mexico, Caribbean Sea and western North Atlantic Ocean margins. *Geological Society, London, Special Publications*, 388(1), 481-501. <https://doi.org/10.1144/sp388.12>
- Wang, P., & Horwitz, M. H. (2007). Erosional and depositional characteristics of regional overwash deposits caused by multiple hurricanes. *Sedimentology*, 54(3), 545-564. <https://doi.org/10.1111/j.1365-3091.2006.00848.x>
- Williams, H. (2009). Stratigraphy, Sedimentology, and Microfossil Content of Hurricane Rita Storm Surge Deposits in Southwest Louisiana. *Journal of Coastal Research - J COASTAL RES*, 25, 1041-1051. <https://doi.org/10.2112/08-1038.1>
- Williams, H., Choowong, M., Phantuwongraj, S., Surakietchai, P., Thongkhao, T., Kongsen, S., & Simon, E. (2016). Geologic records of Holocene typhoon strikes on the Gulf of Thailand coast. *Marine Geology*, 372, 66-78. <https://doi.org/10.1016/j.margeo.2015.12.014>
- Williams, H. F. L. (2010). Storm Surge Deposition By Hurricane Ike On The MCFaddin National Wildlife Refuge, Texas: Implications For Paleotempestology Studies. *Journal of Foraminiferal Research*, 40(3), 210-219. <https://doi.org/10.2113/gsjfr.40.3.210>
- Xiong, H., Huang, G., Fu, S., & Qian, P. (2018). Progress in the Study of Coastal Storm Deposits. *Ocean Science Journal*, 53(2), 149-164. <https://doi.org/10.1007/s12601-018-0019-x>



จุฬาลงกรณ์มหาวิทยาลัย
CHULALONGKORN UNIVERSITY

VITA

NAME Chanakan Ketthong

DATE OF BIRTH 1 September 1995

PLACE OF BIRTH Suphan Buri

INSTITUTIONS ATTENDED Department of Geology, Faculty of Science, Chulalongkorn University

HOME ADDRESS 159 M.4 U-Thong, U-Thong, Suphan Buri, Thailand 72160

